TUTKIMUSRAPORTTI
REPORT OF INVESTIGATION 125

Markku Tiainen and Helene Viita

Determination of ore potential areas in the Häme belt, southwestern Finland, by integration of geological, geophysical and till geochemical data

GEOLOGIAN TUTKIMUSKESKUS
GEOLOGICAL SURVEY OF FINLAND

Espoo 1994

GEOLOGIAN TUTKIMUSKESKUS

Tutkimusraportti 125

GEOLOGICAL SURVEY OF FINLAND

Report of Investigation 125

Markku Tiainen and Helene Viita

DETERMINATION OF ORE POTENTIAL AREAS IN THE HÄME BELT, SOUTHWESTERN FINLAND, BY INTEGRATION OF GEOLOGICAL, GEOPHYSICAL AND TILL GEOCHEMICAL DATA

Espoo 1994

Tiainen, Markku & Viita, Helene 1994. Determination of ore potential areas in the Häme belt, southwestern Finland, by integration of geological, geophysical and till geochemical data. Geologian tutkimuskeskus, Tutkimusraportti - *Geological Survey of Finland, Report of Investigation* 125. 49 pages, 51 figures and 7 tables.

The mineral potential of the Early Proterozoic Svecofennian Häme belt in Southern Finland was assessed by analysing and integrating bedrock geological, till geochemical and geophysical data sets from an explorational viewpoint. The data were collected during the regional mapping projects conducted by the Geological Survey of Finland (GSF). The geochemical and ore geological data were available in digital data bases of the GSF. The geophysical data were compiled from small airborne survey areas, and the geological data were digitised by the project. The study area covers about 120 km x 60 km.

The main metallogenic ore deposit types of the area are of Zn-Cu-S, Ni-Cu, Fe, Fe-Ti, Au-(Cu), W, Mo, U and Sn. Ore deposit fingerprints were investigated with till geochemical data by applying factor analysis and various element ratios. The explorationally interesting till geochemical patterns were enhanced by filtering away the regional background level. Image processing enhancement methods were applied to the geophysical data to reveal the dominant structural patterns. Colour composites, principal component analysis and classifications were applied to the geophysical data to reveal indications of rock alterations related to ore formation. The geological, till geochemical and geophysical variables were integrated with similarity analysis using the Katumajärvi Cu-Zn-Au, Tupala Zn-Pb-Ag and Särkisuo Ni-Cu deposits as models. The results are presented as ore-potential maps of zinc, copper and nickel.

The most promising ore deposit types and targets for exploration in the Häme belt are 1) the Tupala-type Zn deposits hosted by volcanic rocks in the southern part of the belt, 2) the Au-bearing Cu(-Zn) deposits in the volcanic belts west of Hämeenlinna and 3) the Cu-bearing tourmaline breccias in the surroundings of synorogenic granitoids intruding volcanic belts, e.g. the Aulanko and Onkimaa granodiorites. The likelihood of finding Ni-Cu deposits outside the Särkisuo area is not very high.

Key words (GeoRef Thesaurus, AGI): mineral exploration, metal ores, potential deposits, data integration, statistical analysis, structural geology, geophysical surveys, imagery, geochemical surveys, till, prediction maps, Proterozoic, southwestern Finland

Markku Tiainen and Helene Viita
Geological Survey of Finland
FIN-02150 Espoo
Finland

ISBN 951-690-553-6
ISSN 0781-4240

CONTENTS

Introduction 5
Data and methods 6
Geological setting 6
Metallogenic features 7
  Zn-Cu deposits 7
  Ni deposits 10
  Fe-Ti deposits 10
  Fe deposits 10
Preprocessing and analysis of data 10
  Geological data 10
    Structural data 10
    Main structural units 11
  Geophysical data 16
  Image processing 18
    Principal component analysis 23
    Classification 23
  Geochemical data 27
  Factor analysis 28
    Regional factors 28
    Factors indicating mineral deposits 30
  Element and element ratio data 33
    Zinc 35
    Copper 36
    Nickel 37
Data integration 39
  Deposit models 39
    The Tupala Zn-Pb deposit 39
    The Katumajärvi Cu-Zn deposit 40
    The Särkisuo Ni-Cu deposit 41
  Similarity analysis 41
    Variables in the Tupala and Katumajärvi models 41
    Variables in the Särkisuo model 43
  Results 43
    Cu-Zn-Pb potential areas 43
    Ni-Cu potential areas 43
Conclusion 46
Acknowledgements 46
References 47

INTRODUCTION

The Häme belt is a Palaeoproterozoic fault-bounded tectonic unit of the Svecofennian domain in southwestern Finland, bordered in the north by the metagreywacke-granodioritic gneiss complex and in the south by the high metamorphic West Uusimaa gneiss complex (Fig 1). The schists of the Häme belt consist of volcanic-sedimentary rocks intruded by synorogenic I-type granitoids and late-orogenic S-type granitoids (Fig. 1).

The Häme belt has characteristic metallogenic features, that distinguish it clearly from the migmatitic greywacke schist belt with Ni-bearing ultramafic intrusions to the north and from the Cu-Zn-bearing volcanogenic leptite zone to the south. Several Cu, Zn, Au, Ni, W, and Fe mineralisations and mineralised boulders have been found in the region but no economic deposits as yet.

The aim of this study was to determine the main metallogenic features of the Häme belt and to select potential areas and targets for exploration by analysing and integrating the geological, geophysical and geochemcal data collected by the Geological Survey of Finland (GSF). The study is part of the Mineral Resource Assessment Project of Southwestern Finland (Tiainen 1989).

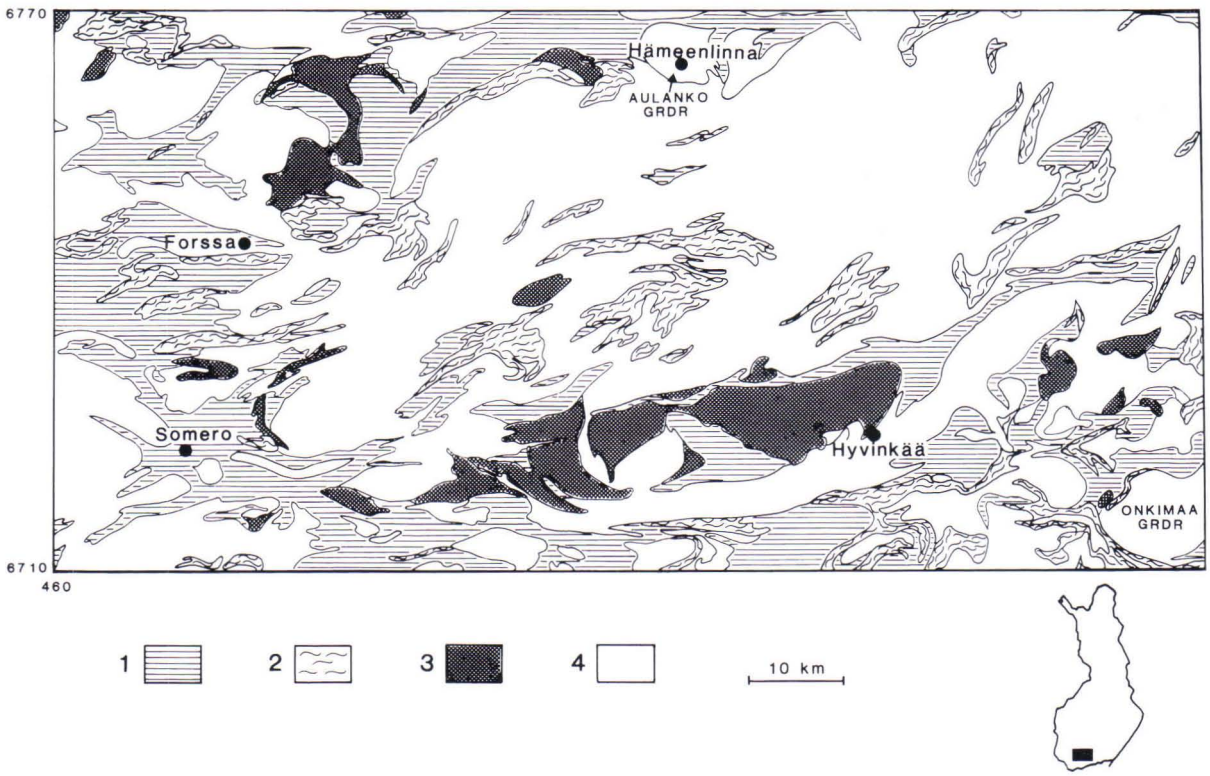

Fig. 1. Location of the study area and the main geological features, simplified after Simonen 1949a, Härme 1953, Neuvonen 1954, Simonen 1955, Kaitaro 1956 and Lehijärvi 1961. 1. volcanic rocks; 2. mica schists and gneisses; 3. mafic and ultramafic plutonics; 4. synorogenic and late-orogenic granitoids.

DATA AND METHODS

The data were largely acquired from the geological, aerogeophysical and till geochemical regional mapping programmes of the GSF. The metallogenic data were compiled from the explorational data bases of the GSF (Gaál et al. 1977, Saltikoff & Tarvainen 1990) and from the archives of the Ministry of Trade and Industry.

The Lithological and structural data were digitised with the FINGIS program, developed by the National Board of Survey of Finland, from 1:100,000-scale geological maps (Fig. 2) published by the Petrological Department of the GSF.

The high altitude aeromagnetic total anomaly field data (Korhonen 1980) were provided by the Geophysical Department. The gravity data were supplied by the Geodetic Institute of Finland and processed by Seppo Elo at the Geophysical Department of the GSF. The low-altitude aerogeophysical data were compiled and processed from the data on 66 sheets of 1:20,000-scale maps (Fig. 13).

The geochemical data were produced by the Geochemistry Department of the GSF as part of their regional geochemical till mapping programme. The sampling density was about 1 sample/4 km^2. Each sample is composed of four sub-samples, which were taken by a motor-driven percussion drill with a through-flow bit from till below the water table at 20-metre intervals along a line perpendicular to the direction of glacier movement. The fine fraction (<0.06 mm) of the samples was leached in aqua regia and analysed by ICP. The analytically reliable elements were Al, Ba, Ca, Co, Cr, Cu, Fe, K, La, Li, Mg, Mn, Ni, P, Sc, Sr, Th, Ti, V, Y and Zn.

The integration, analysis and prediction of ore potential areas were carried out by statistical and image processing methods. The statistical studies were done with the SPSS-X program package (SPSS Inc. 1988) in a Vax/VMS 8250. The image processing was carried out with the DISIMP program package (CSIRO 1990) in a Vax/VMS and an HP-Apollo 3550 UNIX workstation. Similarity analysis was performed with the SIMANA software (Koistinen 1984, Gaál & Koistinen 1988).

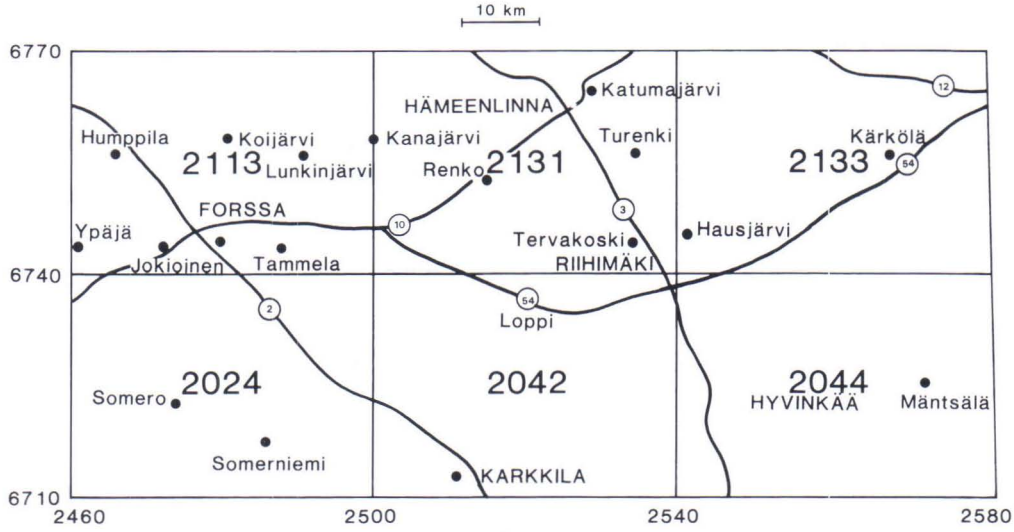

Fig. 2. Index map with 1:100,000 map sheets, showing the main roads, cities and localities in the study area.

GEOLOGICAL SETTING

The Palaeoproterozoic Häme belt in southwestern Finland lies in the Svecofennian domain of the Fennoscandian shield (Hietanen 1975, Simonen 1980, Gaál & Gorbatschev 1987). The belt is mainly composed of intermediate metavolcanic rocks and to a lesser extent of mafic and felsic metavolcanites and metapelites (Fig. 1). The stratigraphy of the Svecofennian schist zones in southern Finland can be divided into three major units: the upper, middle and lower Svecofennian Groups (Latvalahti 1979, Simonen 1980, Mäkelä 1989). The upper group represents epiclastic sedimentation, the middle group mainly mafic volcanism and the lower group greywackes and local felsic volcanism. In the northern part of the Häme belt, however, the metapelites rest on volcanic rocks, and the mafic volcanites are overlain by felsic volcanites (Hakkarainen 1989, Papunen 1990). The metapelites and altered

volcanites include andalusite-, cordierite- and garnet-bearing mica schists and mica gneisses (Ruskeeniemi 1990).

The volcanic rocks of the Häme schist belt include massive lavas, pillow lavas, pyroclastics and other fragmentary volcanic rocks. The depositional environment of the schist belt varies from subwater and shallow water to subaerial, the subwater environment being the more characteristic (Lindroos 1980, Mäkelä 1980, Hakkarainen 1989). The chemical composition of the volcanites varies considerably, mafic basalts dominating in the north and intermediate volcanites in the south. The tholeiitic basalts in the north exhibit certain oceanic rift affinities, although calc-alkalic and alkalic basalts also exist (Hakkarainen 1990). In the south of the belt (Kiipu, Forssa and Somero), intermediate to felsic calc-alkalic volcanites with island arc affinities dominate (Mäkelä 1989, Hakkarainen 1990).

There are two different genetic groups of granitoids in the Häme belt — synorogenic granitoids and late-orogenic microcline granites. The synorogenic granitoids with ages of 1.88 Ga (Patchett & Kouvo 1986) are mainly I-type granodiorites and quartz diorites (Front & Nurmi 1987); the late-orogenic microcline granites with ages of 1.83 Ga (Huhma 1986) are mainly migmatitic, but have homogenous, porphyritic, muscovite-bearing and pegmatitic parts (Simonen 1948, Härme 1965, Nurmi et al. 1984). The late-orogenic granites have been interpreted by Nurmi and Haapala (1986) as S-type granites.

The mafic intrusions of the study area are concentrated in three main areas: 1) the gabbro belt from Hyvinkää to Somerniemi; 2) the gabbros of Mäntsälä and 3) the gabbros of Forssa. Petrologically, the gabbros range from diorites to pyroxenites and lherzolites, with amphibolite gabbros as dominat variants (Härme 1954, Mäkinen 1987). The Hyvinkää and Forssa gabbros grade into subvolcanic uralite porphyrites (Härme 1954, Neuvonen 1956). The mafic and ultramafic plutonites, which are surrounded by intermediate and mafic volcanites, have been interpreted as subvolcanic magma chambers (Härme 1978).

The Häme belt was metamorphosed under low pressure amphibolite facies conditions (Haataja 1987, Mäkelä 1980, Mäkelä 1989). However, the presence of hyperstene-bearing gneisses within the late-orogenic granites is an indication of local high-grade metamorphism (Simonen 1949b).

METALLOGENIC FEATURES

The main metallogenic types of mineral deposit in Häme belt are Zn-Cu(-Pb-Ag), Ni-Cu, Fe and Fe-Ti deposits, but indications of Au-Cu, W, U, Mo and Sn-Fe deposits also occur. There are three types of Cu-Zn indication: 1) chalcopyrite and 2) chalcocite bearing types in the north of the belt between Katumajärvi and Kiipu and 3) Zn-bearing types in the surroundings of the Tupala Zn deposit (Fig. 3). Sulphur poor chalcocite bearing Cu deposits have been correlated by Saltikoff (1992) with porphyry copper deposits. Gold indications seem to favour the same areas as Cu; some are clearly related to fault/shear zones. The Satulinmäki Au deposit (Fig. 3) is associated with tourmalinised aplitic and quartz veins (Haga 1984). Nickel indications form a distinct zone to the west of Särkisuo (Fig. 3). According to ore deposit data, only Cu-Zn, Ni-Cu and, possibly, Au deposits have some economic potential in this area. The most important mineralisations in the study area are listed in Table 1.

Zn-Cu deposits

The Zn-Cu deposits are associated with cordierite-anthophyllite-rocks or sericite schists in volcanic complexes. They are usually interpreted as volcanic hydrothermal massive sulphide deposits (Mäkelä 1980, Mäkelä 1989, Papunen 1990, Ruskeeniemi 1990).

The Tupala Zn-Pb-Ag deposit (Fig. 3) with estimated ore reserves of 763 000 t assaying 3.86% Zn, 0.71% Pb, 39 ppm Ag and 12% S (Papunen 1990), is the most important mineralisation in the Häme belt. The main ore minerals are pyrite, pyrrhotite, sphalerite, galena, tetrahedrite and native silver. The Tupala mineralisation was interpreted by Mäkelä (1989) as a strata-bound distal ore deposit. The orebodies are hosted by cordierite-mica gneisses, diopside-tremolite skarns and altered acid metavolcanites at the contact of intermediate and basic metavolcanites. The metavolcanites in the surroundings of the Tupala deposit differentiated from a calc-alkalic magma (Mäkelä 1989).

The other known Zn-Cu deposits in the Häme belt are clearly smaller than Tupala. The Kiipu Zn mineralisation (Fig. 3), for example, which is a banded, disseminated, partly massive stratabound deposit in altered felsic metavolcanites, is only some tens of centimetres thick (Mäkelä 1980, Papunen 1990).

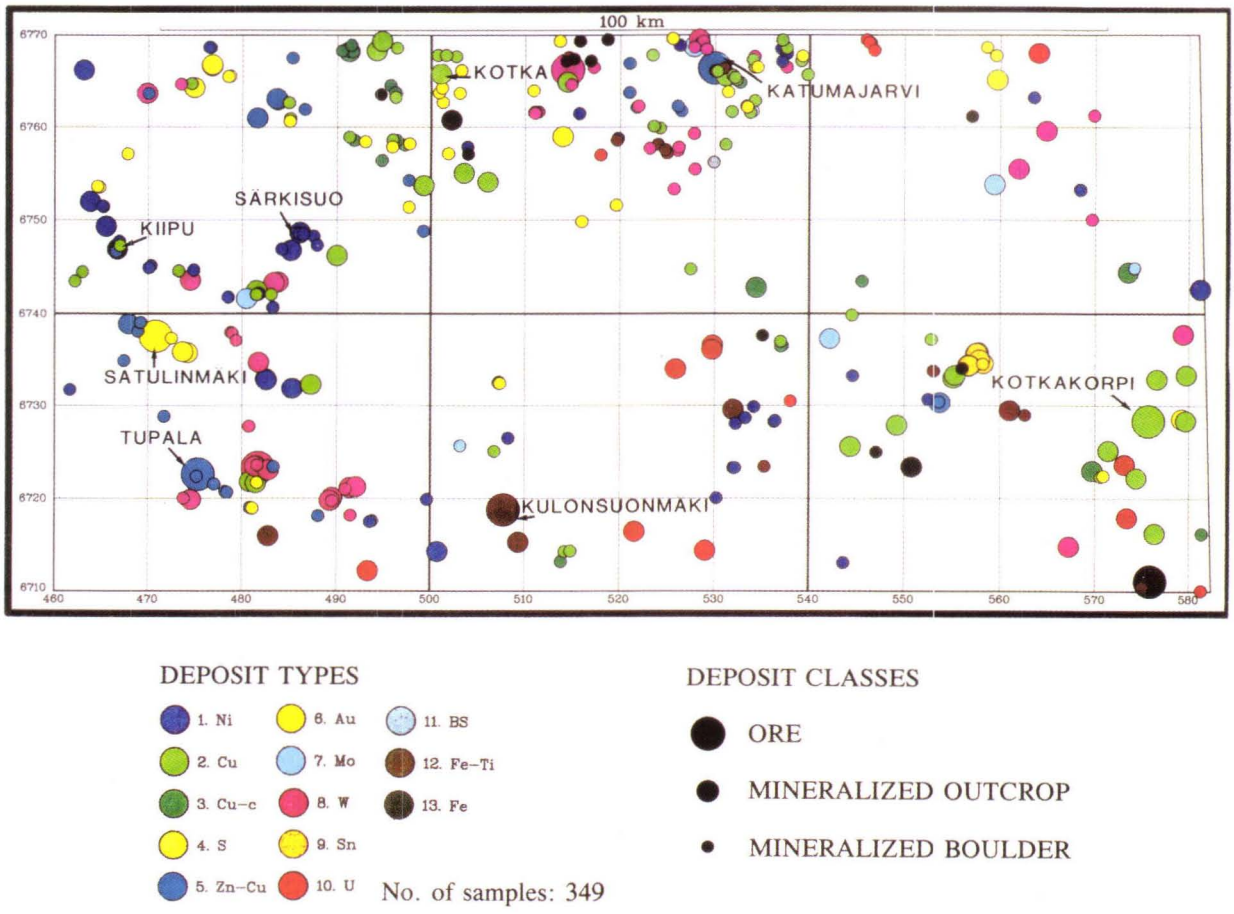

Fig. 3. Ore deposits and indications plotted from the explorational data bases of the Geological Survey of Finland. Modified from Saltikoff (1992).

The highest observed metal contents are: 450 ppm Zn, 150 ppm Cu and 130 ppm Pb (Papunen 1990). Kiipu lies in a calc-alkalic felsic and intermediate metavolcanite formation altered to cordierite gneisses, cordierite-mica gneisses and cordierite-anthophyllite gneisses by circulating sea water (Lindroos 1980, Mäkelä 1980, Ruskeeniemi 1990).

The Kotka and Katumajärvi Cu-Zn(-Au) mineralisations (Fig. 3) are hosted by cummingtonite gneisses, cordierite-anthophyllite rocks and sericite schists associated with felsic, intermediate and mafic metavolcanites near the contacts of granodioritic and quartz dioritic stocks or batholits (Kinnunen 1987a,b). The cummingtonite gneisses, cordierite-anthophyllite rocks and sericite schists have been interpreted as metamorphosed products of hydrothermal alteration; the main exploration targets have been Kuroko-type volcanic exhalative massive sulphide deposits (Haataja 1987, Kinnunen 1987a). The drilled mineralisations at Kotka and Katumajärvi are small, low grade disseminated stringer type Cu-S deposits with minor Zn, Co, Au and REE contents.

The main ore minerals at Katumajärvi are pyrite, pyrrhotite, chalcopyrite and sphalerite, and the highest metal contents are 0.1% Cu in a core 2 m long (Kinnunen 1987a), and 0.5% Cu, 0.5% Zn and 2.5 ppm Au found in a couple of small mineralisations sampled in the course of the project.

The main ore minerals at Kotka are pyrite, chalcopyrite, cobaltite, arsenopyrite, sphalerite and molybdenite (Kinnunen 1987b). The highest metal contents 0.34% Cu, 0.14% Co and 0.17 ppm Au in a core 0.55 m long and 0.228% La, 0.356% Ce, 0.039% Pr and 0.104% Nb in a 0.7-m core.

The Kotkakorpi Cu deposit (Fig. 3) is hosted by mafic, intermediate and felsic metavolcanites (Lindmark 1982a). The main ore mineral is pyrite, which is most abundant in the felsic metavolcanites. Chalcopyrite is the only mineral of any value and usually appears together with pyrite. The drilled mineralised section is about 60 m thick and 150 m long, and contains at best 8 m of 0.3% Cu (Lindmark 1982).

Table 1. Ore mineralisations of the Häme schist belt according to the explorational data bases of the Geological Survey of Finland and other published data.

N:o	Name	x-coord y-coord	Metals	Ore minerals	Assosiated rocks	References
1.	Tupala	6722.620 2475.350	Zn, Ag, Pb	pyrrhotite, sphalerite, pyrite	cordierite-mica gneiss, skarn, chert, mafic, felsic and intermediate volcanites	Mäkelä (1989) Papunen (1990)
2.	Kiipu	6746.720 2466.540	Zn, Cu, Pb	sphalerite, pyrite, chalcopyrite, galena	cordierite, cordierite-mica and cordierite-antofyllite gneisses	Mäkelä (1980) Papunen (1990) Ruskeeniemi (1990)
3.	Katumajärvi	6766.400 2529.950	Cu, Zn, W, Au	pyrrhotite,chalcopyrite, pyrite, sphalerite, magnetite	cordierite-antofyllite rocks, cummingtonite amfibolite sericite schist	Haataja (1987) Kinnunen (1987a)
4.	Kotka	6764.550 2500.750	Cu, Zn, Co, Ag	chalcopyrite, cobaltite, molybdenite	andesite, dasite, chlorite schist	Kinnunen (1987b)
5.	Kotkakorpi	6728.350 2575.700	Cu	chalcopyrite, pyrite, pyrrhotite, magnetite	uralite porphyrite, mafic, felsic and intermediate volcanites	Lindmark (1982)
6.	Särkisuo	6748.665 2486.125	Cu, Ni		peridotite, gabbro	Huopaniemi (1978)
7.	Kulonsuon-mäki	6718.780 2507.820	Fe, Ti	titanomagnetite, ilmenite, magnetite	gabbro	Sipilä (1981)
8.	Laha	6711.120 2575.910	Fe	magnetite	garnet-kordierite gneiss, banded iron formation	Pyy (1978)
9.	Satulinmäki	6737.550 2470.850	Au		applite, intermediate tuff, uralite porphyrite, turmaline breccia	Haga (1984)

Ni deposits

The Ni deposits in the Häme belt are associated with the Hyvinkää, Somerniemi and Forssa gabbros (Lindmark 1982b, 1983, Huopaniemi 1978). The Särkisuo Ni-Cu deposit (Fig. 3) is hosted by a hornblende gabbro possibly connected to the Forssa gabbro. The drill intersected 5.8 m of weak Cu-Ni mineralisation (Huopaniemi 1978). The Ni-Cu deposits detected in the Hyvinkää and Somerniemi gabbros are also small. However, at the southwest border of the Hyvinkää gabbro, there are a couple of Cu rich cummingtonite-norite glacial erratics with an unknown source.

Fe-Ti deposits

The Fe-Ti deposits of the study area are associated with the gabbros from Hyvinkää to Somerniemi (Figs 3 and 4) (Härme 1955). According to Talvitie and Paarma (1980), the Fe-Ti-V bearing mafic intrusions in southwestern Finland are controlled by a northwesterly wrench fault. In the 19th century, about 24 000 t of iron ore with about 30% Fe was extracted from a gabbro at Kulonsuonmäki (Fig. 3) (Laine 1952). The deposit contains magnetite and ilmenite as separate minerals, variable amounts of apatite and some iron sulphides (Sipilä 1981).

Fe deposits

Iron deposits in southern Finland include both skarn Fe deposits and banded iron formations (Sipilä 1981); to date, however, all have proved to be subeconomic. One documented Fe deposit in this area is the 1.5-km-long and 50-m-wide banded iron formation of Laha (Fig. 3). Hosted by garnet-cordierite gneisses it lies at the contact with the Onkimaa granodiorite (Pyy 1978).

PREPROCESSING AND ANALYSIS OF DATA

Geological data

The geological data were digitised from published geological maps at 1:100 000 scale. Lithological and structural elements were extracted into separate coverages (Figs 4, 5 and 6). The data were slightly generalised and modified in order to get an unambiguous lithological classification and continuous lithological boundaries between the map sheets.

The digitised lithological data were pixelled by FINGIS into a regular 1 km x 1 km grid. The pixel data were later used in the similarity analysis, in which geological, geophysical and till geochemical data were integrated into ore-potential maps.

Structural data

The structural observations, schistosities and lineations were digitised from published bedrock geological maps and were interpolated into a regular grid according to the dip of schistosity. The general trends of the structures were visualised by plotting the interpolated dip values of the schistosities as greytone maps (Fig. 7). The structural interpretation is based on visual and statistical analysis of the structural observations and on the interpretation of high- and low-altitude aerogeophysical data.

Several filtering operations were executed to enhance the magnetic pixel range data for structural interpretation. Edge enhancements, directional gradients and 3-D shaded relief surfaces etc. were generated. Figure 8 shows edge-enhanced low- altitude magnetic data, obtained by applying a 31 x 31-sized box filter. This map emphasizes the main structures. A relief surface as created by a directional gradient and a 3 x 3-sized low pass filter is shown in Fig. 9. It is also useful to detect structures in areas with low and homogeneous magnetic intensity. To increase variance within magnetically smooth areas, a nonlinear difference operator with a user-supplied variance and neighbourhood size was applied (Fig. 10).

The oldest faults, shear zones and structural deformation patterns can be interpreted from the aeromagnetic total intensity map and from the filtered aeromagnetic maps (Figs 8–10), whereas the younger fractures are best shown by the electromagnetic and radiometric data (Figs 16–20). The compilation of patterns, faults and fractures (Fig. 11)

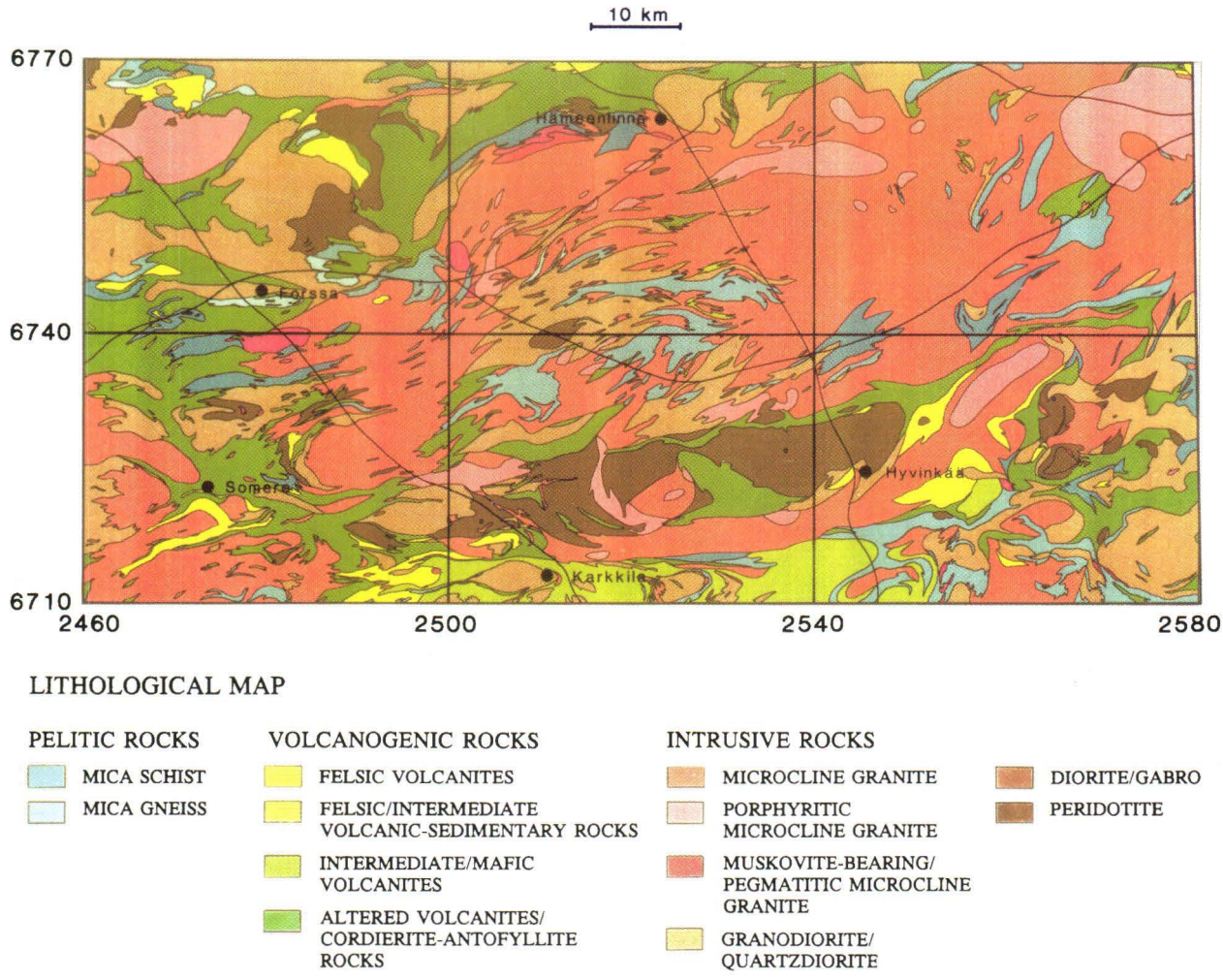

Fig. 4. Lithological map compiled from 1:100,000-scale bedrock geological maps published by the Petrological Department of the Geological Survey of Finland (Simonen 1949a, Härme 1953, Neuvonen 1954, Simonen 1955, Kaitaro 1956 and Lehijärvi 1961).

served as the basis of the structural interpretation.

The areas with gently dipping schistosities and geophysical patterns indicating large folds were interpreted as antiforms or synforms according to the direction of the dip of the schistosity and the plunge of the lineation. The main structures, antiforms, synforms, faults and shear zones, generalised as a synthesis of structural studies, are shown in Fig. 12a.

Main structural units

The Häme belt is a fault-bounded structural unit between the Valkeakoski migmatitic greywacke-granodiorite belt and the high metamorphic West Uusimaa complex (Fig. 12b). The fault zones delineating the Häme belt show up clearly as strong lineaments on the geophysical maps and are called the Pääjärvi lineament at the northern boundary and the Hirsjärvi lineament at the southern boundary. Both lineaments have been interpreted as fault/shear zones that were active during the main deformation phase, when they caused ductile deformation structures, and, still in the brittle stage of deformation, when they fractured late-orogenic granites. Today, the youngest fractures are seen as straight, long and narrow lakes in deep valleys.

The earliest structures were rotated near the Pääjärvi and Hirsjärvi shear zones, indicating sinistral horizontal movement in both fault zones. Vertical movement was, however, obviously even more important, as shown by the geology, which is very different in the two fault zones. The Häme belt is sub-divided by faults and shear zones into still smaller structural units (Fig 12b), many of which have characteristic metallogenic features.

The Hyvinkää block, with its structural continuation to the east, the Mäntsälä block and its western continuation, and the zone between the Ypäjä and Hirsjärvi faults contain the most important gabbros of the area with the exception of the Forssa gabbro. The Mäntsälä block is separated from the Hyvinkää block by late orogenic granites and younger faults. Metallogenically these are different from each other, the Mäntsälä block having mainly Cu indications

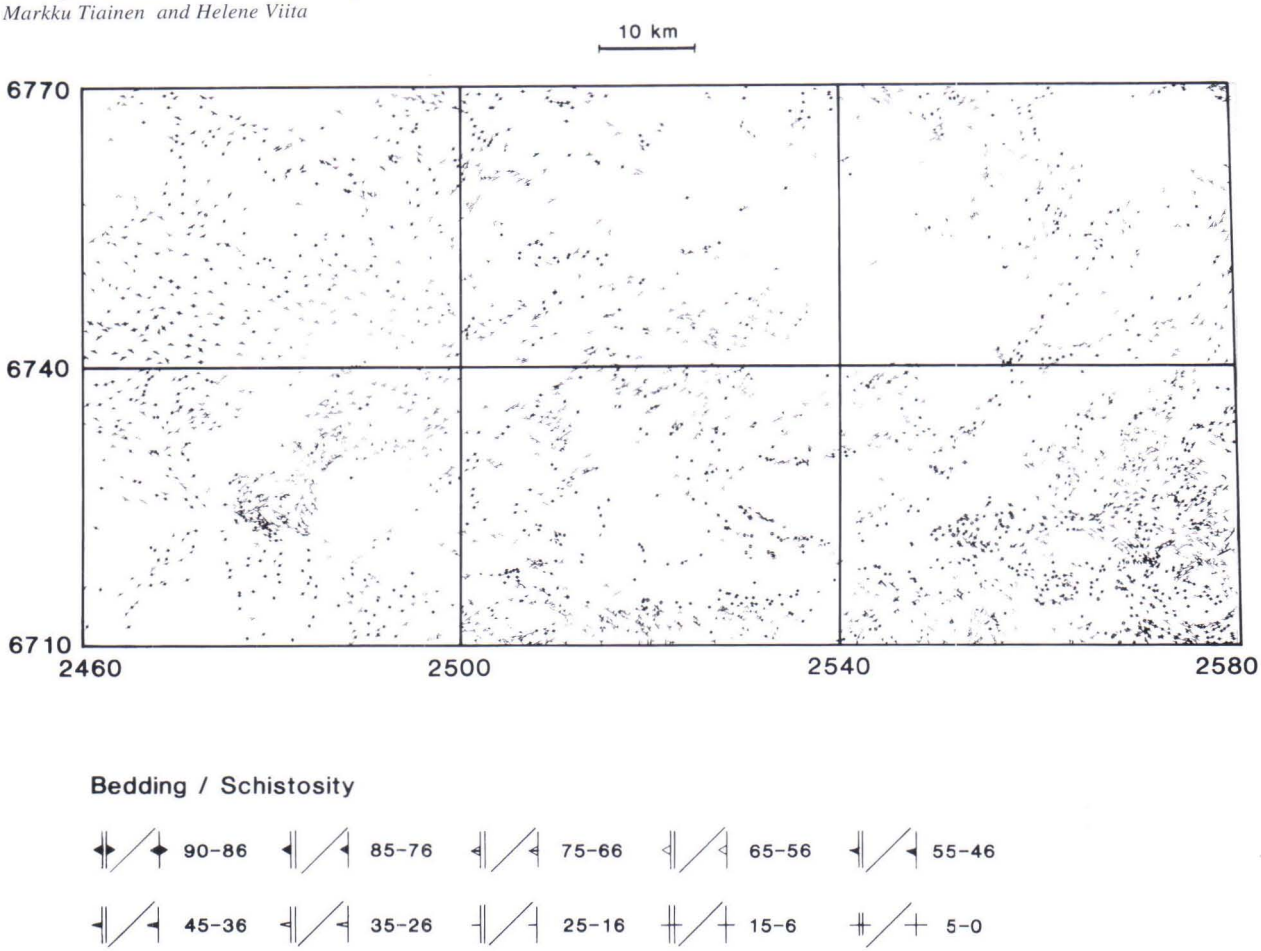

Fig. 5. Digitised structural plane observations.

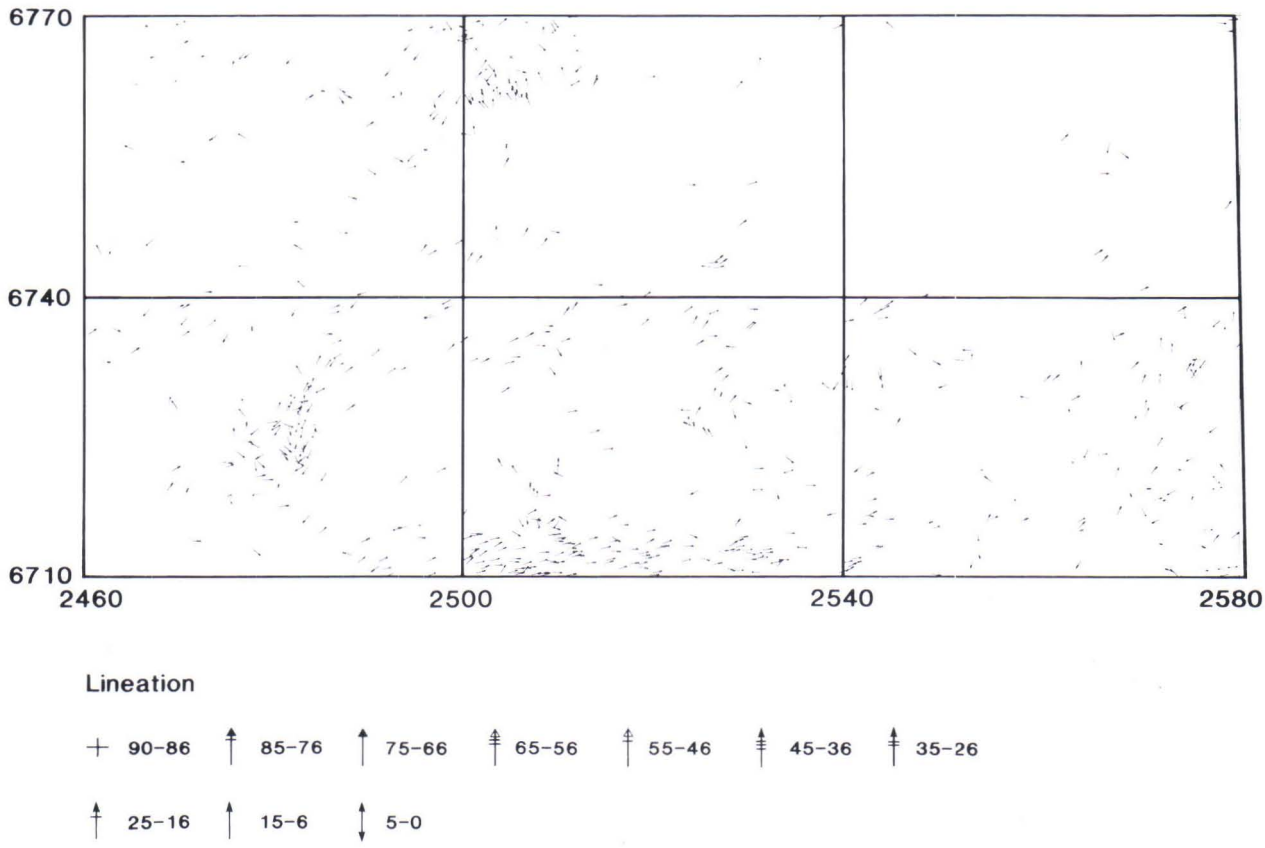

Fig. 6. Digitised structural linear observations.

and the Hyvinkää block mainly Ni indications. Several Ni indications have also been found at the southern end of the Forssa gabbro and in the sheared Forssa block.

Although it includes some Zn indications, the Humppila block can be characterised as the Au-Cu province of the Häme belt. Another important Au province is the Ypäjä fault/shear zone.

The Terttilä block is a slab separated by the Hirsjärvi fault zone from the other units of the Häme belt and the West Uusimaa complex. The block includes the Tupala Zn deposit and is structurally related to the Orijärvi-Aijala Zn province.

Structural data indicate that, the high metamorphic migmatised Tervakoski structure in the middle of late-orogenic granites is a large antiform. The

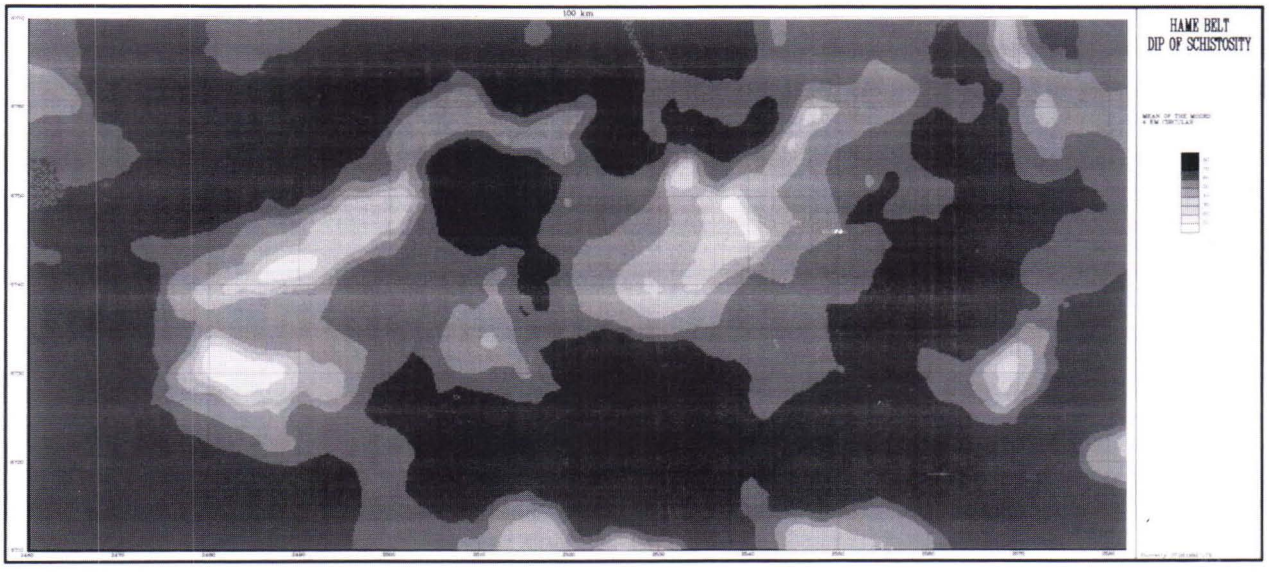

Fig. 7. Structural patterns indicated by the dip values of the schistosities.

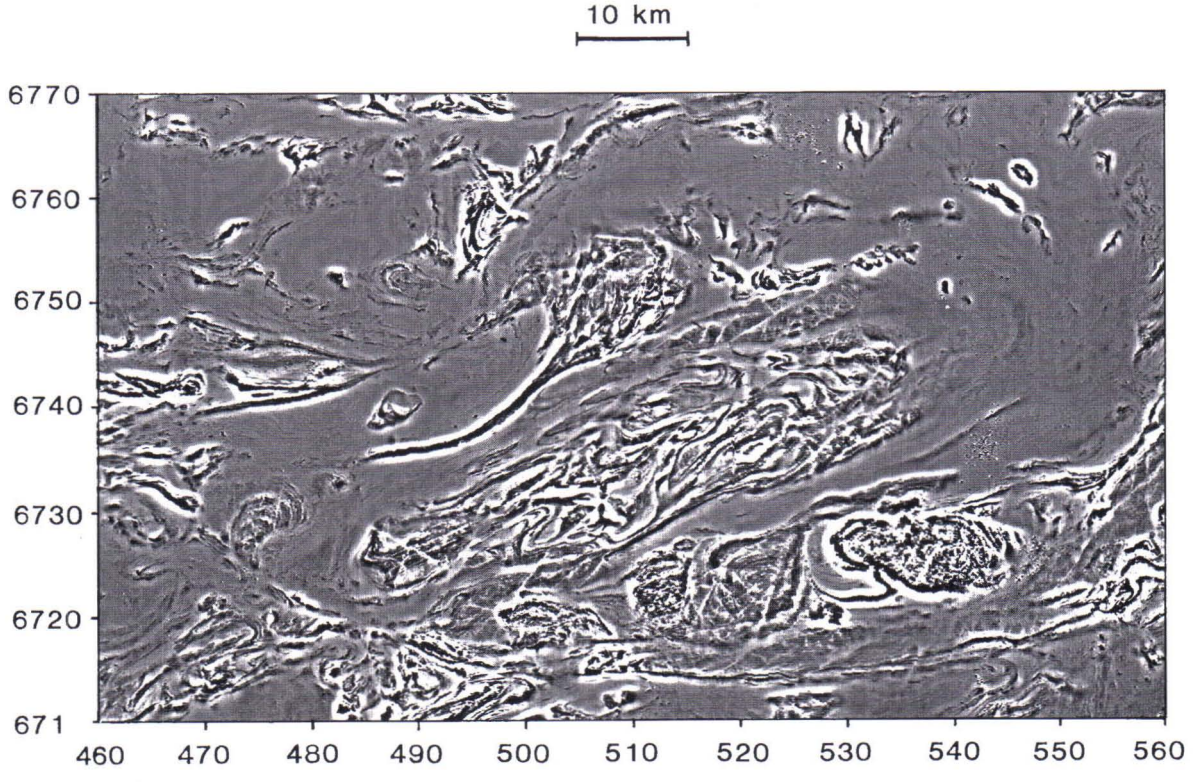

Fig. 8. Edge detection from the low altitude magnetic data by a 31 x 31 box filter.

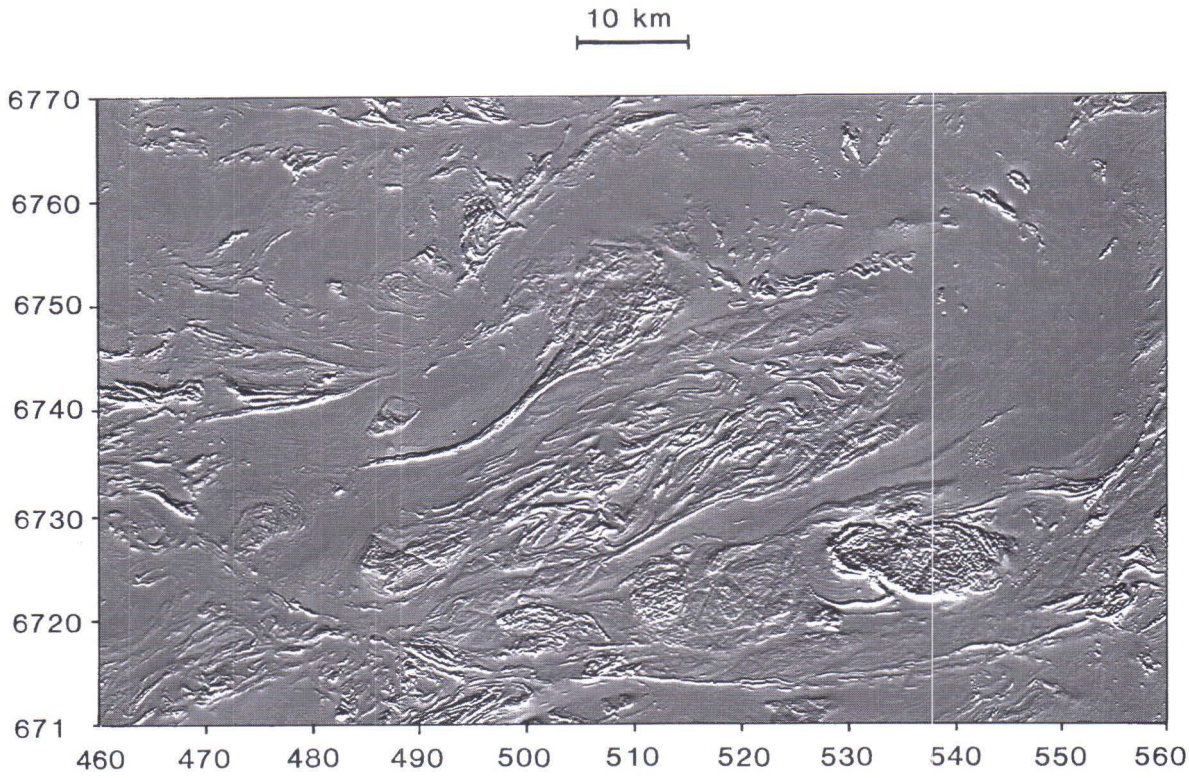

Fig. 9. Relief surface obtained by a directional gradient and a 3 x 3 low-pass filter. Low-altitude magnetic data.

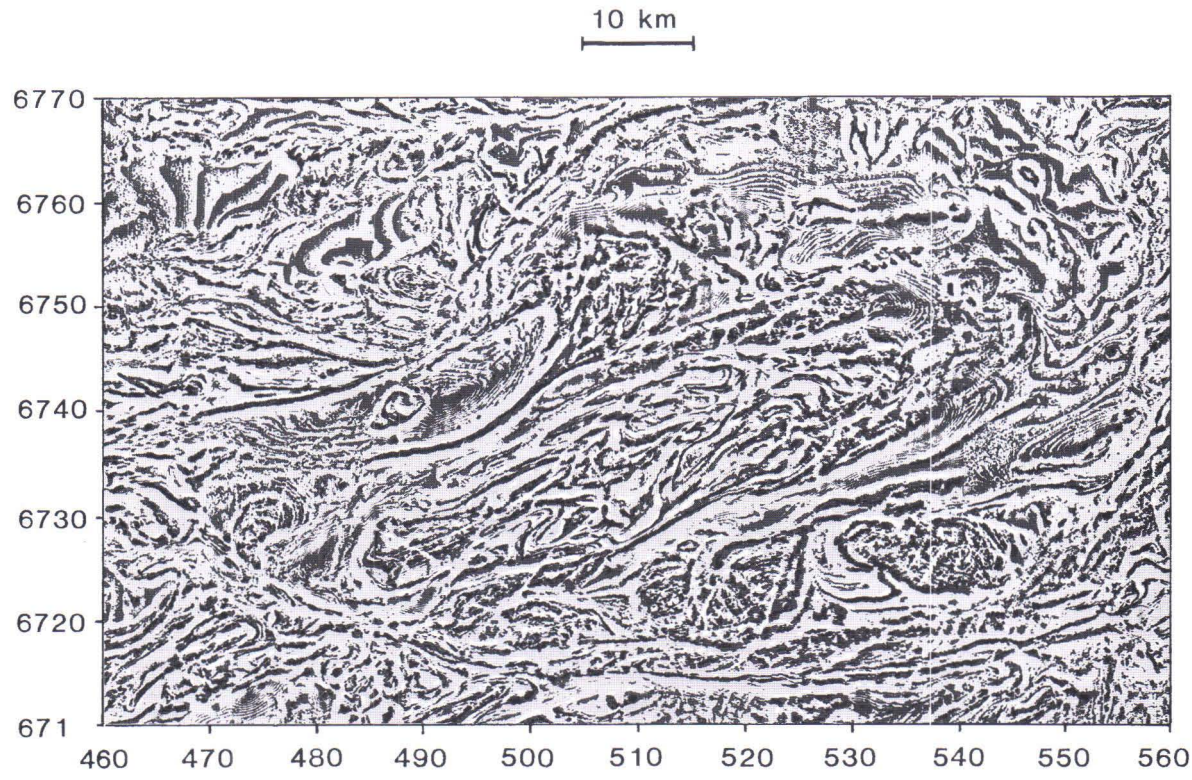

Fig. 10. Statistical difference operator applied to the low altitude magnetic data with the neighbourhood size of 31 x 31 and variance 2.

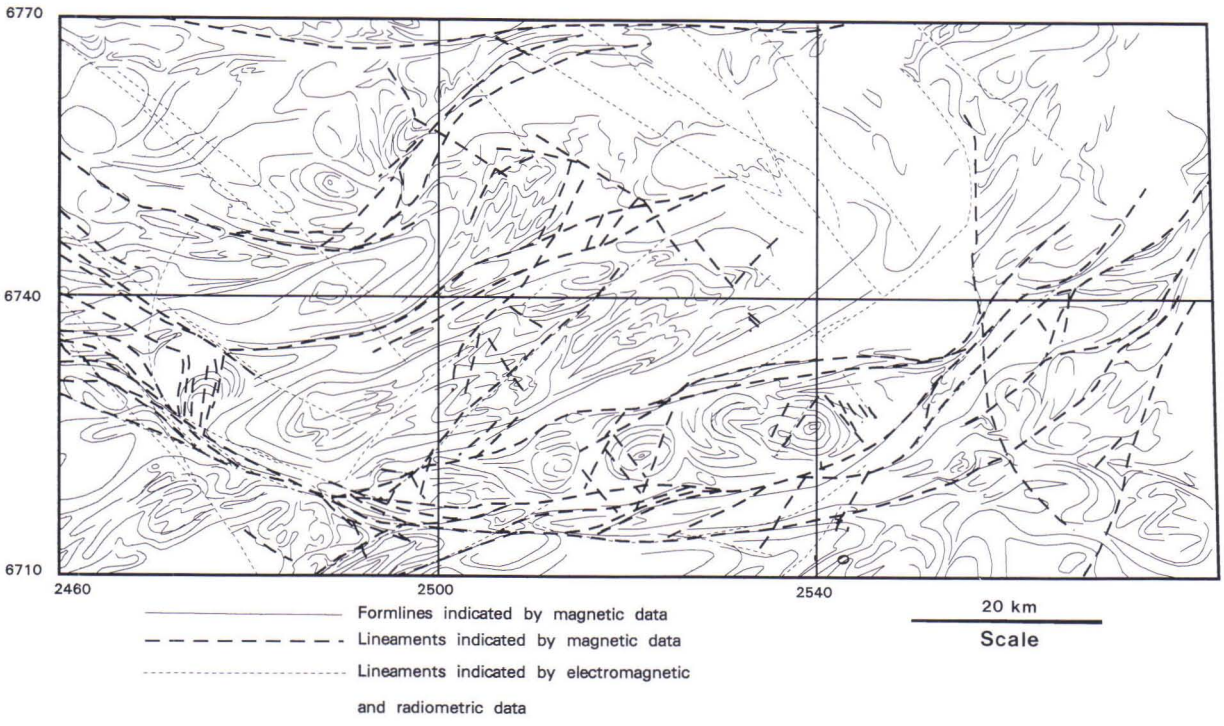

Fig. 11. Structural form lines and lineaments indicated by aerogeophysical data.

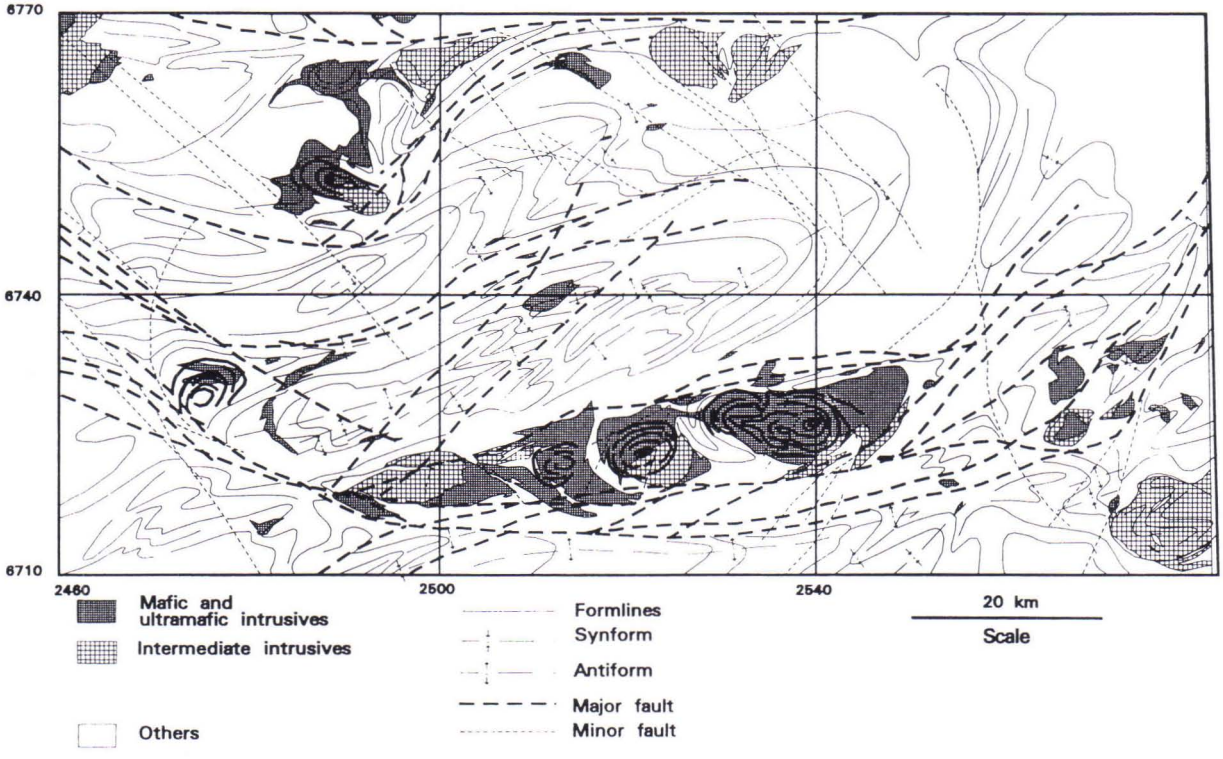

Fig. 12. a) Main structures interpreted by intergration of form lines and lineaments in fig. 11 with structural and lithological field observations in figs. 4–7.

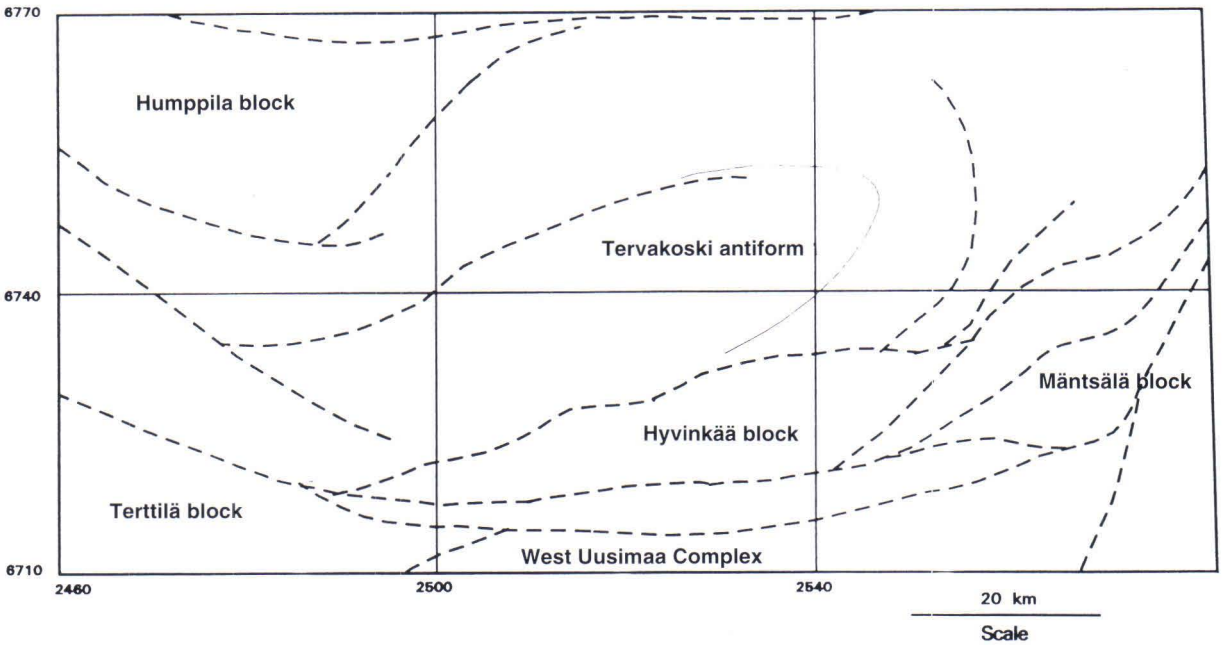

Fig. 12.b) Main structural units of the Häme belt. Thick dashed lines show the boundaries of the units and the thin continuous line indicates the form of the Tervakoski antiform.

migmatised intensely folded garnet-cordierite and pyroxene bearing gneisses in the centre of the antiform probably represent the deepest erosion level in the Häme belt.

Geophysical data

The geophysical data used in image processing are from systematic airborne low-altitude (30–50 m) measurements conducted by the Geophysical Department of the Geological Survey of Finland since 1972 (Oksama 1986, Poikonen 1991). Several small parts of the Häme belt area were measured during 1978–1988. The aerogeophysical surveys comprised the digital recording of magnetic, electromagnetic and gamma-ray data onboard aircraft using proton magnetometers (Korhonen 1985), coaxial and coplanar rigid coil slingram systems (Peltoniemi 1982, 1986), and multi-channel gamma-ray spectrometers (Vironmäki & Multala 1981).

The study area covered six 1:100 000-scale map sheets. Geophysical data were available from map sheets 2113, 2131, 2133, 2024, 2042 and the first half of 2044 (Fig. 13) for the following variables:

1. magnetic total intensity
2. electromagnetic in-phase component
3. electromagnetic out-of-phase component
4. radiometric potassium
5. radiometric thorium
6. radiometric uranium
7. radiometric total

Before the data can be analysed in appropriate image processing format, several preprocessing operations e.g. corrections, interpolations and conversions, have to be done. The results of measurements are stored by the Geophysical Department on 1:20 000-scale sheets as shown in Fig. 14a.

All the sheets in the study area were surveyed along N-S flight lines. The line spacings and sampling intervals were about 200 m x 50 m for the electromagnetic and radiometric components, but varied for the magnetic components (Table 2.).

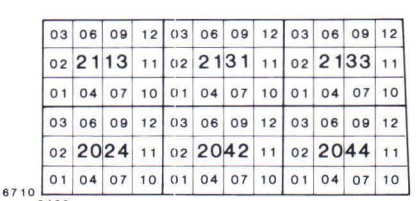

Fig. 13. 1:100,000- and 1:20,000-scale map sheets of the study area.

As the sheets had to be gridded on the same scale, a gridding of 50 m x 50 m was chosen. Two sheets, 2131 and 2133 were already available on a 50 m x 50 m grid. Most of the programs used in correcting, interpolatig and compiling the data were developed by the Mineral Resource Assessment unit in the Department of Economic Geology.

The data from the Geophysical Department were in ASCII array format. Lines overlapping the sheets were deleted and the data were checked for abnormal values. These were replaced by uniform dummy values characteristic of each component. The dummy values were 0 for the magnetic data -32000 for the electromagnetic data and -10 for the radiometric data. The dummy values were then eliminated by interpolation based on the weighted mean value of the closest neighbours. This was done mainly to delete disturbing small "holes" from the picture.

Owing to the different coil configurations used in the electromagnetic survey in 1972, 1973–79 and after 1980, the electromagnetic data on the sheets 2113 01–03 and 2024 03 had opposite signs, which were corrected.

All the data matrices shown in Fig. 14a were interpolated separately to form a 50 m x 50 m grid. The interpolation was done linearly between lines. When the sampling interval was 12.5 m or 25 m, as was the case with some magnetic components, the extra points were deleted. To facilitate comparison of the data with the geological maps the 50 m x 50 m gridded areas were warped to form 1:100 000-scale map sheets (Fig. 14b). The matrices then had a size of 801 pixels per line x 601 lines. All these sheets were united to form the final big matrix covering the whole study area and having a size of 2441 pixels per line x 1201 lines (Fig. 14c).

Data on areas measured at different times and partly with different equipment tended to show level differences between the areas. This was particularly true of the electromagnetic and radiometric data. The differences were corrected with linear scaling by equilizing the mean and standard deviation values calculated from a narrow zone on both sides of the sheets, and by taking one of them as the base level. It should be remembered however, that, owing to differences in the flight periods and equipment of the low-altitude surveys, it is impossible to get identical levels, and minor differences will always have to be expected.

The data varied within the following ranges:

Magnetic total intensity (48790–57201 nT), electromagnetic in-phase component (-4761–19354 ppm), electromagnetic out-of-phase component (-2709–11270 ppm), radiometric potassium (-5.820–8.000% eK), radiometric thorium (-3.930–62.040 ppm eTh), radiometric uranium (-8.690–74.680 ppm eU) and radiometric total (-4.030–37.300 Ur)

The gridded matrices were converted from ASCII format to 8-bit binary mode within the range of the absolute minimum and maximum and were scaled between 0 and 255. This presentation was chosen to save disc space and because many of the image-processing programs require 8-bit data. Some smaller areas were, however, converted into a 16-bit mode.

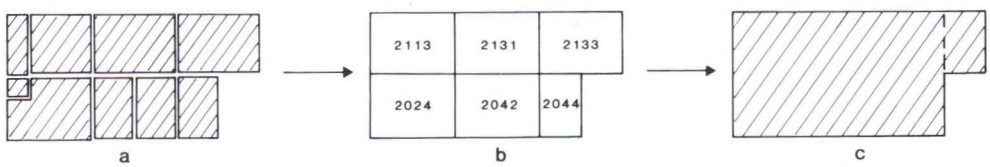

Fig. 14. Stages in compiling the low altitude geophysical data. a) Pieces compiled from 1:20,000-scale sheets mostly by the Geophysics Department b) the matrices compiled as 1:100,000-scale sheets c) the matrix covering the study area.

Table 2. Line spacings and sampling intervals for the magnetic data.

Mapsheets	Linespacing	Sampling interval
2113 01-03	100m	25m
2113 04-12	50m	12,5m
2024 03	200m	25m
2024 01-02, 04-12	50m	12,5m
2042 01-12	100m	25m
2044 01-06	50m	12,5m

Image processing

In Finland image processing of low-altitude geophysical data is a useful tool for geologists working in exploration and mineral assessment (Aarnisalo 1984, 1990, Aarnisalo et al. 1982, Arkimaa 1982, Ketola 1989, Gaál 1988, Kuosmanen 1988), as it provides them with quick overall information about large areas and helps in the outlining of interesting zones and structures for ground surveys.

The image processing was done using DISIMP (Device-Independent Software for Image Processing) (CSIRO 1990). It operates on an Apollo 3500 workstation in the UNIX environment and also on a VAX 6310 computer in the VMS environment; the files are interchangable through an Ethernet connection. With the exception of byte swapping between UNIX and VMS the data format for DISIMP is identical in both systems.

The DISIMP package contains more than 150 programs covering most of the standard image-processing routines such as contrast manipulation, intensity and geometric transformations, spatial filtering operations, statistical analyses, classifications and 3-D display, and the Apollo workstation enables interactive viewing and image modification. Composite pictures accompanied by contrast stretching provide a quick and easy way to see spatial correspondence and to improve visual discriminability and interpretation. Images were viewed both in colour and in black-and-white. The human eye can distinguish hundreds of thousands of different colour shades but only 20–30 greytones (Drury 1987). Colour images are therefore, best suited for detecting intensity changes, and black-and-white combinations for textural interpretation.

Four types of hardcopy were generated:

1. Slides photographed from the Apollo screen direct;
2. Plots by Versatec electrostatic colourplotter transferring files to the Vax system;
3. Montage slideplots operating in a PC environment; and
4. Film plots from files transferred by cartridges or magnetic tape to a filmplotter of the National Board of Survey of Finland.

The main geophysical components were first enhanced by contrast stretching to distinguish the main features in the area (Figs 15–20). Colour composite pictures were made from the magnetic and electromagnetic components (Fig. 21) and the radiometric components (Fig. 22).

The magnetic data (Fig. 15) refer mainly to the distribution of magnetite and pyrrhotite in rocks within different environments. The main geological units and structures such as faults, shear zones and

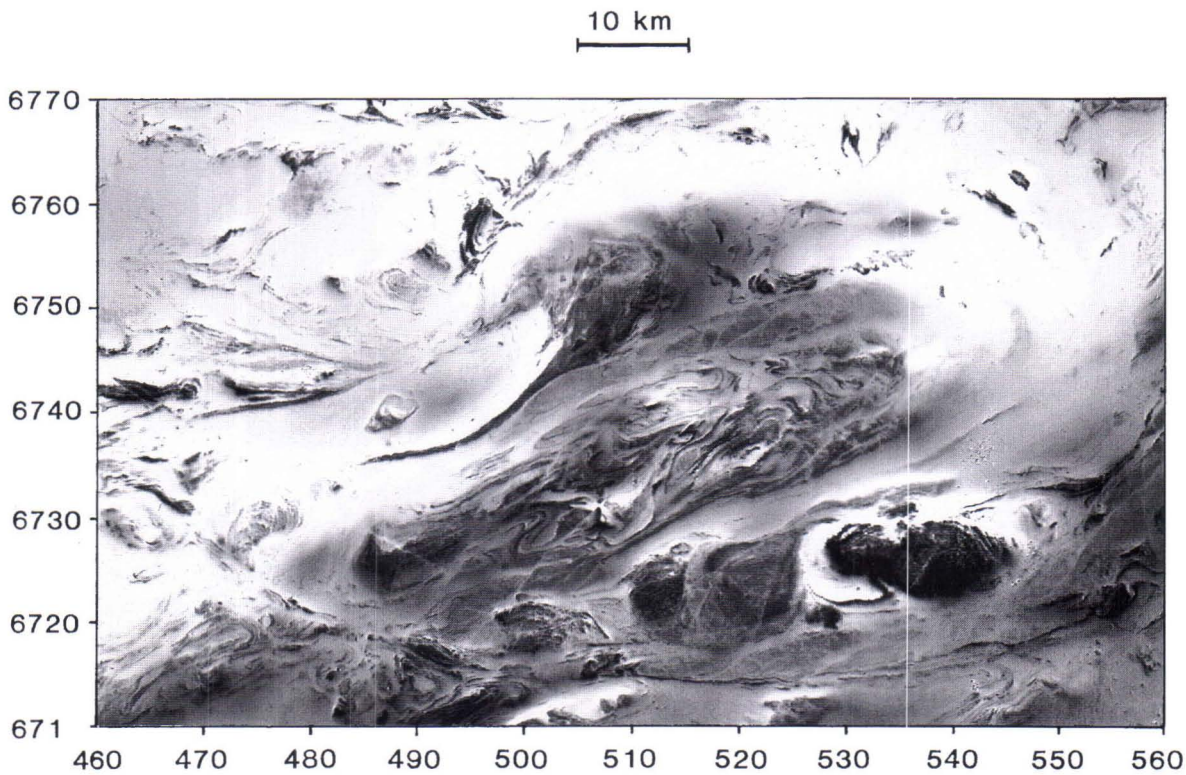

Fig. 15. Magnetic low-altitude total intensity. Positive values are dark.

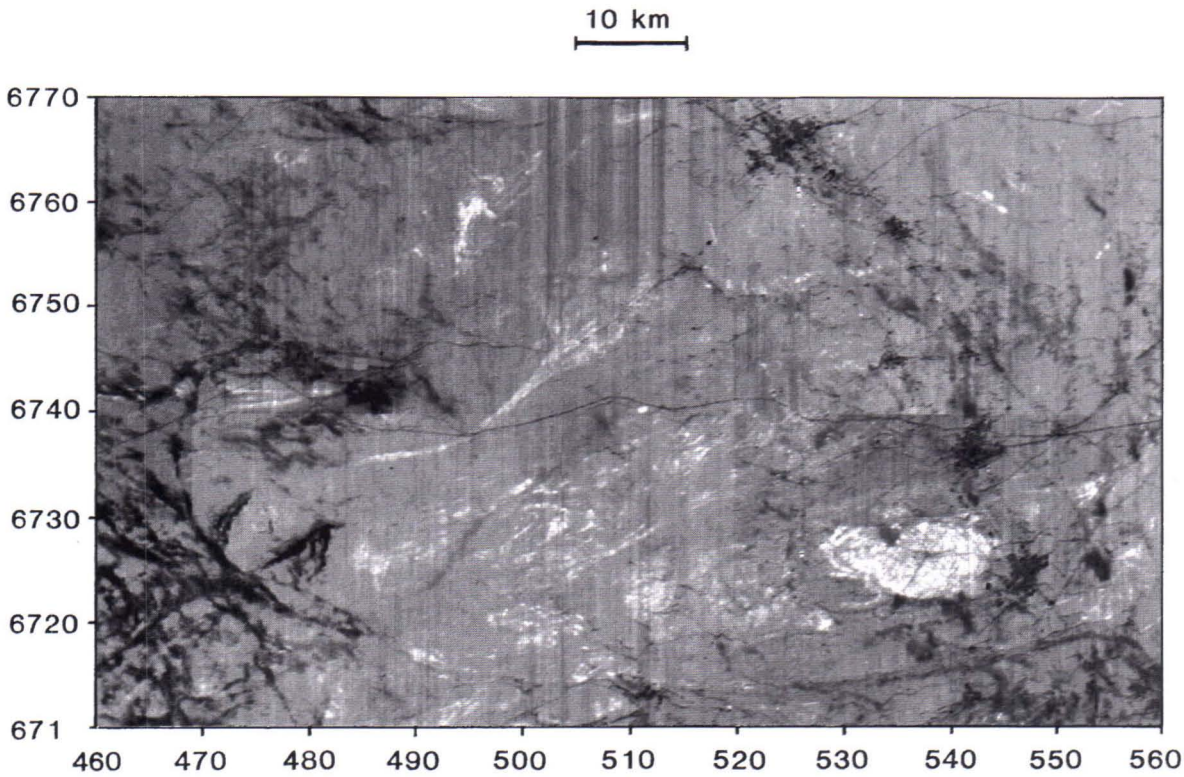

Fig. 16. Electromagnetic in-phase component. Positive values are dark.

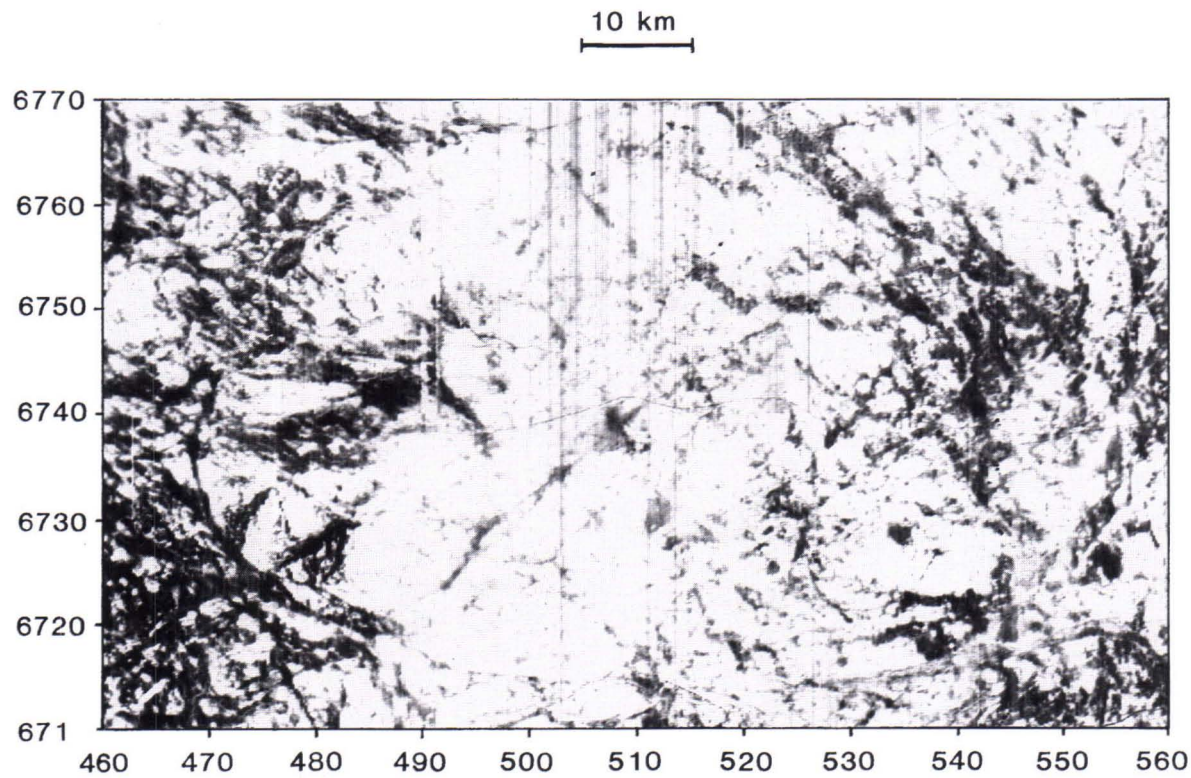

Fig. 17. Electromagnetic out-of-phase component. Positive values are dark.

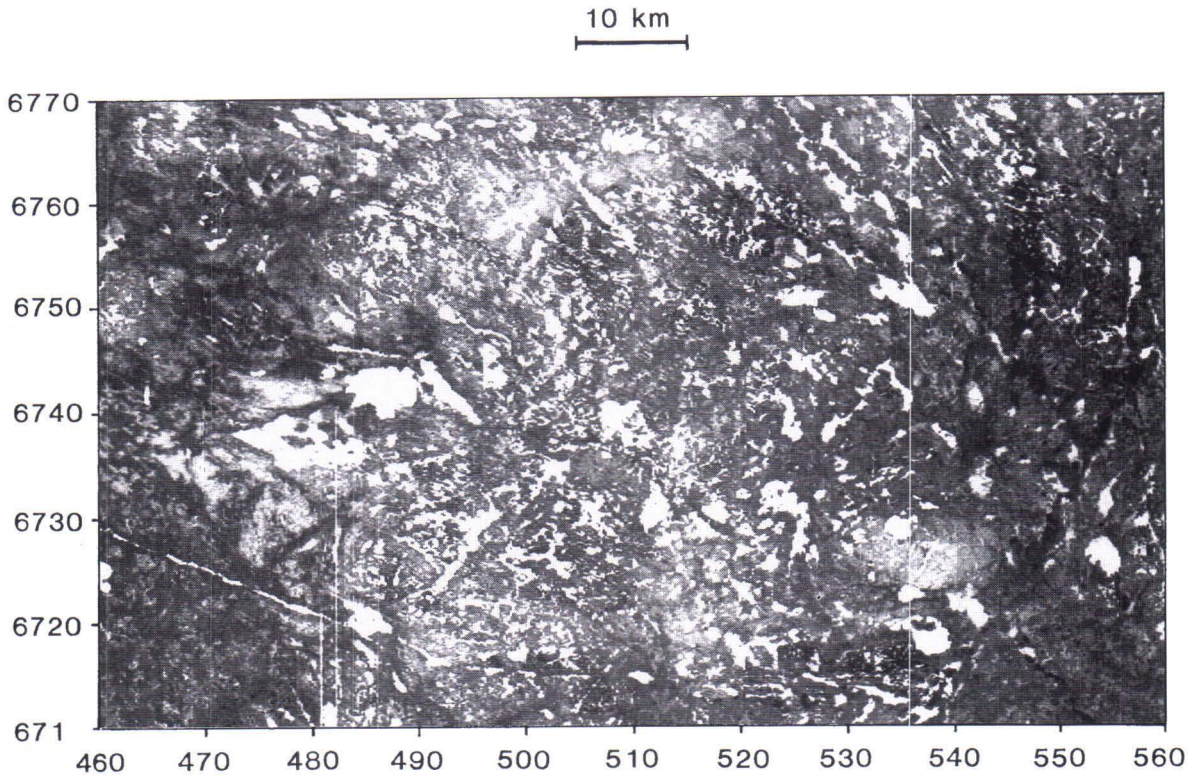

Fig. 18. Radiometric potassium. Positive values are dark.

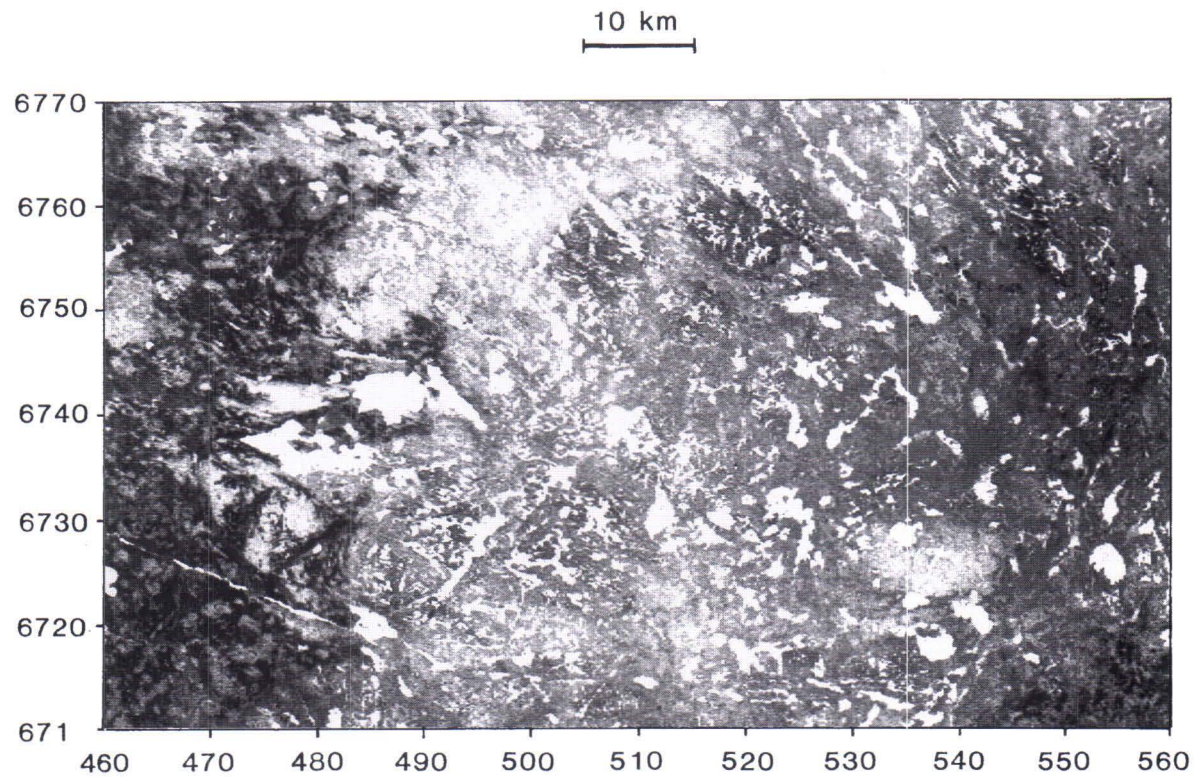

Fig. 19. Radiometric thorium. Positive values are dark.

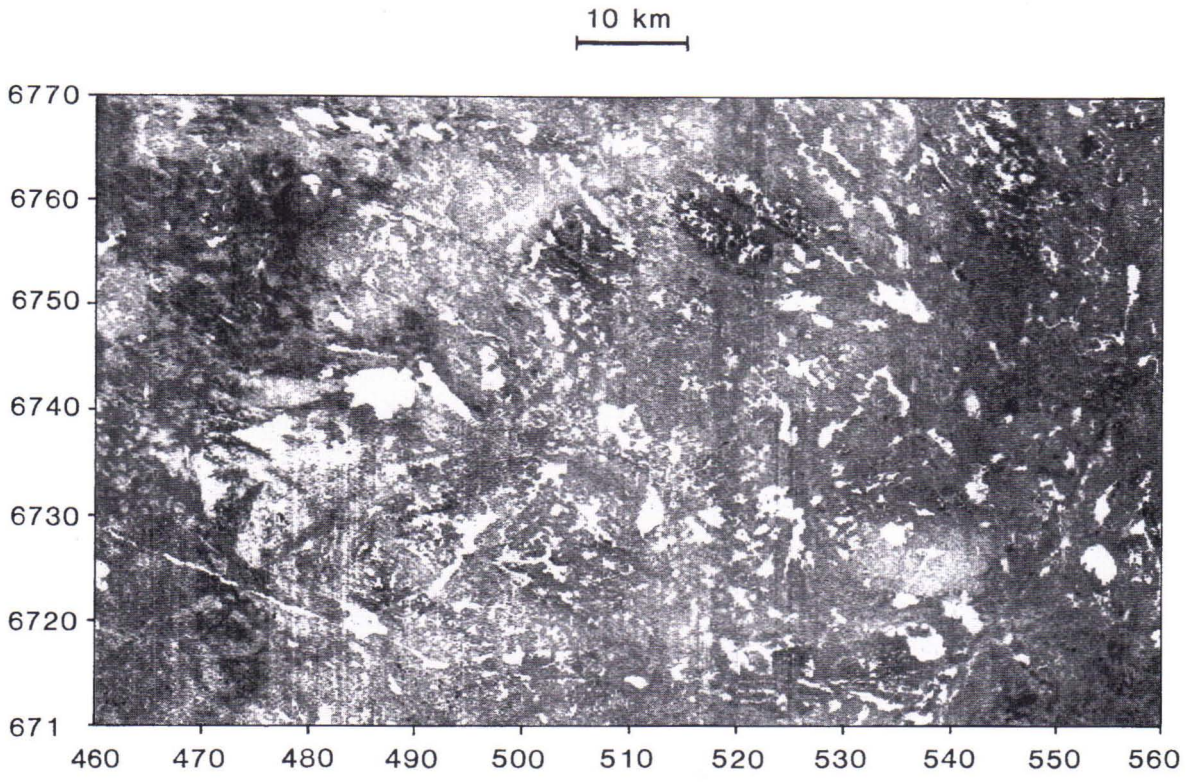

Fig. 20. Radiometric uranium. Positive values are dark.

fold patterns are visible, but the magnetic map should not be directly compared with the lithological map. Rocks with similar chemical compositions will have different magnetic properties if their cooling histories differ. Metamorphism and alteration may also change the magnetic nature, depending on factors such as temperature and oxidation (Grant 1985a,b).

The Hyvinkää gabbro-volcanite complex shows up distinctly in the southeastern part of the Häme belt (Fig. 15). From petrophysical studies the complex has been interpreted as consisting of two 2–3-km-thick sheets with two deeper feeder channels extending to a depth of 12 km and possibly continuing northwards on a still deeper level (Puranen 1968, 1971). On the other hand, the magnetic low altitude-data (Fig. 15) show a strong secondary minimum on the north side of the main gabbro intrusion. Together with structural data, this implies that the northern contact dips to the south. It also seems to have responded to deformation by rotation.

In the south of the study area, a large east-west lineament visible in magnetic, electromagnetic and radiometric components forms a clear boundary and transition between the microcline-granite and pyroxene-gneiss area to the south (Figs 15–21). The structure is interpreted as dipping 45–65 to the north under the microcline granite (Puranen 1971). Known as the Hirsijärvi lineament, the zone is the structural boundary between the Häme belt and the West Uusimaa complex (Fig. 12b).

Another area clearly visible on the magnetic map (Fig. 15) is the intensely deformed high-grade metamorphic migmatite area (the Tervakoski antiform) northwest of the gabbro-volcanite complex. In the north of the Häme belt, narrow highly magnetised horizons running east-west and northeast-southwest follow the volcanic sequences. Their correlation with cordierite-bearing gneisses enhances their value in delineating ore-potential zones.

Generally, the electromagnetic anomalies in the Häme belt are high over clay and certain water areas (Figs 16, 17). They are mainly due to young fault structures filled with clay and water that appear as long narrow lake systems modified by glacial movements. The in-phase component also emphasises cultural features such as cities and power lines. The Hyvinkää gabbro produces a clear minimum in the electromagnetic components.

Both electromagnetic components reveal structures in areas without a clear magnetic pattern, for example, in the circular fault zone in the western part of the Häme belt (Fig. 21). The highly magnetised areas coincide with the conducting areas in only a few places, which appear dark in the composite picture.

The radiometric components covering the Häme

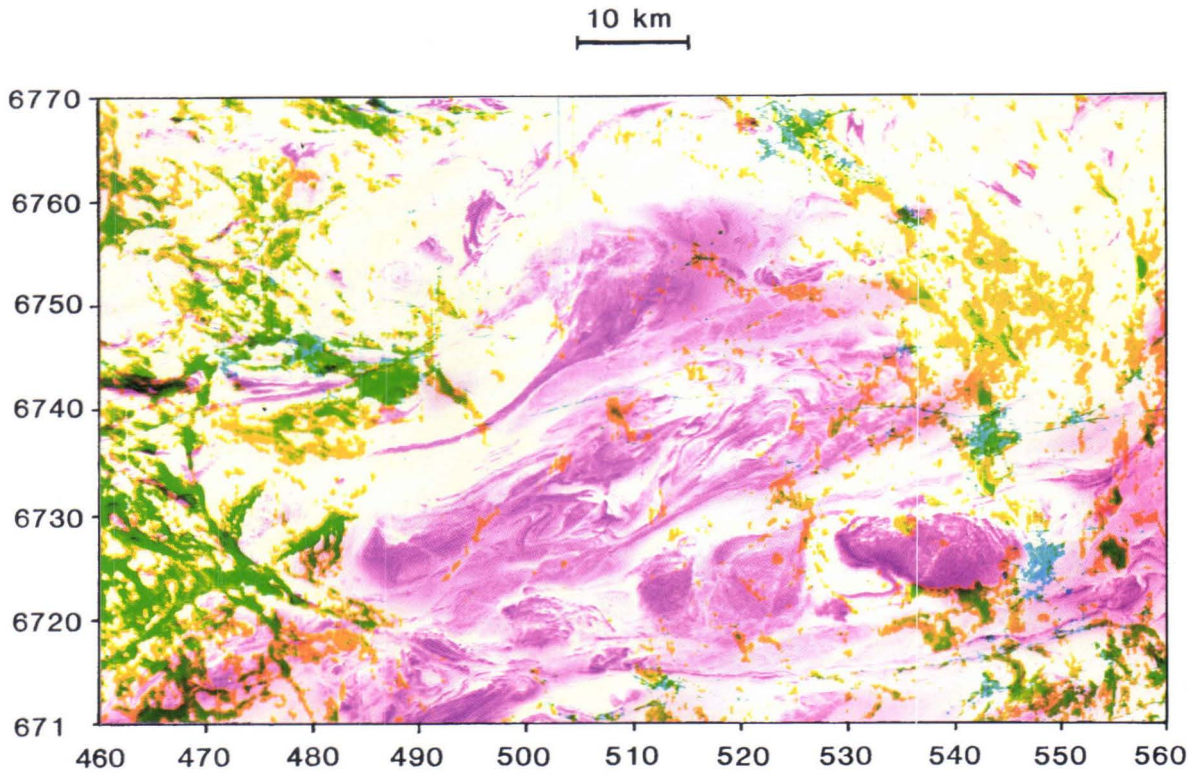

Fig. 21. Colour composite of magnetic and the electromagnetic components. The magnetic component is coloured pink, the in- phase component blue and the out-of-phase component yellow.

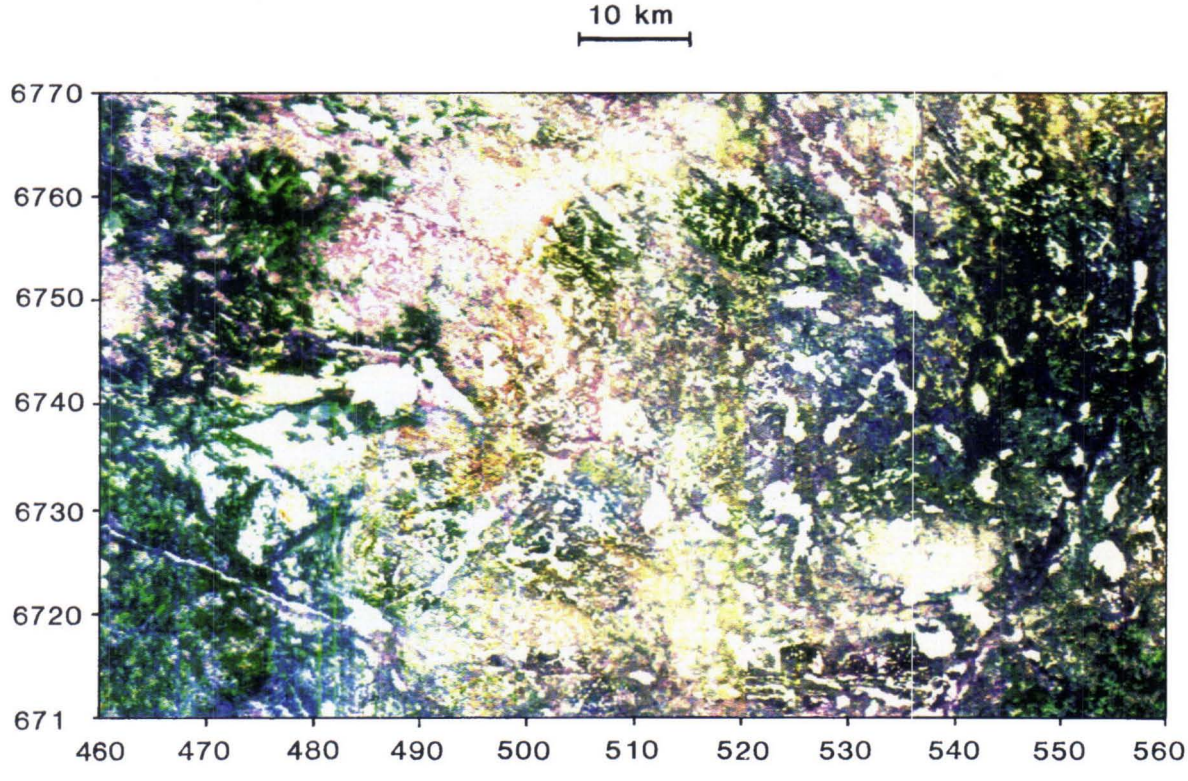

Fig. 22. Colour composite of radiometric components. The colour is dark where the components overlap.

belt (Figs 18–20) seem mostly to reflect the overburden. Radiation levels are elevated in clay areas. The intensity of the thorium component, in particular, is very high and directly related to the clay areas in the western half of the study area (Fig. 19). Use of radiometric components in ore prospecting in these areas is thus questionable. The clays in the western part are generally more than 20 m thick, but thicknesses of up to 77 m are not unknown (Haavisto et al. 1990); thus any radiation from the bedrock is prevented. The thorium content was used as a measure of the clay content in soil by Schwarzer & Adams (1973). In the upper middle part of the study area there are circular areas with high radiation of all the radiometric components (Fig. 22). These anomalies are due to moraine ridges and hummocks resting on late-orogenic K-rich granites. The hummocks range from 1 to 20 m in height (Virkkala et al. 1969).

Owing to the heterogeneity of the radiometric components in the study area, most of the image-processing operations are based on the magnetic and electromagnetic components.

Principal component analysis

Principal component analysis (PCA) is a standard statistical method for decorrelating multivariate data (Siegal & Gillespie 1980, Drury 1987). The multidimensional data are arranged into a new orthogonal coordinate system of independent axes, resulting in a higher contrast between new variables. Some features invisible in a composite image of the original variables may be highlighted in the PC image. The relation between the old and new variables is described by the variance and covariance matrix, and the loadings for each variable onto the principal components are described by the correlation coefficient of the PC axes and the original coordinates.

The three-channel magnetic, electromagnetic in-phase and out-of-phase image was submitted to PCA transform. The variance-covariance matrix was used for calculating the eigenvectors. Table 3 lists the statistics of the principal component transform, and Figures 23a–23c show the principal components. Figure 23d shows the composite picture of the three principal components.

As seen from Table 3, the first principal component (PC1) (Fig. 23a) has a positive loading on all variables and is responsible for the highest variance. As the second principal component (PC2) (Fig. 23b) has a strong negative loading representing the magnetic data, the relationships between the variables can be seen more clearly. The third principal component (PC3) (Fig. 23c) accounts for the smallest variance.

Classification

In image processing, classification is mainly used for interpreting satellite imagery based on spectral differences in surface materials (Drury 1987). It can be geologically rewarding in areas with bare lands (Antón-Pacheo & Gumiel 1991, Wester 1992).

Classification of geophysical data is difficult, because a class with specific intensity values may represent different lithologies and different depths, depending on the location in the study area.

For the classification, the intensity values are divided into classes. The clustering process is supervised with a given training area or is left unsupervised if the number of classes is either user-supplied or chosen by the system. The supervised classification requires prior knowledge of the classes.

The DISIMP image processing system offers a variety of classification techniques: 1) The parallepiped classifier arranges the mean values into

Table 3. Principal component analysis statistics.

COVARIANCE MATRIX

	1	2	3
1	457.13		
2	236.18	242.11	
3	253.98	286.84	422.24

EIGEN VECTORS

	1	2	3
1	0.6143	-0.7714	0.1659
2	0.4895	0.2077	0.8469
3	0.6189	0.6015	0.5052

CORRELATION OF CHANNELS WITH AXES

AXIS		1	2	3
CHANNEL	1	0.86	-0.50	0.04
	2	0.94	0.19	-0.27
	3	0.90	0.41	0.12

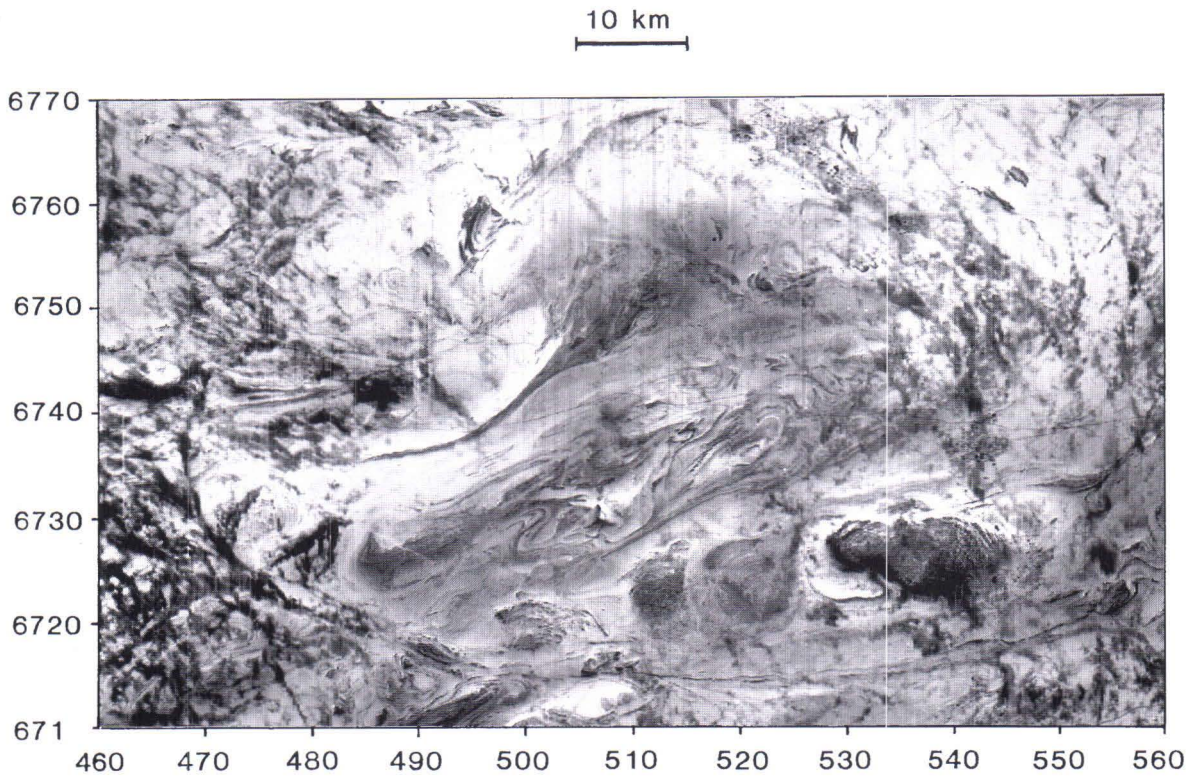

Fig. 23. Principal components calculated from the magnetic and electromagnetic data:
a) PC1.

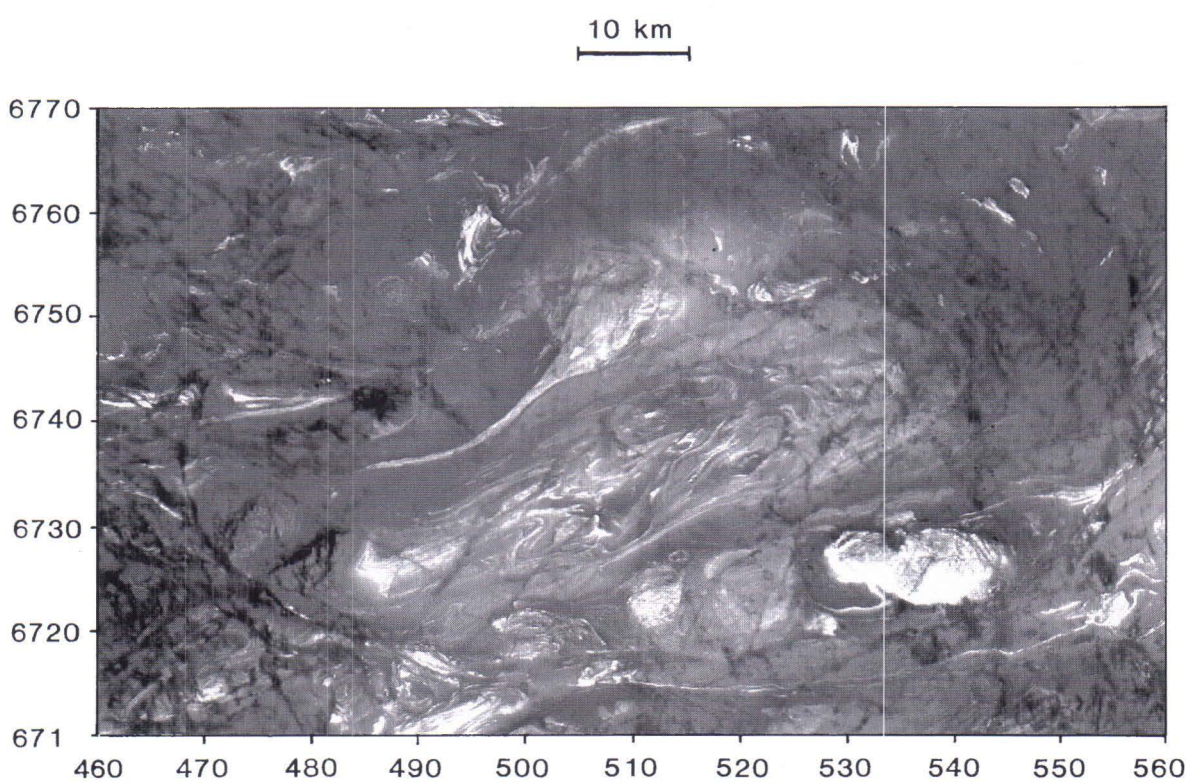

Fig. 23b) PC2.

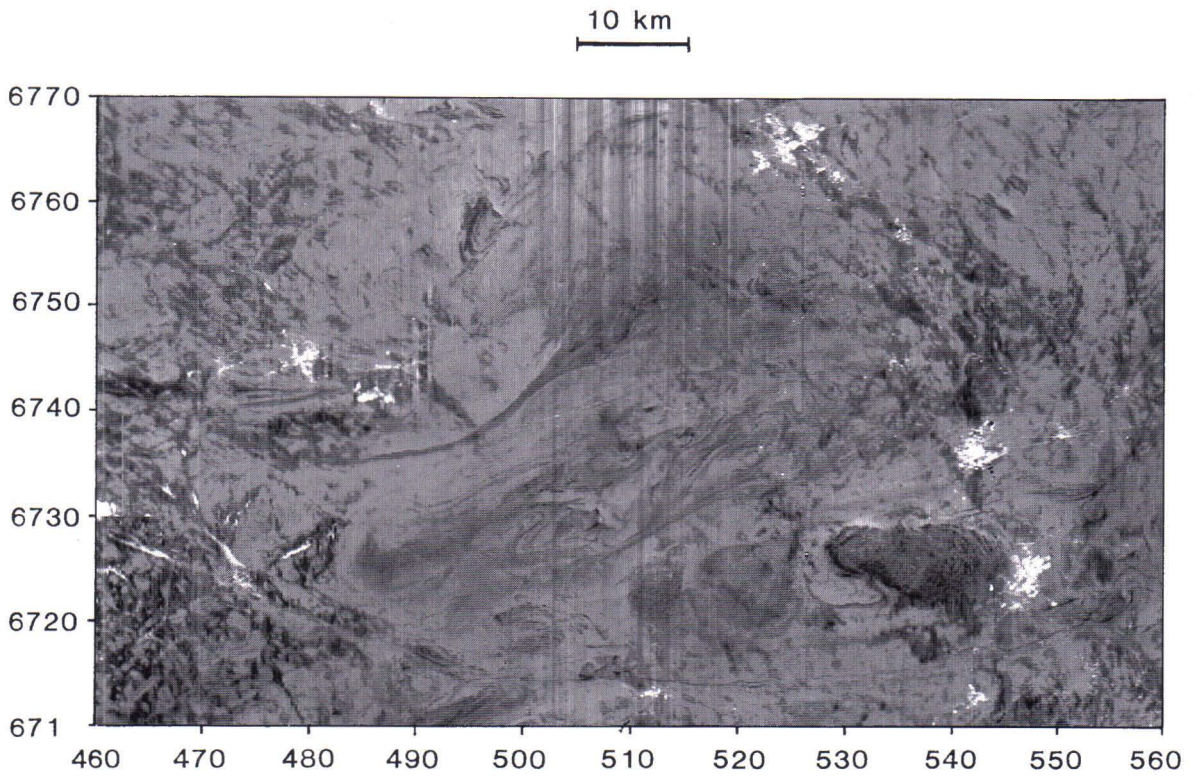

Fig. 23c) PC3.

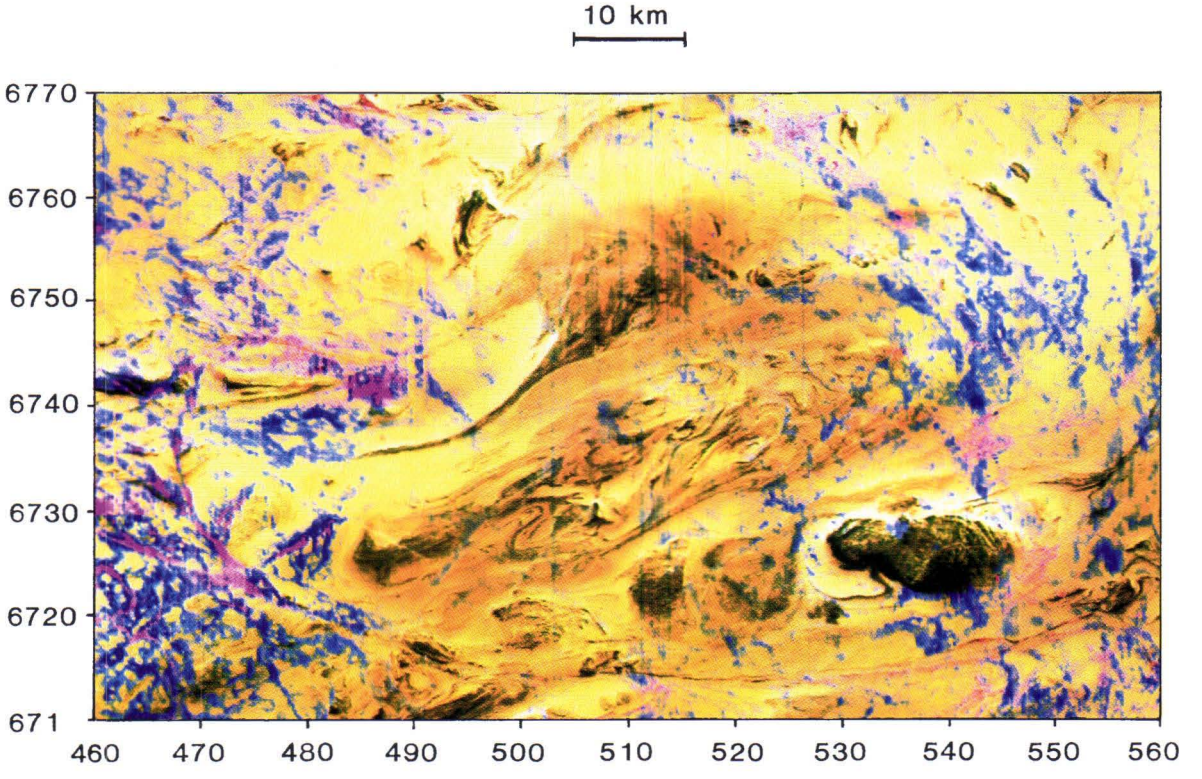

Fig. 23d) composite picture of principal components.

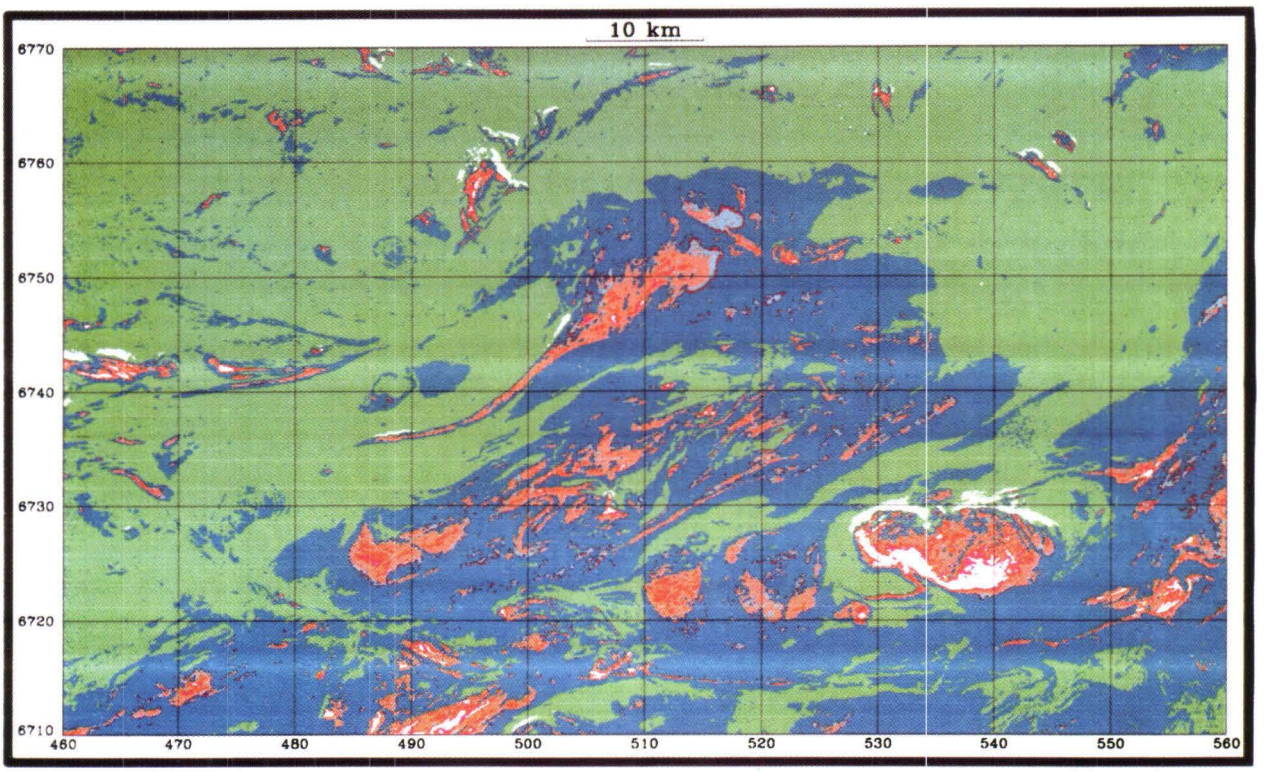

Fig. 24. Classification of the magnetic low-altitude data using a minimum-distance classifier. Training areas are represented by various altered rocks in the study area. Interesting classes are the narrow orange zones in the north part of the area.

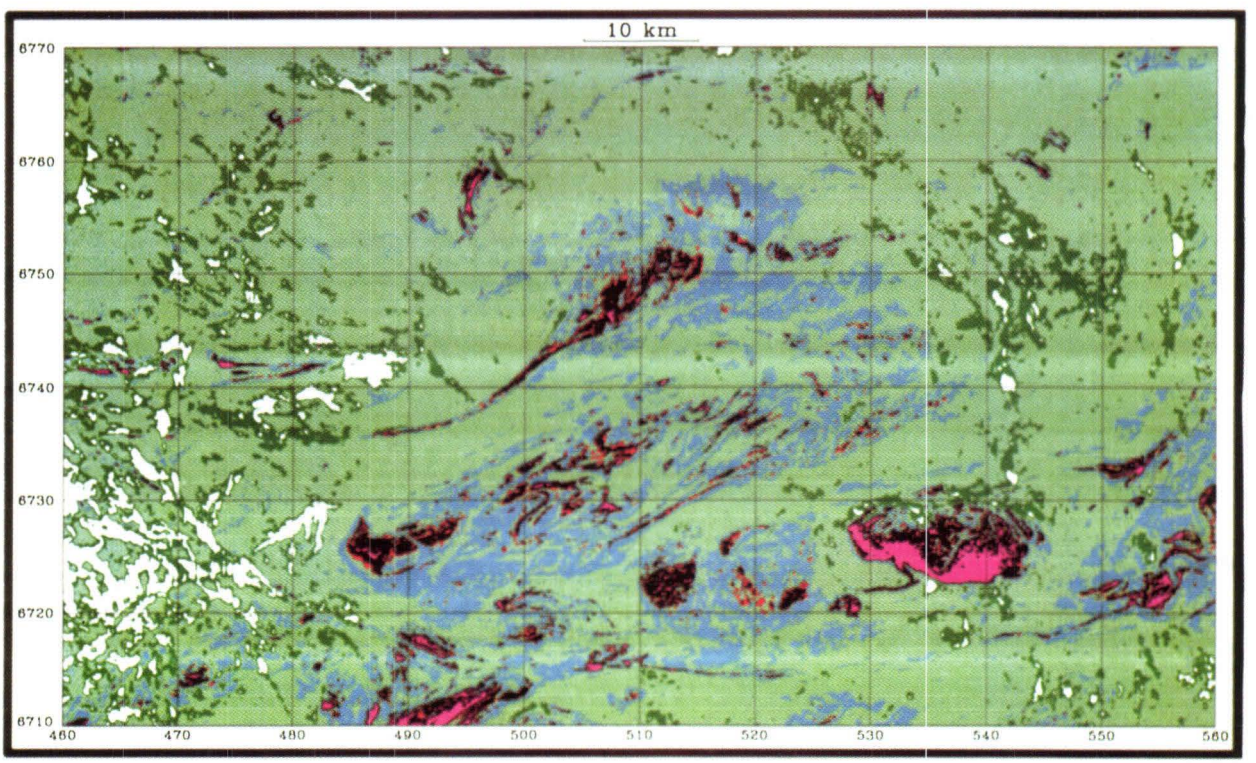

Fig. 25. Classification of the second principal component (from magnetic, electromagnetic in-phase and electromagnetic out-of- phase) using a maximum likelihood classifier. Training areas are the same as in fig. 24. The picture emphasizes the grouping of the electromagnetic components (dark green and white).

classes within a range of values; 2) The minimum-distance classifier, sets the pixel in the class with the closest mean and operates on the basis of Euclidean distance; 3) The maximum-likelihood classifier, places each pixel in the most appropriate class. The methods applied in the study area were the minimum-distance and maximum-likelihood techniques, even though classifiers of this type require the properties of the variables being analysed to be normally distributed.

Numerous training areas, including the main ore deposit model areas, lithological units, areas with known altered rocks etc. were examined and classified. The training areas were first clustered without supervision. The resulting classes were then used to classify the whole study area with the minimum-distance and the maximum-likelihood classifiers. These two classifiers gave similar results. The numbers of variables used varied from one to three: 1) the magnetic alone; 2) the principal components calculated from the magnetic, electromagnetic in-phase and out-of-phase data; and 3) a composite of 1) and 2).

The classification with training areas of supposed lithological units was not successful, because the geophysical fingerprints of different lithologies were not sufficiently homogeneous.

Training areas of altered rocks were used in most of the classification experiments (Figs 24 and 25). Altered rocks and high magnetic intensities coincide in the north of the Häme belt as narrow stripes within volcanic zones.

When the electromagnetic components are included as variables, they form distinct classes coloured white and dark green (Fig. 25).

Geochemical data

The element contents of the aqua regia-leached fine fraction of till reflect the cation composition and the abundance of micas and clay minerals in the sample (Koljonen & Malisa 1991, Lahtinen 1991, Räisänen et al. 1992, Koljonen 1992, Mäkinen 1992, Lintinen 1993). The variation in element contents depends on the mineralogical composition of the bedrock, but it is also affected by glacio-geological processes, fracturing of the bedrock and weathering processes which change the abundance of clay in till.

In addition to micas and clay minerals, sulphides, carbonates and phosphates dissolve almost totally in aqua regia, thus causing local variations in certain element contents. For explorational purposes it is useful to apply partial solution, which enhances the anomalies caused by sulphides and phosphates.

Oxides and many silicates such as quartz, feldspars, zircon, amphiboles and pyroxenes are poorly soluble (Koljonen & Malisa 1991). The amount of poorly soluble material in the sample naturally affects the abundance of elements in the dissolved part of the sample.

The leached proportion (partial/total solution) of elements in the fine fraction of till ranges from < 10% for Ba, Ca, K and Sr to nearly 90% for Cu and P (ref. op cit.). The sum of the partially leached Al, Ca, K, Fe and Mg represents about 4 wt% of the fine fraction of till (Koljonen 1992), but about 95 wt% of the sum of the analytically reliable elements analysed by ICP: Al, Ba, Ca, Co, Cr, Cu, Fe, K, La, Li, Mg, Mn, Ni, P, Sc, Sr, Th, Ti, V, Y and Zn. The Al, Ca, K, Fe, Mg referred to account for c. 21 wt% of the Earth's crust and together with O and Si for c. 96 wt% (Mason 1966).

Because the analytical data from the selective leaching depend on several processes, the element contents cannot be directly correlated with the underlying bedrock, even though it is basically the source of the analysed material. If the abundance of clay minerals in the sample is known, some of the secondary processes can be filtered away. To a certain extent the processes can be distinguished statistically and taken into account in the interpretation of the data. That is what was done here, because only the numerical values of the chemical analysis were available.

The basic statistics of the till geochemical data show that some minor elements such as Ba, Cu, Mn, P, Ti and Zn have a high standard deviation and anomalously high maximum values, implying different sources and possibly local enrichment of these elements in the bedrock (Table 4.). Chromium and Ni, too, have high maximum values although, the variation tends to be moderate.

Table 4. Basic statistics from till geochemical data.

Element	Mean	Standard Deviation	Minimum	Maximum	Valid N
Al %	1.620	.654	.379	4.800	1732
Ca %	.258	.141	.036	1.940	1732
Fe %	1.993	.742	.595	7.730	1732
K %	.254	.153	.017	.942	1732
Mg %	.523	.254	.108	3.040	1732
Ba ppm	58.063	30.001	10.700	197.000	1732
Co ppm	8.424	3.896	.900	39.600	1732
Cr ppm	25.105	14.218	5.590	236.000	1732
Cu ppm	36.442	25.327	2.600	510.000	1732
La ppm	31.335	9.266	12.300	95.400	1732
Li ppm	21.774	11.654	3.340	130.000	1732
Mn ppm	222.846	124.686	48.400	2190.000	1732
Ni ppm	17.620	10.943	3.370	168.000	1732
P ppm	800.636	319.334	120.000	4060.000	1732
Sc ppm	3.451	1.540	.920	10.000	1732
Sr ppm	11.232	5.538	2.420	67.000	1732
Th ppm	11.280	4.193	1.600	36.200	1732
Ti ppm	1328.849	500.325	428.000	4050.000	1732
V ppm	39.193	16.156	12.400	155.000	1732
Y ppm	11.977	3.548	4.470	55.200	1732
Zn ppm	45.381	24.697	7.630	365.000	1732

Factor analysis

The processes causing till geochemical anomalies were studied statistically by R-mode factor analysis. The element values were lognormalised and Kaiser-normalised before factoring (SPSS 1988) and the factors were extracted by the principal component method applying oblique Oblimin rotation. The oblique rotation method was selected as rotation technique, because the existing processes in nature are seldom orthogonal, and oblique rotation allows interrelated phenomena to be represented by the factor correlations. On the other hand, factor solution using oblique rotation is more sensitive to the number of factors extracted (Tiainen 1991). The geological significance of the factors was interpreted by studying the geological implication of the correlations between the elements. To do this the factor score maps were compared visually with the bedrock geological and Quaternary geological maps and with the data on ore deposits and ore indications.

Regional factors

The main regional variation in till contents was extracted into three factors (Table 5). To obtain the regional variation in siderophile elements in till, the chalcophile elements Co, Cu, Ni and Zn and also Cr were omitted from this factor analysis. The three factors extracted explain about 80% of the variance in the variables. The factors mainly reflect the bedrock lithology, but some glacial processes and bedrock fracturing are also shown on the factor score maps (Figs 26–28).

Factor 1 (Fig. 26) explains 53.8% of the variance in analysed elements. The rotated factor 1 has high loadings on Al (0.91), Ba (0.87), Fe (0.96), K (0.75), Li (0.82), Mg (0.97), Mn (0.76), Sc (0.92), Ti (0.91) and V (0.98). The highest factor scores plot mainly in till above schist belts and on mafic and ultramafic intrusions (cf., Fig. 4). Factor 1 was interpreted as a mica and clay mineral factor by Lahtinen (1991) and Tiainen et al. (1991) and as a mafic factor by Koistinen & Gaal (1988), but it could also be called more generally a schist belt factor.

Factor 2 (Fig. 27) explains 15% of the variance in analysed elements before rotation. The rotated factor 2 has the highest loadings on Ca (0.95) and P (0.74), and the highest factor scores plot on the mafic volcanics from Hämeenlinna through Forssa to Somero and also partly on certain mafic intrusions, e.g. the Forssa and Hyvinkää gabbros (cf. Fig. 4). The clearly lower level of factor scores in the eastern third of the study area than in the two western thirds is not easily explained by lithology. It might be due to glacio-geological processes. Owing to the number of geological processes involved, factor 2 cannot be named unambiguously.

Factor 3 (Fig. 28) represents 12% of the variance in analysed elements. After rotation it has the highest loadings on La (0.92), Th (0.88) and Y (0.74). Factor 3 was interpreted as a granite factor with the highest scores plotting on granitic rocks, late-orogenic potassium granites in particular. The factor score map of factor 3 correlates with the radiometric data (cf. Figs 18–20) on the late-orogenic granites (cf. Fig. 4).

Table 5. Statistics in a 3-factor model factor analysis with an oblique Oblimin rotation technique. Regional factors.

INITIAL STATISTICS:

VARIABLE	COMMUNALITY	*	FACTOR	EIGENVALUE	PCT OF VAR	CUM PCT
		*				
AL	1.00000	*	1	8.60903	53.8	53.8
BA	1.00000	*	2	2.40542	15.0	68.8
CA	1.00000	*	3	1.91653	12.0	80.8
FE	1.00000	*	4	.71341	4.5	85.3
K	1.00000	*	5	.66477	4.2	89.4
LA	1.00000	*	6	.37433	2.3	91.8
LI	1.00000	*	7	.27304	1.7	93.5
MG	1.00000	*	8	.25860	1.6	95.1
MN	1.00000	*	9	.18227	1.1	96.2
P	1.00000	*	10	.16056	1.0	97.2
SC	1.00000	*	11	.11292	.7	97.9
SR	1.00000	*	12	.09661	.6	98.5
TH	1.00000	*	13	.08532	.5	99.1
TI	1.00000	*	14	.07196	.4	99.5
V	1.00000	*	15	.04981	.3	99.8
Y	1.00000	*	16	.02543	.2	100.0

PC EXTRACTED 3 FACTORS.

FACTOR MATRIX:

FACTOR	1	2	3
AL	.779	-.461	-.008
BA	.892	-.008	-.108
CA	.233	.847	-.372
FE	.946	-.140	-.080
K	.819	.050	.016
LA	.387	.326	.775
LI	.814	-.233	.123
MG	.953	-.089	-.138
MN	.867	.239	-.141
P	.044	.668	-.301
SC	.926	-.206	.095
SR	.566	.593	-.260
TH	.251	.205	.807
TI	.915	-.113	-.036
V	.939	-.139	-.188
Y	.379	.556	.495

OBLIMIN ROTATION 1 FOR EXTRACTION 1 IN ANALYSIS 1 - KAISER NORMALIZATION.

OBLIMIN CONVERGED IN 6 ITERATIONS.

FINAL STATISTICS:

VARIABLE	COMMUNALITY	*	FACTOR	EIGENVALUE	PCT OF VAR	CUM PCT
		*				
AL	.82002	*	1	8.60903	53.8	53.8
BA	.80803	*	2	2.40542	15.0	68.8
CA	.91201	*	3	1.91653	12.0	80.8
FE	.92123	*				
K	.67501	*				
LA	.85837	*				
LI	.73318	*				
MG	.93694	*				
MN	.82997	*				
P	.53943	*				
SC	.90976	*				
SR	.74079	*				
TH	.75737	*				
TI	.85251	*				
V	.93759	*				
Y	.69876	*				

PATTERN MATRIX:

FACTOR	1	2	3
AL	.906	-.324	-.096
BA	.870	.137	-.000
CA	-.000	.954	.004
FE	.962	.012	-.018
K	.749	.122	.133
LA	.050	-.036	.915
LI	.822	-.181	.123
MG	.966	.085	-.053
MN	.763	.370	.062
P	-.129	.741	-.020
SC	.924	-.131	.120
SR	.378	.710	.051
TH	-.040	-.173	.882
TI	.913	.012	.029
V	.983	.063	-.122
Y	.028	.299	.737

STRUCTURE MATRIX:

FACTOR	1	2	3
AL	.838	-.216	.102
BA	.888	.252	.243
CA	.126	.954	.115
FE	.959	.137	.234
K	.800	.237	.343
LA	.284	.077	.924
LI	.830	-.058	.316
MG	.963	.206	.208
MN	.829	.478	.305
P	-.036	.721	.032
SC	.939	.004	.347
SR	.486	.766	.234
TH	.166	-.075	.855
TI	.922	.136	.269
V	.959	.179	.142
Y	.260	.389	.779

FACTOR CORRELATION MATRIX:

FACTOR	1	2	3
FACTOR			
1	1.000		
2	.131	1.000	
3	.261	.117	1.000

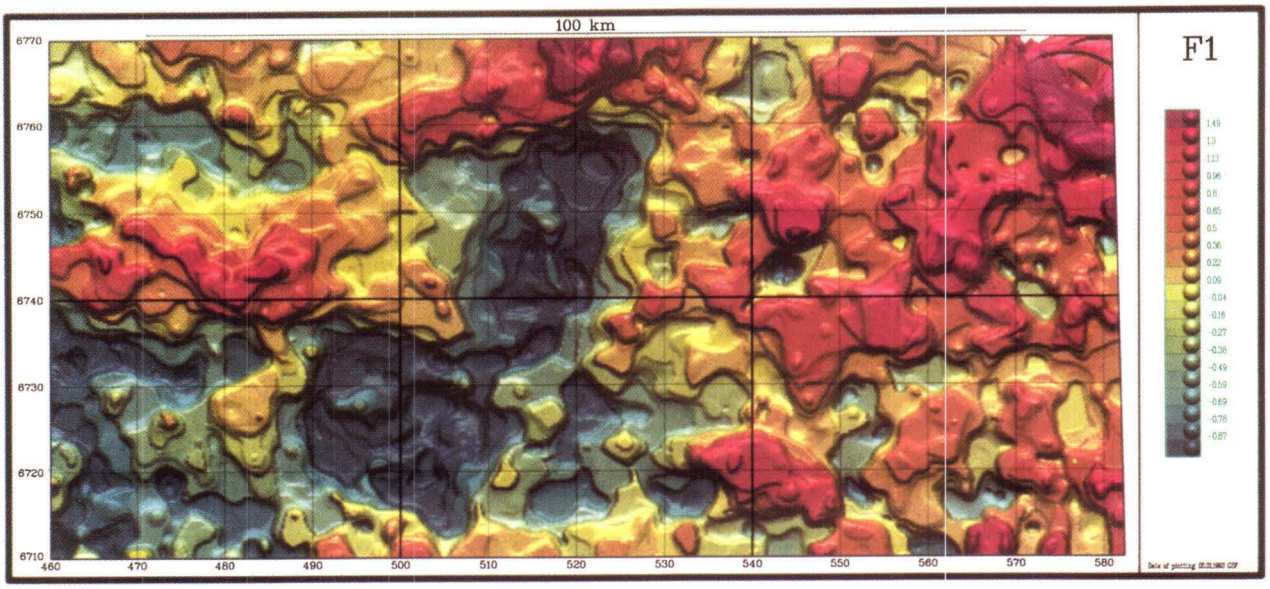

Fig. 26. Schist belt factor. Factor score map of factor 1 in a 3 factor model with highest loadings on Al, Ba, Fe, K, Li, Mg, Mn, Sc, Ti and V.

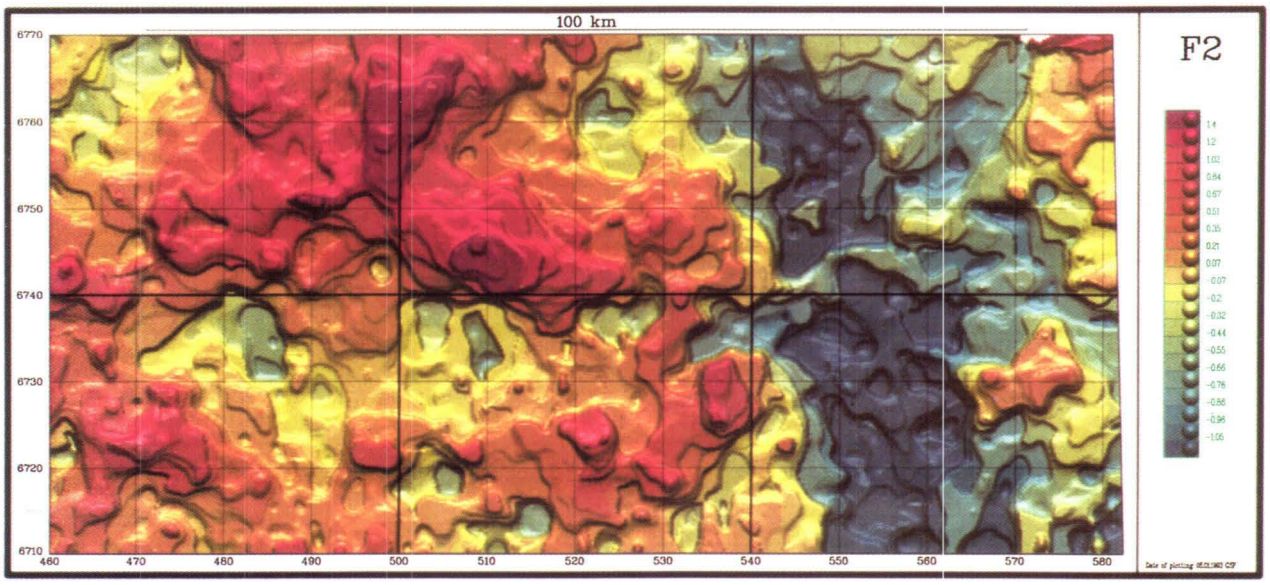

Fig. 27. Factor score map of factor 2 in a 3 factor model with highest loadings on Ca and P.

Factors indicating mineral deposits

The processes related to the formation of sulphide deposits were extracted from till geochemical data by factor analysis applying the principal component method with oblique Oblimin rotation in a nine factors model (Table 6). The number of factors calculated was decided after the factor models had been analysed with three to ten factors. The aim was to find ore-geologically significant correlating element combinations which could be interpreted as signatures of certain sulphide deposit types. Thus only the factors of ore-geological interest were plotted and interpreted (Figs 29–31).

Factor 1 (Fig. 29) has the highest loadings on Zn (0.67), Mn (0.60) and Fe (0.42). These elements are among the ones that have typically elevated concentrations in lithogeochemistry in volcanic-hosted massive Zn-Pb-Cu sulphide deposits and/or in their surroundings. Factor 1 was therefore interpreted as a Zn factor. The Zn factor has the highest factor scores in two zones: 1) The volcanic belt between Hämeenlinna and Humppila, and 2) the volcanic belt from Karkkila to Hyvinkää and Mäntsälä (cf. Fig. 4). The Tupala Zn deposit can also be distinguished, although not with very high factor scores.

Factor 6 (Fig. 30) has the highest loading on Cu

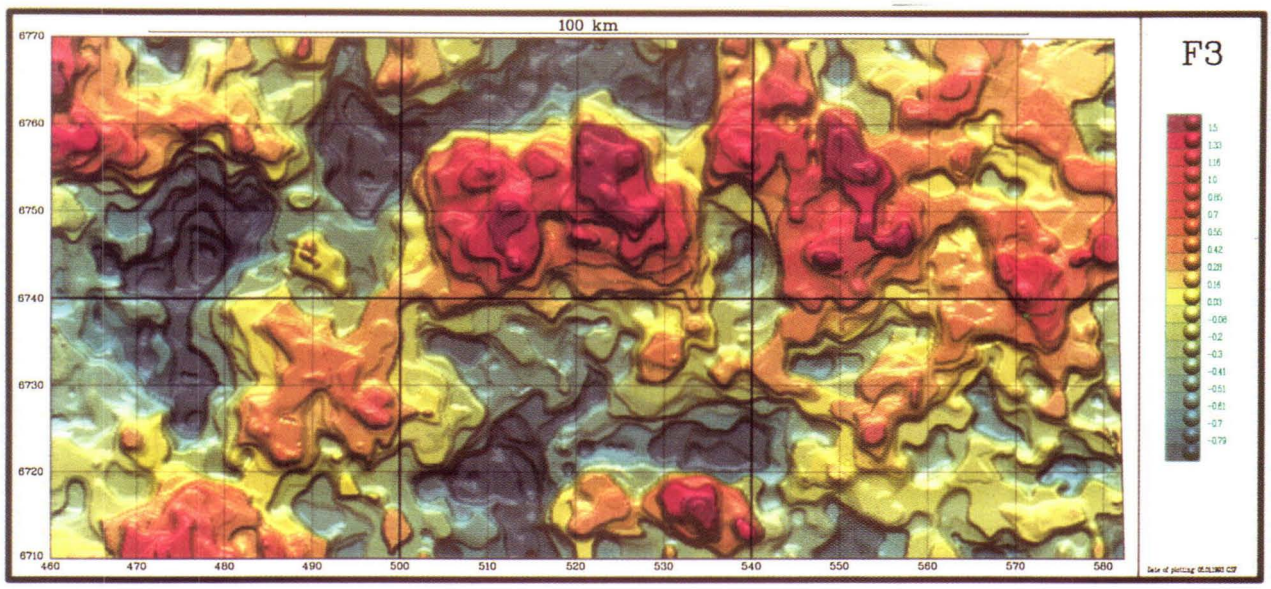

Fig. 28. Granite factor. Factor score map of factor 3 in a 3 factor model with highest loadings on La, Th and Y.

(1.01); the loadings on all other elements are insignificant. Factor 6 was interpreted as a Cu factor. It has highest factor scores in the volcanic belt between Hämeenlinna and Forssa, especially in the surroundings of Lunkinjärvi and Kanajärvi (cf. Figs 2–4). The volcanic belt in the surroundings of the Onkimaa granodiorite in Mäntsälä is also very distinct.

Factor 6 anomalies indicate several deposit types. According to the mineral indication data, other possibilities besides volcanic hosted stratiform Cu-Zn-Pb deposits are Ylöjärvi-type Cu-W-Au deposits, the related Au-Cu deposits and vein-type Au-Cu deposits. There are also indications of low-grade porphyry Cu deposits in intermediate granitoids and their country rocks in the mineral indication data bank (Saltikoff 1992). Their economic viability is, however, questionable.

Factor 7 (Fig. 31) has the highest loadings on Ni (0.97), Cr (0.85), Co (0.36) and Mg (0.32). This metallic combination indicates clearly mafic or ultramafic rocks with possible Ni deposits and the factor was consequently interpreted as a Ni factor. The highest factor scores show two geological formations: the Hyvinkää and Forssa gabbros. The small Ni-Cu deposit at Särkisuo near the Forssa gabbro is also visible due to high factor scores (cf. Figs 3 and 4), whereas, the Ni potential of the Hyvinkää and Forssa gabbros is not so clear. Their high P and elevated Ti contents rather refer to the presence of P and/or (Fe) Ti-V deposits.

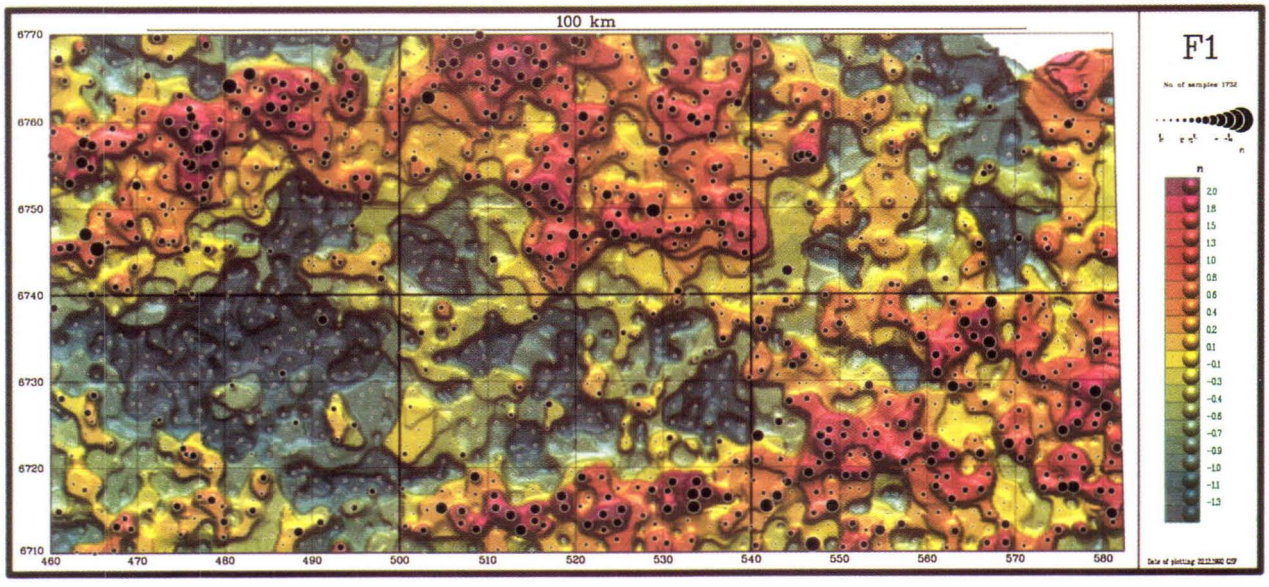

Fig. 29. Zinc factor. Factor score map of factor 1 in a 9 factor model with highest loadings on Zn, Mn and Fe.

Table 6. Statistics in a 9-factor model factor analysis with an oblique Oblimin rotation technique. Factors indicating mineral deposits.

EXTRACTION 1 FOR ANALYSIS 1, PRINCIPAL-COMPONENTS ANALYSIS (PC)

INITIAL STATISTICS:

VARIABLE	COMMUNALITY	*	FACTOR	EIGENVALUE	PCT OF VAR	CUM PCT
AL	1.00000	*	1	11.88959	56.6	56.6
BA	1.00000	*	2	2.60897	12.4	69.0
CA	1.00000	*	3	2.09012	10.0	79.0
CO	1.00000	*	4	.71560	3.4	82.4
CR	1.00000	*	5	.68652	3.3	85.7
CU	1.00000	*	6	.50150	2.4	88.1
FE	1.00000	*	7	.45350	2.2	90.2
K	1.00000	*	8	.37964	1.8	92.0
LA	1.00000	*	9	.31695	1.5	93.5
LI	1.00000	*	10	.26342	1.3	94.8
MG	1.00000	*	11	.21808	1.0	95.8
MN	1.00000	*	12	.16800	.8	96.6
NI	1.00000	*	13	.13836	.7	97.3
P	1.00000	*	14	.11744	.6	97.8
SC	1.00000	*	15	.10237	.5	98.3
SR	1.00000	*	16	.09348	.4	98.8
TH	1.00000	*	17	.07516	.4	99.1
TI	1.00000	*	18	.06412	.3	99.4
V	1.00000	*	19	.05022	.2	99.7
Y	1.00000	*	20	.04322	.2	99.9
ZN	1.00000	*	21	.02374	.1	100.0

PC EXTRACTED 9 FACTORS.

FACTOR MATRIX:

FACTOR	1	2	3	4	5	6	7	8	9
AL	.785	-.433	-.043	.285	-.010	.023	-.110	.194	.013
BA	.889	.020	-.040	-.132	.104	-.139	-.052	-.103	.116
CA	.234	.896	-.201	-.139	-.030	-.081	.089	.027	.045
CO	.880	.112	-.240	.040	-.013	.162	.007	-.073	-.169
CR	.840	-.315	-.069	.013	-.079	.079	.338	-.019	.127
CU	.647	.362	-.256	-.008	.188	.438	-.331	.093	.157
FE	.950	-.115	-.037	.122	-.009	-.058	-.055	.006	-.097
K	.808	.058	.086	-.333	.292	-.157	-.025	-.188	.191
LA	.331	.187	.844	.110	-.050	-.002	.047	.131	.081
LI	.801	-.242	.144	.032	.244	-.190	-.027	.042	.025
MG	.965	-.057	-.094	-.035	.002	-.013	.027	.009	-.005
MN	.870	.268	-.038	-.091	-.116	-.021	-.094	-.145	-.226
NI	.837	-.011	-.161	-.013	.006	.290	.383	-.061	.001
P	.051	.706	-.176	.524	.366	-.146	.127	-.001	-.005
SC	.916	-.211	.120	-.031	-.136	-.004	-.072	-.001	.075
SR	.556	.623	-.100	-.246	-.259	-.123	.037	.311	-.059
TH	.208	.078	.826	-.182	.317	.168	.080	.150	-.155
TI	.901	-.105	.020	.112	-.166	-.148	-.030	.121	.105
V	.949	-.097	-.149	.081	-.056	-.033	-.004	.083	.017
Y	.339	.460	.604	.237	-.335	.083	-.080	-.284	.098
ZN	.895	-.114	.097	.021	.075	-.068	-.077	-.116	-.268

OBLIMIN ROTATION 1 FOR EXTRACTION 1 IN ANALYSIS 1 - KAISER NORMALIZATION.

OBLIMIN CONVERGED IN 23 ITERATIONS.

FINAL STATISTICS:

VARIABLE	COMMUNALITY	*	FACTOR	EIGENVALUE	PCT OF VAR	CUM PCT
AL	.93908	*	1	11.88959	56.6	56.6
BA	.86783	*	2	2.60897	12.4	69.0
CA	.93753	*	3	2.09012	10.0	79.0
CO	.90894	*	4	.71560	3.4	82.4
CR	.95478	*	5	.68652	3.3	85.7
CU	.98648	*	6	.50150	2.4	88.1
FE	.94905	*	7	.45350	2.2	90.2
K	.95804	*	8	.37964	1.8	92.0
LA	.89895	*	9	.31695	1.5	93.5
LI	.82265	*				
MG	.94740	*				
MN	.93584	*				
NI	.96345	*				
P	.98131	*				
SC	.93049	*				
SR	.95386	*				
TH	.94804	*				
TI	.91329	*				
V	.95190	*				
Y	.96668	*				
ZN	.92681	*				

PATTERN MATRIX:

FACTOR	1	2	3	4	5	6	7	8	9
AL	.202	-.122	-.000	-.045	.047	.225	.189	.024	.660
BA	.138	.084	-.078	-.009	-.059	.107	.097	-.618	.096
CA	-.084	.643	-.085	.324	-.081	.082	.008	-.127	-.287
CO	.457	.100	-.056	.057	-.029	.256	.366	.032	-.010
CR	-.060	-.022	-.046	-.083	-.021	-.095	.853	-.154	.169
CU	-.058	.015	.020	.021	-.015	1.006	-.033	-.032	.019
FE	.423	.055	-.014	.028	-.058	.091	.185	-.163	.329
K	.005	.011	.065	-.022	-.002	.091	.042	-.924	-.126
LA	-.141	.105	.569	.021	-.459	-.073	.013	-.027	.255
LI	.199	-.074	.178	.084	.100	-.008	.061	-.500	.363
MG	.246	.144	-.016	-.035	.001	.121	.323	-.264	.194
MN	.597	.285	-.038	-.033	-.203	.091	.051	-.141	-.083
NI	.049	.025	.064	.053	.011	.088	.972	.046	-.124
P	.021	-.002	-.012	.996	-.022	.016	.013	.003	.064
SC	.165	.060	-.016	-.248	-.201	.129	.207	-.270	.306
SR	.055	.970	.055	-.034	.039	.039	.008	.036	.078
TH	.052	.004	.975	-.026	.015	.032	.018	-.029	-.089
TI	.102	.219	-.106	-.061	-.152	.032	.183	-.222	.509
V	.218	.157	-.091	-.008	-.003	.144	.296	-.163	.364
Y	.053	-.041	.015	.033	-.983	.032	-.011	.023	-.057
ZN	.672	-.019	.136	.008	-.052	-.004	.073	-.210	.119

STRUCTURE MATRIX:

FACTOR	1	2	3	4	5	6	7	8	9
AL	.679	.039	.056	-.218	-.097	.452	.706	-.540	.876
BA	.712	.436	.099	-.016	-.273	.590	.717	-.880	.470
CA	.093	.846	-.084	.629	-.317	.444	.109	-.210	-.346
CO	.838	.483	-.041	.094	-.233	.736	.809	-.622	.381
CR	.626	.202	.051	-.232	-.158	.403	.945	-.670	.619
CU	.471	.483	-.010	.248	-.202	.990	.496	-.472	.156
FE	.863	.355	.097	-.048	-.286	.582	.800	-.743	.686
K	.596	.389	.256	-.027	-.251	.532	.625	-.967	.297
LA	.091	.210	.798	.015	-.748	.026	.147	-.286	.322
LI	.662	.153	.291	-.094	-.173	.382	.638	-.789	.671
MG	.814	.445	.079	-.065	-.249	.637	.858	-.803	.587
MN	.848	.633	.089	.082	-.442	.641	.667	-.687	.300
NI	.660	.375	.059	.004	-.195	.605	.965	-.607	.357
P	.009	.340	-.067	.986	-.183	.265	-.030	-.001	-.137
SC	.739	.310	.188	-.282	-.373	.512	.781	-.764	.691
SR	.374	.967	.043	.256	-.354	.507	.373	-.397	.077
TH	.091	.041	.967	-.077	-.408	.021	.078	-.268	.077
TI	.695	.418	.079	-.102	-.358	.493	.751	-.713	.755
V	.795	.422	-.000	-.051	-.226	.628	.844	-.735	.681
Y	.190	.349	.417	.186	-.980	.191	.151	-.209	.091
ZN	.907	.288	.242	-.085	-.305	.495	.713	-.748	.558

FACTOR CORRELATION MATRIX:

FACTOR FACTOR	1	2	3	4	5	6	7	8	9
1	1.000								
2	.291	1.000							
3	.031	.001	1.000						
4	-.059	.321	-.071	1.000					
5	-.184	-.365	-.423	-.150	1.000				
6	.513	.469	-.042	.219	-.174	1.000			
7	.662	.302	.031	-.099	-.170	.530	1.000		
8	-.610	-.349	-.222	.052	.231	-.473	-.631	1.000	
9	.442	-.030	.116	-.222	-.142	.165	.484	-.403	1.000

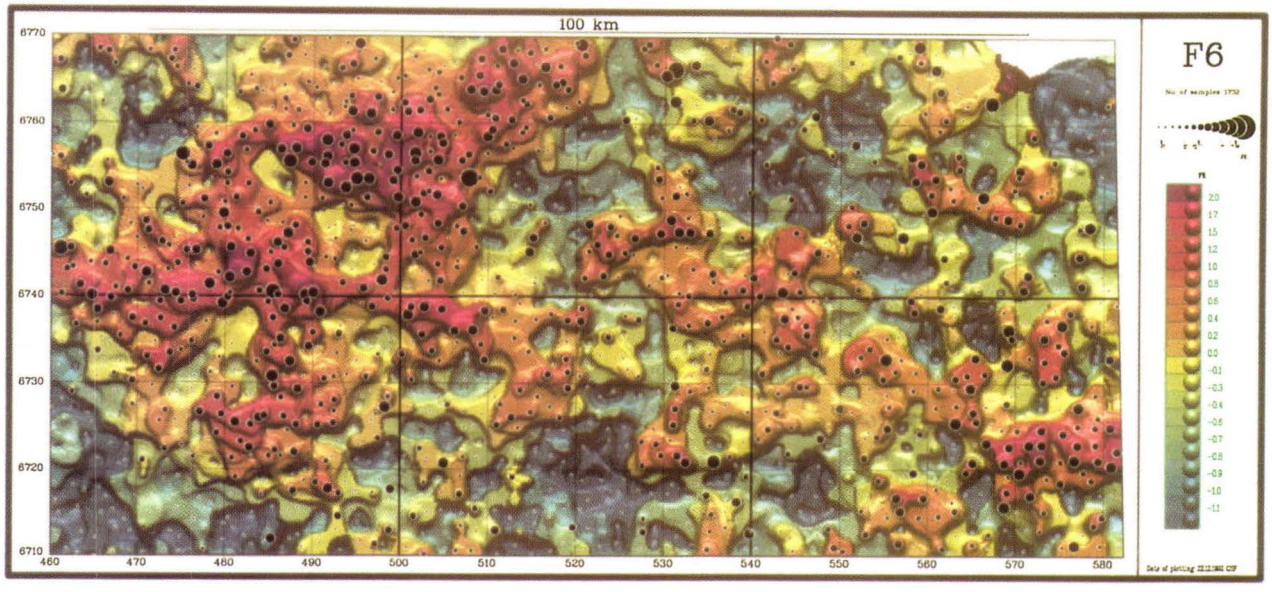

Fig. 30. Copper factor. Factor score map of factor 6 in a 9 factor model with highest loadings on Cu.

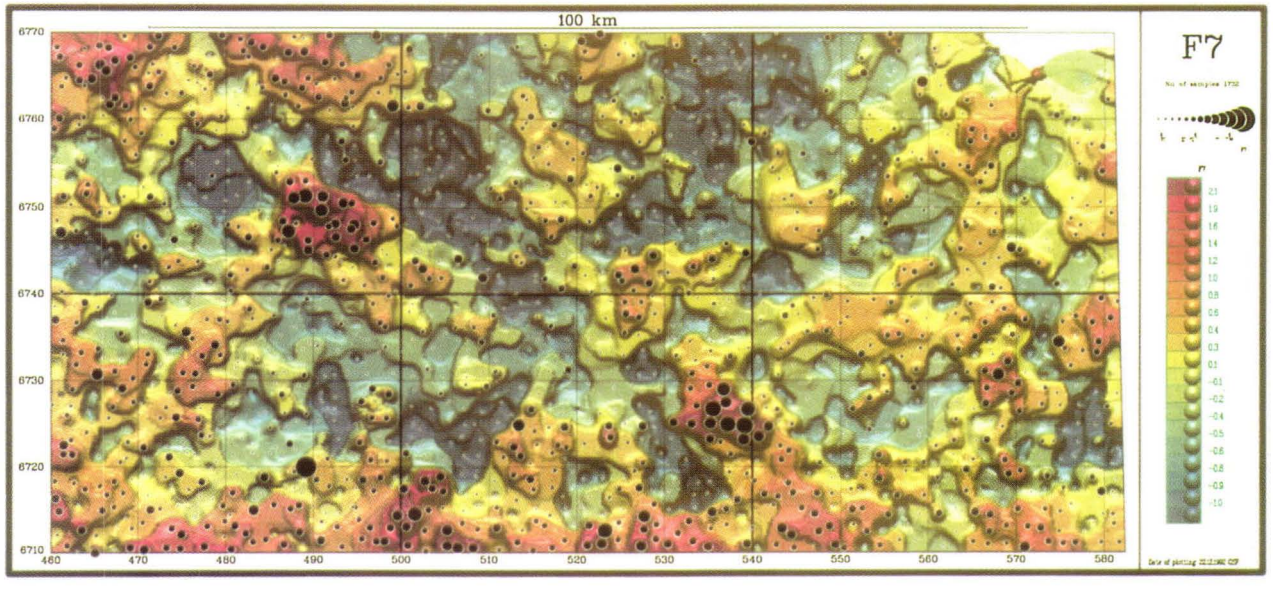

Fig. 31. Nickel factor. Factor score map of factor 7 in a 9 factor model with highest loadings on Ni, Cr, Co and Mg.

Element and element ratio data

The till geochemistry of the explorationally interesting elements was investigated by comparing the original data with normalised data from which the regional background level had been filtered away. Both the original and the filtered data on Cu, Cr, Ni, Zn and the Cr x Ni/Co ratio were plotted upon the interpolated maps as dot maps to show the regional patterns and local anomalies of the elements (Figs 32–42).

The filtering was carried out by dividing the element content in question by the weighted sum of Al, Ba, Ca, Fe, K, La, Li, Mg, Mn, P, Sc, Sr, Th, Ti, V and Y with the loadings of factor 1 (Table 5) as weighting coefficients. The filtering reduces base metal anomalies due to high abundances of micas and clay minerals, but enhances anomalies caused by sulphide deposits or metal precipitates. However, if the sum of the elements used as denominator is very small this method may cause anomalies even when the base metal contents are very low. Therefore, the filtered maps should be compared with the original element content maps when interpreting and evaluating the results.

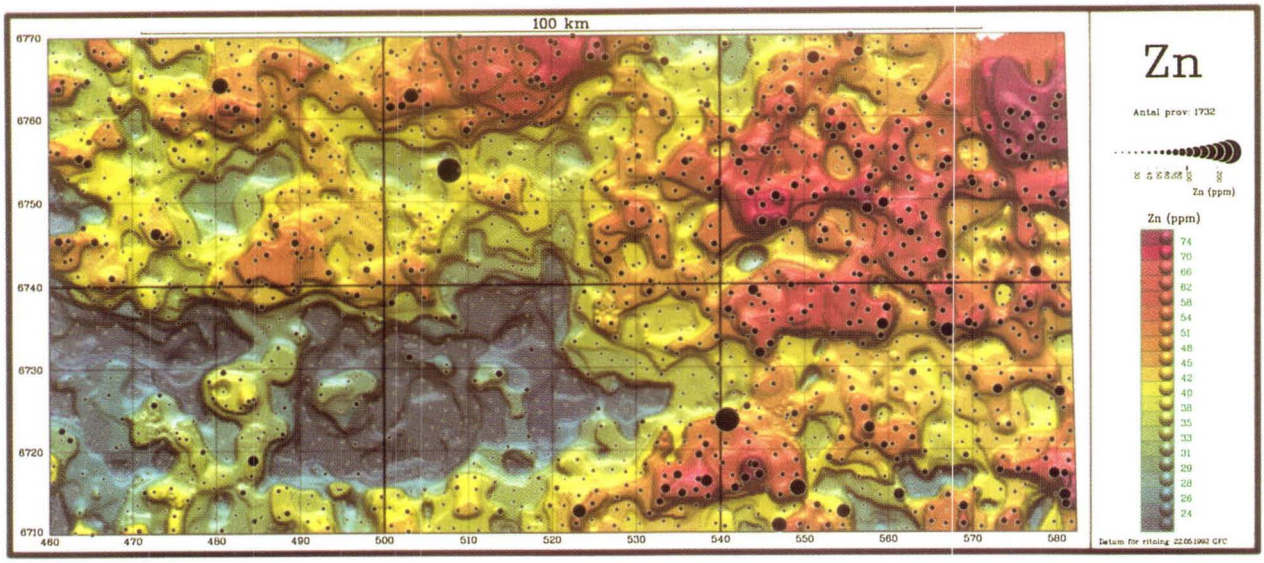

Fig. 32. Zn content in till, partial leaching of -0.06 mm fraction. About 1 sample/4 km^2.

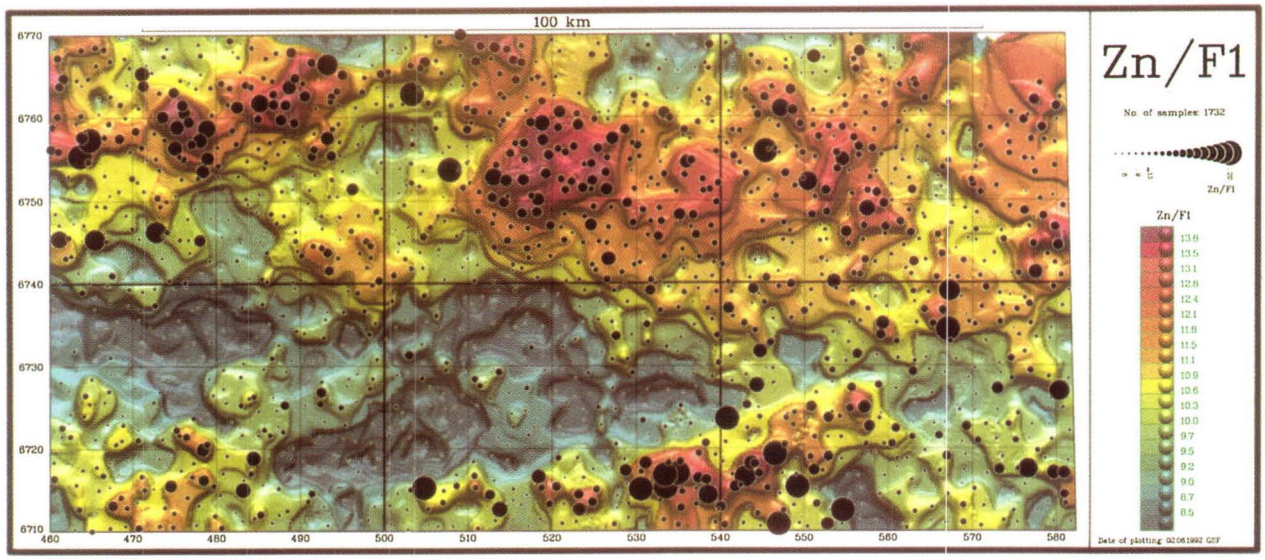

Fig. 33. Zn/F1 ratio for till. The variation caused by the leachable material in samples has been filtered away by regional factor 1.

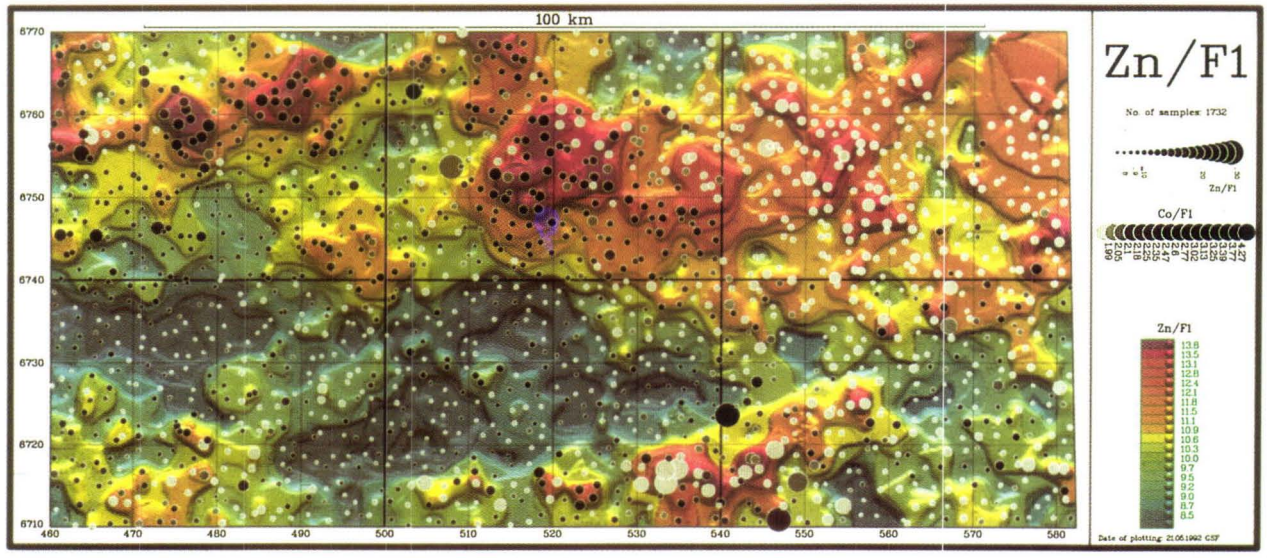

Fig. 34. Zn/F1 and Co/F1 ratios in till. The main variation between the samples has been filtered away by regional factor 1.

Zinc

Zinc occurs in sulphides mainly as sphalerite but also in lattices of some other sulphide minerals and mafic silicates. The common occurrence of Zn in silicate minerals is one reason for its low solubility, about 50% by partial leach (Koljonen 1992).

The anomaly patterns of Zn are similar to those of Co, Mn and Fe as was already noted in factor analysis. The statistical behaviour of Zn in factor analysis can be partly attributed to its occurrence in the lattices of mafic minerals and its geochemical character resembling Fe and Mn under the conditions prevailing on the Earth's surface. Iron, Mn and Co, too, often have high contents in massive sulphide deposits and their surroundings in the Svecofennian domain (Mäki 1986, Rasilainen 1991, Papunen 1990, Lagerblad 1988). Zinc anomalies in till are obviously the caused by several processes, of which ore formation is only one.

In the Häme belt the Zn anomalies form two clear zones in till geochemistry: the volcanic belts from Hämeenlinna to Humppila and from Somero to Hyvinkää (Figs 4, 32 and 33). Both belts have elevated concentrations of Fe and Mn, but differ in Co, having a high Co content in the belt between Hämeenlinna and Humppila but a low Co content in the belt between Somero and Hyvinkää (Fig. 34). Another difference is the occurrence of mineralized Zn indications. The volcanic zone from Hämeenlinna to Humppila has several mineralised boulders or outcrops as Zn indications (Fig. 3), whereas the Zn potential of the eastern part of the Somero—Hyvinkää schist belt was not evident in the mineral indication data.

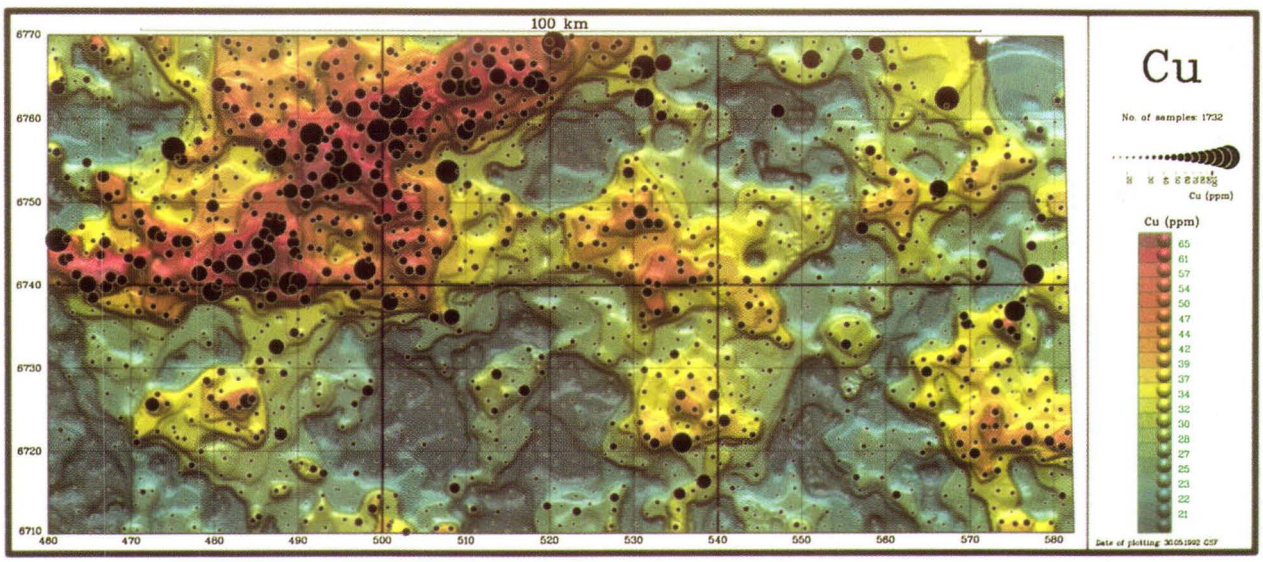

Fig. 35. Cu content in till, partial leaching of -0.06 mm fraction. About 1 sample/4 km^2.

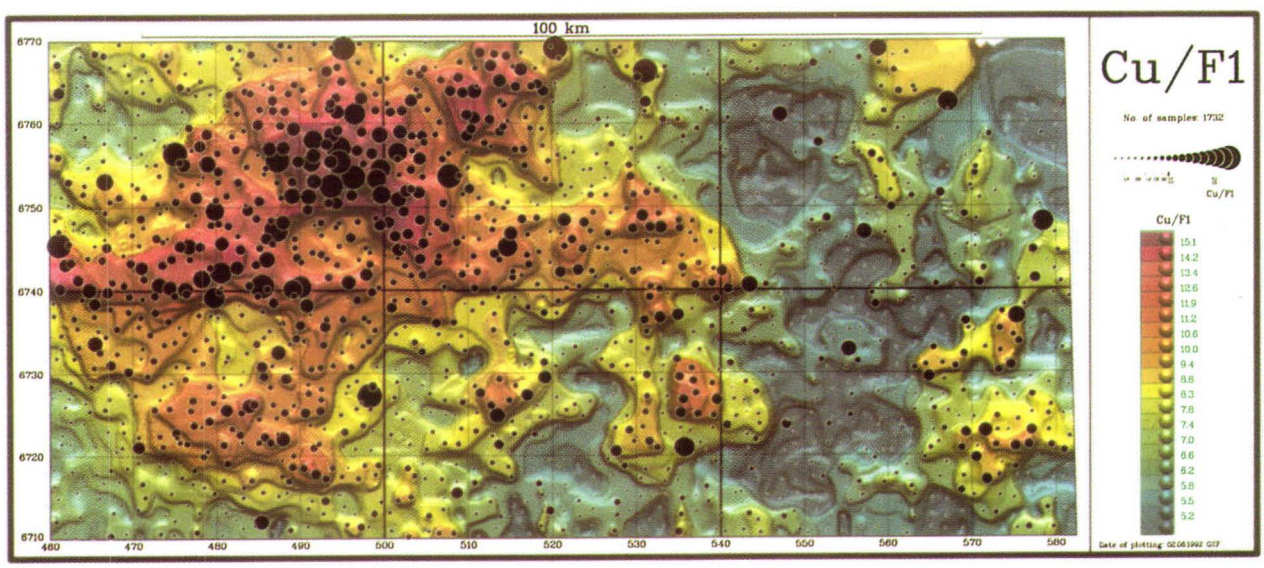

Fig. 36. Cu/F1 ratio for till. The variation caused by the leachable material in samples has been filtered away by the regional factor 1.

In addition to the two volcanic belts, the eastern part of the Hyvinkää gabbro shows high Zn concentrations in till probably due to the Zn content in the mafic minerals of the gabbro. The Zn prospects of Tupala and Kiipu show up poorly in till geochemistry.

Copper

The Cu present in the fine fraction of till is almost totally dissolved in partial leach (Koljonen 1992). The Cu anomalies in till are mainly caused by sulphides but possibly also by oxidic and metallic Cu deposits and hydroxidic precipitates.

In the Häme belt three main types of Cu deposit are indicated by boulders or mineralised outcrops: 1) Volcanic-sedimentary hosted massive sulphide Cu-Zn-Pb deposits, 2) Au-bearing Cu deposits including Ylöjärvi-type tourmaline breccia pipes (Himmi et al. 1979), other breccia pipes and vein deposits and 3) porphyry Cu deposits (Saltikoff 1992).

These deposit types have geochemical fingerprints. Cu-Zn-Pb deposits show elevated Cu, Zn and Pb contents. Ylöjärvi-type Cu-W deposits have anomalous Cu, W and As values in till geochemical data (Kinnunen 1979) and porphyry Cu deposits often have clear Cu and Mo haloes (Nurmi & Isohanni 1984). The deposit types are unfortunately not easy to distinguish on the basis of till geochemical data, because the reliability of the W and Pb analyses was not good and that of the As data was variable. The exploration strategies for these deposit types differ from each other so much, however, that it is useful to have an idea of the deposit type causing the till geochemical anomaly before starting exploration.

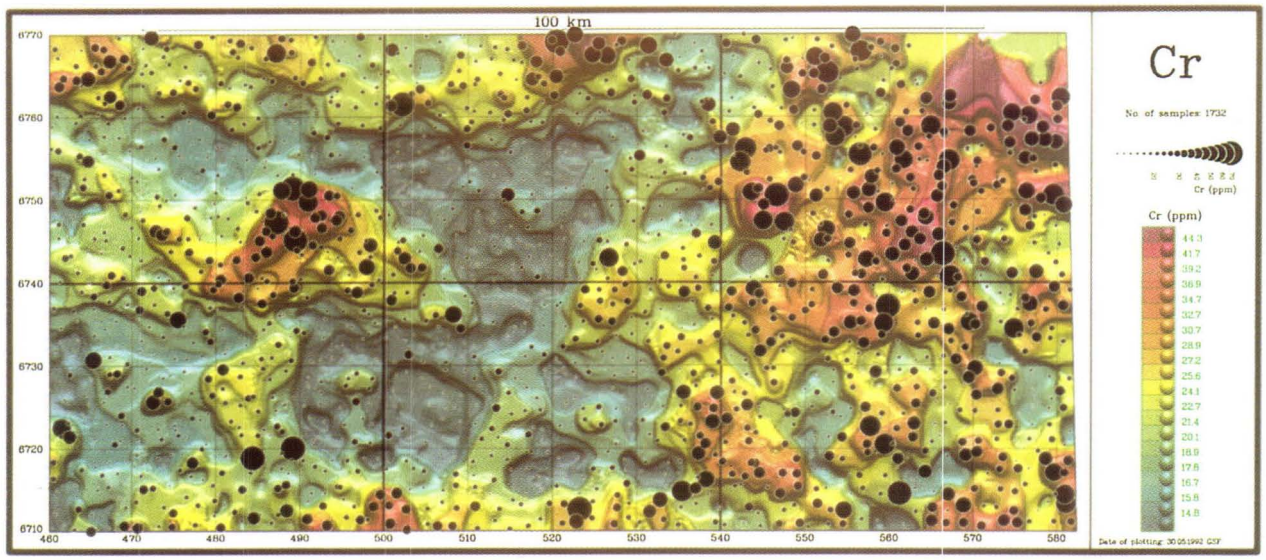

Fig. 37. Cr content in till, partial leaching of -0.06 mm fraction. About 1 sample/4 km^2.

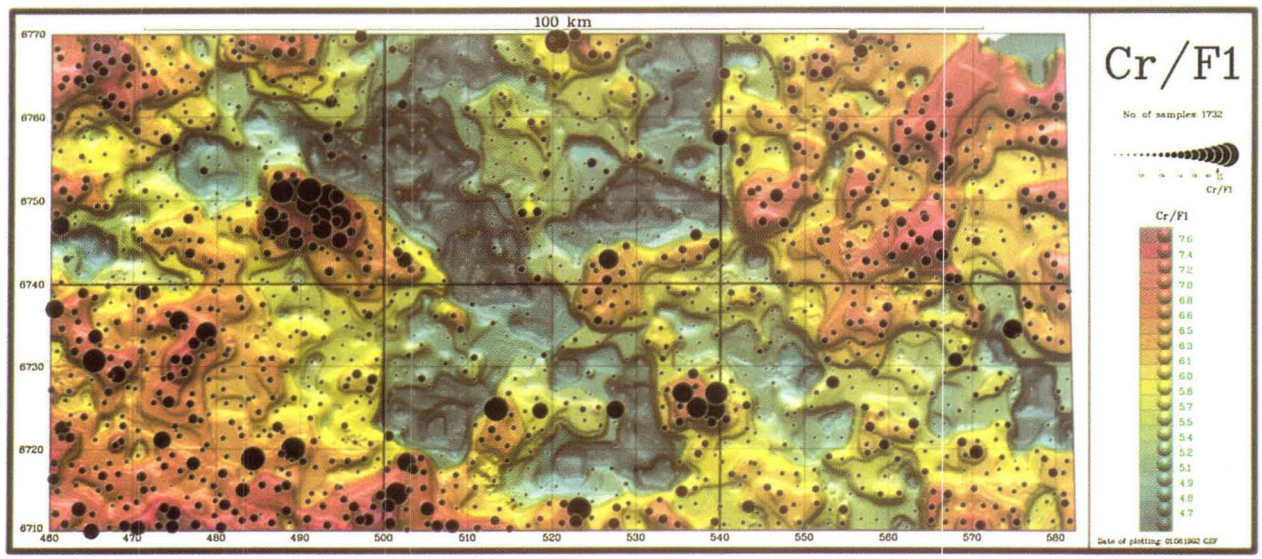

Fig. 38. Cr/F1 ratio from till. The variation caused by the leachable material in samples has been filtered away by regional factor 1.

The most anomalous zone for Cu in the Häme belt is the volcanic-sedimentary zone between Hämeenlinna and Forssa (Fig. 35, 36). High Cu and As contents in the same area as mineralised Cu and W-bearing boulders indicate the existence of Ylöjärvi-type Cu deposits. Several mineralised Cu indications related to Cu-Zn-Pb-type deposits as at Katumajärvi, and mineralised Au indications related to Cu indications were also observed in the same volcanic-sedimentary zone (Fig. 3). The highest Cu anomalies are in the Lunkinjärvi area, which also has Au-bearing mineralised boulders.

The Cu anomalies in the surroundings of Tupala obviously indicate Tupala-type Zn-Pb-Cu deposits. According to till geochemistry, new Cu-Zn deposits should be found in the felsic-intermediate/mafic volcanics northeast of the Tupala Zn deposit, on map sheets 202405D-202408B (Figs 32 and 33, 35 and 36).

The third Cu-anomalous area revealed by till geochemistry in the Häme belt is the Mäntsälä area, that is the volcanic rocks to the north of and in the surroundings of the Onkimaa granodiorite. The geological setting of the Onkimaa granodiorite with the known Ylöjärvi-type Cu-W boulder found in map sheet area 302103B about 10 km southeast of the northern contact of the batholith resembles the Ylöjärvi area so closely that there should be potential for unknown Cu deposits.

The Hyvinkää and Mäntsälä gabbros and the high metamorphic area north of the Hyvinkää gabbro also have elevated Cu contents in till; however, their Cu potential is not clear.

Nickel

Nickel occurs in mafic and ultramafic rocks both as sulphide minerals and in lattices of some silicates

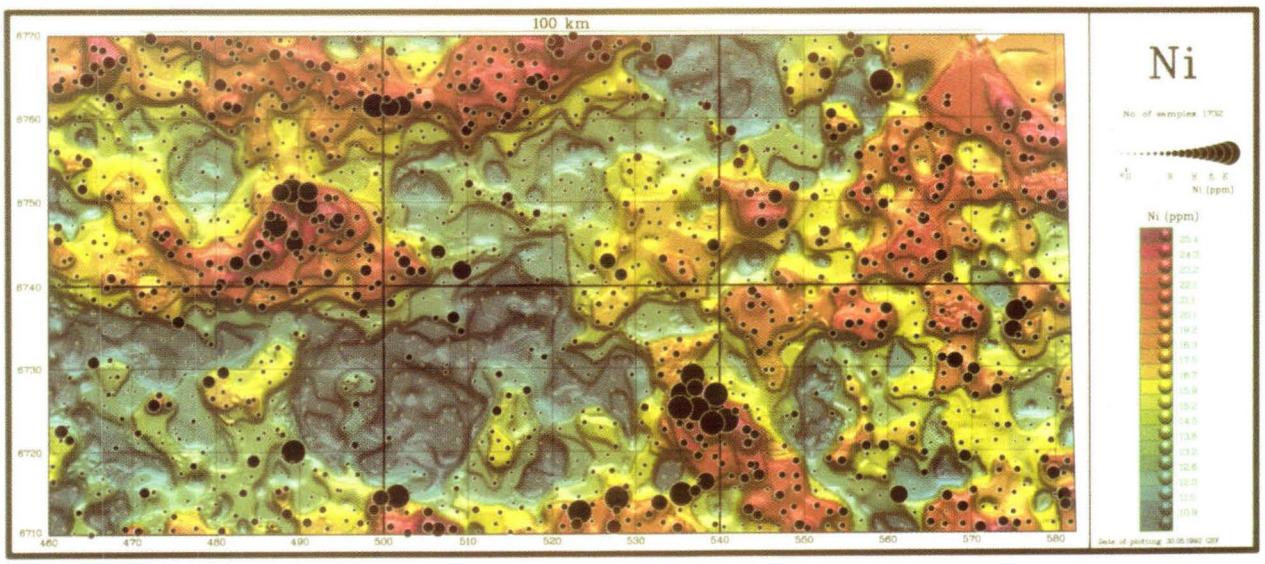

Fig. 39. Ni content in till, partial leaching of -0.06 mm fraction. About 1 sample/4 km^2.

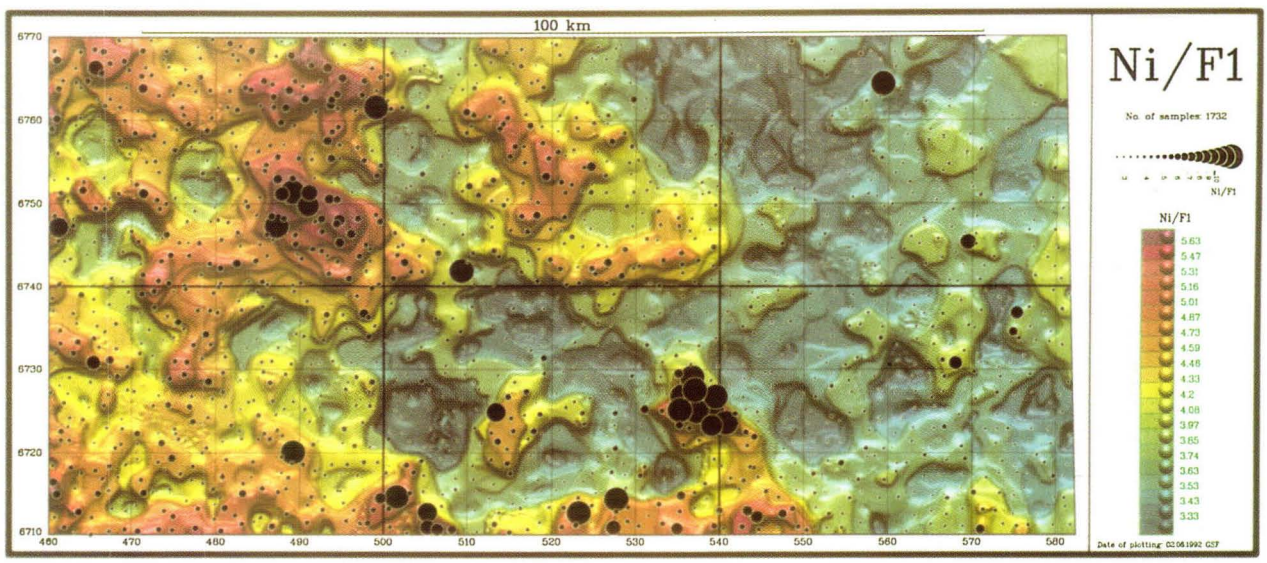

Fig. 40. Ni/F1 ratio for till. The variation caused by the leachable material in samples has been filtered away by regional factor 1.

and sulphide minerals. Silicates such as olivine and pyroxenes and their pseudomorphs are poorly soluble in partial leach, whereas sulphides incorporating Ni are almost totally soluble.

Since sulphide Ni mineralisations are usually located at the stratigraphic bottom of ultramafic intrusions, having only small and low-grade, if any, mineralised outcrops (Naldrett 1981, Makkonen 1992), it is important first to detect the nickel-bearing ultramafic formations and then establish the intrusions likely to contain sulphide nickel.

Chromium is one of the best elements at indicating ultramafic formations (Figs 37 and 38). Its occurrence correlates with Co, Ni and Mg (Table 6). The highest Cr anomalies clearly reveal parts of the Hyvinkää and Forssa gabbros, slighly so some other gabbros and probably some mafic volcanites. Many gabbros or diorites, for example, those in the Mäntsälä area, that show up on the lithological map do not have a Cr anomaly in till. The gabbros without a Cr anomaly are possibly less mafic. Another explanation is that because Cr is more easily leached from the sulphide phase than from silicates or oxides, the highest Cr anomalies indicate mafic and ultramafic intrusions with a magmatic sulphide phase.

The Ni content in till is shown in Fig. 39. Ni-potential ultramafic intrusions were detected in mafic/ultramafic formations by Ni/F1, Ni x Cr/Co and (Ni x Cr/Co)/F1 and ratio plots (Figs 40, 41 and 42). The use of the Ni x Cr/Co ratio in the search for Ni-bearing ultramafic formations using till geochemical data is based on the observations of Bleeker (1990) on the

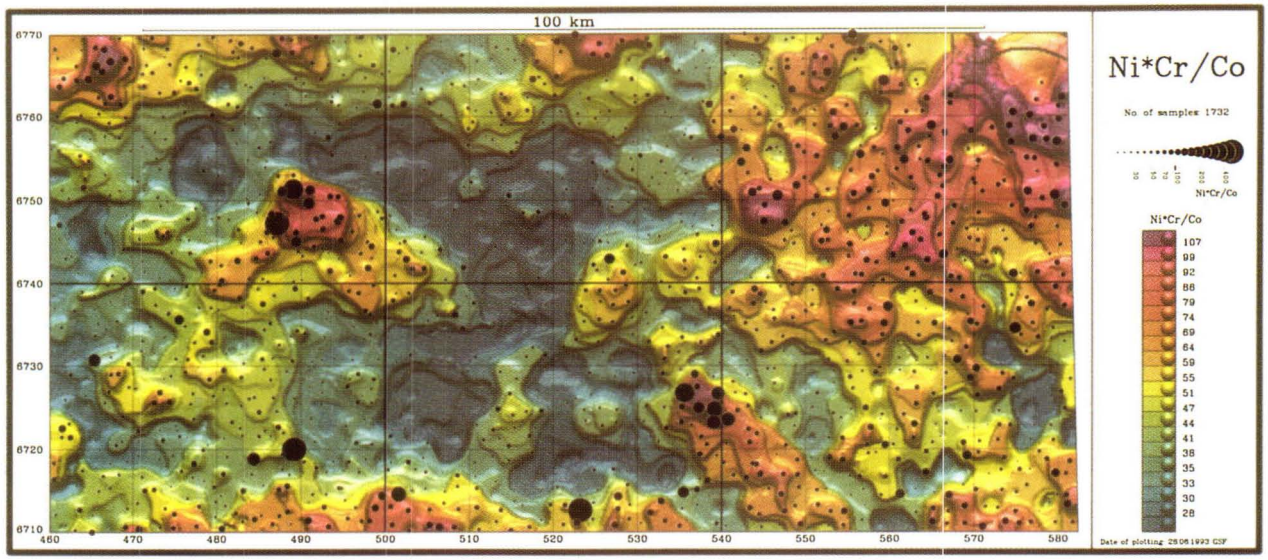

Fig. 41. Cr x Ni/Co ratio indicating mafic and ultramafic Ni-bearing formations.

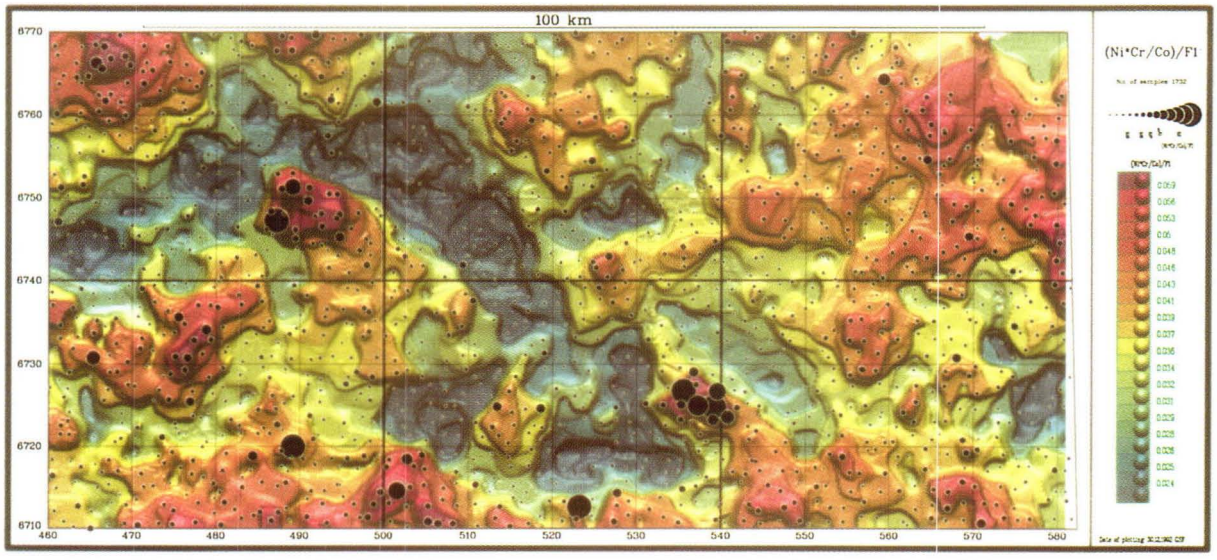

Fig. 42. (Cr x Ni/Co)/F1 ratio. The variation caused by the leachable material in samples has been filtered away by regional factor 1.

Thompson Ni belt in Canada. There the sulphides of Ni-bearing intrusions and the sulphides of graphitic schists in the proximity of Ni orebodies show elevated Ni/Co ratios, and the Cr content was highest in magmatic sulphides.

The highest anomalies on the (Ni x Cr/Co)/F1 maps indicate the presence of mafic or ultramafic intrusions with a Ni-bearing sulphide phase. The Ni/F1 map enhances the Ni mineralisations more than the (Ni x Cr/Co)/F1 map does. These maps should be used together because the dispersion caused by ultramafic rocks is usually greater than that caused by Ni deposits and because Ni deposits may also occur outside the intrusion.

Analysis of the till geochemical data (elements as well as factors) indicates only one area clearly potential for Ni deposits in the Häme belt: the Särkisuo area, which includes one known small low grade Ni-deposit. Potential exists for other, as yet unknown, Ni deposits in this area, because not all the Ni-anomalous till geochemical samples can be due to the known deposit. In till geochemistry the Särkisuo area resembles the Vammala and Kylmäkoski deposits. This was detected in the similarity analysis, in which the till geochemical samples from the surroundings of the Vammala and Kylmäkoski Ni deposits were used as signatures for this deposit type (Tiainen et al. 1991). The Hyvinkää gabbro, too, has Ni anomalies in till, and small low grade unneconomic Ni mineralisations have been located (Lindmark 1983). Its P-Ti(-V) potential seems, however, to be higher than the Ni potential (Pakarinen 1984). The situation is similar to that prevailing in the Forssa gabbro. The Somernimi gabbro hosting small Ni deposits (Pääkkönen 1964a,b, Lindmark 1982b) also shows up in till geochemistry. In addition, there are two anomalous areas with indications for Ni mineralisations on map sheets 211303 and 204401.

DATA INTEGRATION

Selected geological, till geochemical and geophysical variables, interpolated into a 1 km x 1 km regular grid, were integrated by similarity analysis into predictive Zn, Cu and Ni potential maps. Each pixel in the study area was compared with the pixels of the Tupala Zn-Pb deposit, the altered rocks related to the Katumajärvi Cu-Zn and Cu-Au mineralisations and the Särkisuo Ni-Cu deposit by applying the SIMANA program of the GSF, which uses cosine theta as a distance measure (Tontti et al. 1981, Gaál & Koistinen 1988).

Low-altitude airborne geophysical magnetic and electromagnetic data were classified with the aid of training areas representing the same deposits as those in the similarity analysis.

Deposit models

The Tupala Zn-Pb deposit

The Tupala volcanic hosted Zn(-Pb-Ag-S) deposit has been interpreted by Mäkelä (1989) and Papunen (1990) as a volcanic-exhalative hydrothermal massive sulphide deposit formed in a distal basin in an island-arc environment and represents the Kuroko-type of massive sulphide deposit. Although the deposit itself does not show up in the data sets analysed, the formation hosting the ore deposit has features that can be used as fingerprints of this deposit type in locating other similar areas in the study area.

Kuroko-type ore deposits are typically associated with bimodal volcanism, caldera formation and hydrothermal activity in an extentional tectonic regime (Sawkins 1990). Most of the deposits are hosted by felsic volcanites (Sillitoe 1982).

The Tupala ore deposit is hosted by felsic volcanites and hydrothermally altered rocks such as skarns and cordierite-mica gneisses (Mäkelä 1989, Papunen 1990). Cordierite-anthophyllite rocks, sericitised schists and intermediate volcanites are also closely related to the deposit. The deposit is situated in a fault zone that probably follows the fractures of an early rift zone which controlled igneous and hydrothermal activity at the time of ore formation. Although it is difficult to prove a genetic relationship between the faults and ore deposition without detailed studies of the deposit, the faults are included in the Tupala deposit model because of their spatial relationship with the deposit. The fault zone values were expressed as the number of faults within 1.5 km of the centre of each pixel.

The hydrothermally altered cordierite-anthophyllite rocks typically have low-grade magnetite dissemination causing aeromagnetic anomalies in the neighbourhood of massive sulphide deposits (Nikander 1988). In this they resemble the metamor-

phosed rocks after propylitic alteration around porphyry Cu deposits (Grant 1985b). In the surroundings of the Tupala deposit the magnetic anomalies are not very strog, but they can be enhanced by filtering. This gives an impression of an isoclinal fold in the area and shows the direction of possible continuations of the known deposit (Fig. 43). The same rocks also have higher density than mica gneisses and schists or unaltered felsic volcanics. Massive sulphide deposits with pyrrhotite are usually shown by electromagnetic measurements (Huhtala 1988). In Tupala, however, the thick clay deposits in deep fracture valleys hamper the use of electromagnetic data.

The surroundigs of the Tupala ore deposit are faintly visible on the till geochemical Zn and Zn/F1 maps (Figs 32 and 33).

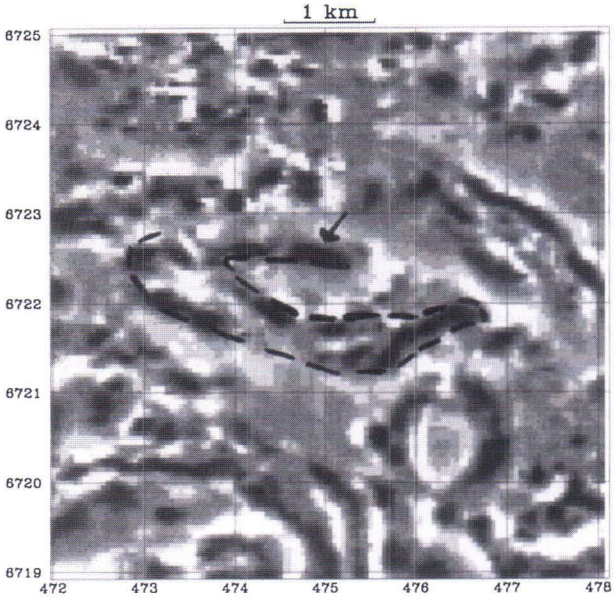

Fig 43. Surroundings of the Tupala Zn-Pb-Ag deposit shown by filtered low-altitude aeromagnetic data. The arrow indicates the known deposit and the dashed line the structure and possible continuations of the deposit.

The Katumajärvi Cu-Zn deposit

The cordierite- and cummingtonite-bearing rocks in the Katumajärvi area are interpreted as metamorphosed equivalents of the propylithic alteration zone at the footwall of the Kuroko-type deposits; the sericite schists are interpreted as the sericitic alteration zone.

The volcanic rocks at Katumajärvi contain felsic, intermediate and mafic pyroclastics, lavas and veins. The ore mineralisations include both stockwork and stratiform deposits. The stockwork deposits comprise Au-bearing Cu deposits and pyritic veins hosted by hydrothermally altered, locally silicified, garnet-cordierite and cordierite-anthophyllite rocks and sericitic rocks. The stratiform disseminated Zn-Cu deposits occur at the contact of felsic and intermediate or mafic volcanites. These two ore deposit types represent different levels of the same mineralising process. Although they have different host rocks with different geophysical properties, the accuracy of the data sets used and the 1 km x 1 km pixel size make it difficult to determine their potential separately. The aim of the prediction of Katumajärvi-type deposits was first to find the areas that contain altered rocks.

The altered rocks have more distinctive characteristics than the disseminated pyritic Cu-Zn deposits. The magnetite-bearing cordierite-anthophyllite rocks, including the Cu-Au vein deposits, show strong positive magnetic anomalies (Fig. 44), a moderate gravity anomaly and a high Cu content in till geochemistry. In low-altitude geophysics with

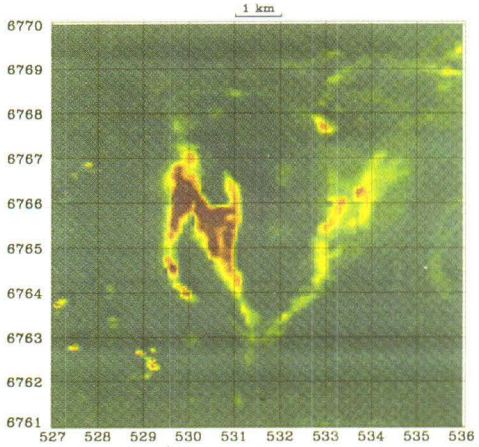

Fig. 44. Hydrothermally altered cordierite-anthophyllite rocks and the structure of Katumajärvi are shown by the high positive low- altitude magnetic anomaly dark purple in colour.

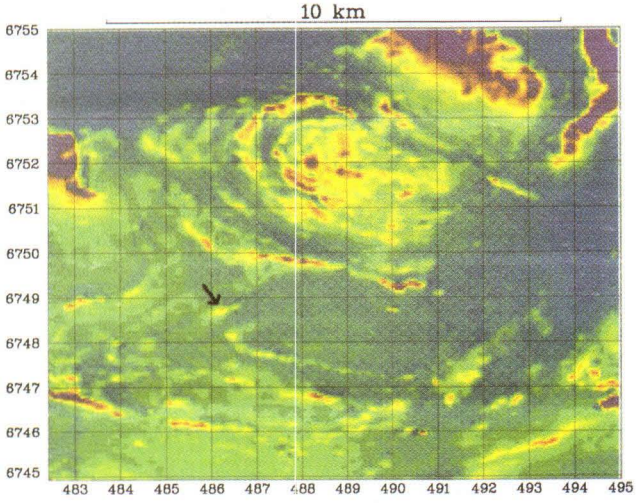

Fig. 45. Särkisuo Ni-Cu deposit is hosted by a small hornblende gabbro shown by a weak magnetic anomaly (arrow). The circular structure northeast of Särkisuo indicates the layered structure of the Forssa gabbro.

a 50 m x 50 m pixel size the pyritic Zn-Cu deposits are situated either at the boundary of areas with low and high magnetic intensity or in areas with low magnetic intensity, whereas in the high altitude magnetic data and in the other data sets the pixels containing the known deposits show more variation than the pixels containing altered rocks and stockwork deposits.

The Särkisuo Ni-Cu deposit

Small and poorly documented though it may be, the Särkisuo Ni-Cu deposit is the most significant Ni deposit in the study area. It therefore served as a nickel deposit model in the similarity analysis to determine whether the study area includes any other Vammala-type deposits.

The Särkisuo Ni-Cu deposit is hosted by a slightly magnetic gabbro in a mica schist environment (Huopaniemi 1978). The mineralisation is like a satellite of the Forssa gabbro, which is a circular mafic to ultramafic intrusion (Fig. 45). According to the aeromagnetic data, the gabbro is not as wide as shown by the map of Neuvonen (1954); the circular intrusion, at least, should be separated from the northern volcanic or subvolcanic mafic rocks.

In his statistical study of the lithogeochemistry of Ni-bearing intrusions in the Svecofennian domain, Mäkinen (1987) classifies the Forssa gabbro as a group with low Ni potential. However, in till geochemistry the Forssa gabbro resembles the intrusions in the Vammala area, having high Mg, Ni, Cr and Co contents: it differs from Vammala in its high P and Ti contents. This could indicate the apatite or titanite-potential of the Forssa gabbro.

The Särkisuo intrusion differs from the main Forssa gabbro in having a lower P and Ti content in till. In that respect it resembles the Vammala intrusion, whereas the Forssa gabbro is more like the Hyvinkää gabbro.

Similarity analysis

The similarity analysis was performed using SIMANA, a program which calculates pixel by pixel the similarity values between the model pixels and the analysed pixels as a mean of similarities using cosine theta as a similarity measure:

$$\cos\theta_{ij} = \frac{\sum_{k=1}^{m} x_{ik}\, y_{jk}}{\sqrt{\sum_{k=1}^{m} x_{ik}^2 \sum_{k=1}^{m} y_{jk}^2}},$$

where $\cos\theta_{ij}$ is the $\cos\theta$ coefficient between the analysed cell i and the model cell j, x_{ik} is variable k in the analysed cell i, y_{ik} is variable k in the model cell j, and m is the number of variables (Gaál & Koistinen 1988).

The similarity values, called the favourability index for the metal in question, were divided into tventy classes and displayed graphically in colour tones, where dark red indicates high and blue indicates low favourability (Figs 46, 47 and 50).

The pixels containing the Tupala, Katumajärvi and Särkisuo deposits and the pixels closest to them were used as deposit models to calculate the favourability for volcanic hosted Zn-Pb and Cu-Zn deposits and for Ni-Cu deposits hosted by mafic intrusives. The variables used were selected after the data sets had been analysed. Thus they are either fingerprints or exclude the deposit type in question. To avoid excessive enhancement of known altered rocks, which makes it more difficult to detect unknown altered rocks in the result of the analysis, the features searched for, e.g., the altered rocks in the Katumajärvi model, were not used as a variable. The variables and their numeric values in the models used in the similarity analysis are shown in Table 7.

Variables in the Tupala and Katumajärvi models

Basically, the Tupala and Katumajärvi deposits represent the same genetic, but different metallic, types of Kuroko-type deposit. The Tupala Zn-Pb deposit represents the black ores or distal deposits of the Kuroko deposit model, whereas Katumajärvi is composed of stockwork Cu-Au-pyrite and stratiform Cu-Zn mineralisations.

The metallic types were taken into account by using the Zn derivatives Zn/F1 and the Zn factor as till geochemical variables in the Tupala model and the Cu derivatives Cu/F1 and the Cu factor in the Katumajärvi model.

As to the geological variables, the volcanites were weighted slightly differently for the Tupala and Katumajärvi models. The Zn deposits (black ores in the Kuroko-type) are more clearly related to felsic volcanites. The Au-bearing stockwork-type Cu deposits in the feeder zone can be related equally well to mafic and to felsic volcanites but more often to their alteration products.

In the Tupala model the clear spatial relation between felsic volcanites and the ore deposit was taken into account by using felsic volcanites as a variable in the similarity analysis in addition to the sum of all the volcanites. In the Katumajärvi model,

Table 7. Variables and range of values used in the similarity analysis.

Models	Tupala Zn-Pb	Katumajärvi Cu-Zn	Särkisuo Ni-Cu
Location of model			
x-coord	6722.500 -	6765.500 - 6766.500	{6748.500 {6747.500
y-coord	2474.500 - 2475.500	2529.500 - 2530.500	{2486.500 {2487.500
Number of model pixels	2.00	4.00	2.00
Variables			
Geology			
Volcanic rocks	1.00	0.43 - 0.95	
Felsic volcanics	0.00-0.06		
Pelitic rocks			0.04 -1.00
Intermed. intrusives	0.00	0.05-0.57	
Mafic/ultramafic intrusives		0.00	0.00 -0.17
Faults	1.00		
Geochemistry			
Cu		41.8 -63.5	
Ni*Cr/Co			108.49 - 120.42
Cu/Fl		0.031 - 0.075	
Ni/Fl			0.018 -0.019
Zn/Fl	0.027 -0.028		
(Ni*Cr/Co)/Fl			0.078
F9_6		0.943 - 3.400	
F9_7			2.04
F9_9	-0.707 - 0.346		
Geophysics			
Aeromagnetic		50.00 - 390.00	-176.00 - -146.00
Magnetic edge	-33.00 - -5.00	42.00 - 384.00	-37.00 - -6.00
Bouguer anomaly, horiz. der.	1.17 - 1.46	0.84 - 0.95	0.46 - 0.90
Bouguer anomaly, 2nd vert. der.	-1.35 - -0.56	-2.12 - -1.15	1.44 - 2.86

the sum of volcanic rocks in a pixel alone represents the volcanic processes. The mafic and ultramafic intrusives were included in the Katumajärvi model in order to exclude them from areas that probably contain altered volcanic schists. The mafic and ultramafic intrusives, e.g. the Hyvinkää gabbro, sometimes show geophysical properties similar to those of the cordierite-anthophyllite rocks. Faults were included in the Tupala model because they are so clearly spatially related to the model deposit.

The geophysical variables in the Tupala and Katumajärvi models include gravity data (the horizontal derivative and the second vertical derivative of the Bouguer anomaly interpolated to a 1 km x 1 km grid) and magnetic data (high altitude total intensity in a 1 km x 1 km grid).

Variables in the Särkisuo model

Like the Vammala type deposits, the Särkisuo Ni-Cu deposit is hosted by mafic or ultramafic intrusives in a pelitic schistose or gneissic environment. These lithologies are included in the Ni-Cu deposit model. Migmatites, schollen migmatites in particular, are very important indicators of a Ni province (Gaál 1971). The migmatites are not, however, clearly enough specified on old geological maps to be useful as variables in ore potential mapping.

As till geochemical data show clear fingerprints of this type of Ni deposit, they were weighted using four different variables in the similarity analysis: Ni*Cr/Co, (Ni x Cr/Co)/F1 and Ni/F1. The first two variables indicate Ni-bearing environment and the last one Ni-bearing intrusions.

The geophysical variables are the same as in the Tupala and Katumajärvi models except for the addition of one magnetic variable with edge enhancement. Mafic and ultramafic intrusions usually have some fingerprints in the magnetic data. There are magnetite-rich gabbros because serpentinisation of ultramafites produces magnetite. Some gabbros are, however, nonmagnetic.

Results

Cu-Zn-Pb potential areas

The Cu-Zn-Pb potential areas of the Häme belt were defined applying similarity analysis with the Tupala Zn-Pb and Katumajärvi Cu-Zn deposits as models (Figs 46 and 47) and by comparing the results of the similarity analysis with corresponding till geochemical maps, factor score maps and mineral indication data.

The Zn-potential areas with the Tupala model clearly follow the volcanic belts surrounding the late orogenic granites and the high metamorphic dome. The weakness of the Tupala model is its low Zn content in till. Therefore, the areas with the highest similarities in the Tupala model also lack a high Zn content in till. A more reliable prediction is obtained by comparing the similarities of the Tupala and Katumajärvi models with each other and with the factor score maps and the Cu and Zn till geochemical anomalies.

The known Zn-Cu-Au prospects of Tupala, Katumajärvi and Kotkakorpi have moderate to high Cu-Zn potentiality. Other interesting targets for Cu-Zn exploration are the Pajula volcanic belt to the northeast of Somero (map sheet 202405B-D), the volcanic rocks to the west of the Satulinmäki Au prospect (202403D), Sakarajärvi volcanic belt (204205B-D), the volcanites at the northern boundary of the Onkimaa granodiorite (204410B-202411A, 202411C) and several targets in the volcanic belts surrounding the Koijärvi granodiorite (211302C, 211305, 211309 and 211311) (Figs 48 and 49).

Ni-Cu potential areas

The Ni potential in the Häme belt was assessed applying similarity analysis, with the Särkisuo Ni-Cu mineralisation as a model. According to the model, the most favourable areas should include mafic or ultramafic intrusions in a metapelitic environment, have a till geochemical Ni anomaly and show slight aeromagnetic and gravity anomalies.

The similarity analysis (Fig. 50) indicates four Ni targets in the study area. The same targets are favourable for Ni deposits as shown by factor analysis and till geochemistry anomalies (Fig. 51). The most favourable area is in the surroundings of the Särkisuo deposit. There are also three areas, map sheets 211303, 202410 and 204401 that have high similarity with the Särkisuo Ni deposit. The first two of these have Ni indications in their vicinity. The known geology of these targets is, however, not as favourable for Ni deposits as that in the Särkisuo area.

The Särkisuo area is thus the only clear Ni target in the study area. It shows Ni potential according to both similarity analysis and till geochemical data. Till geochemistry implies that the Hyvinkää and Forssa gabbros also have Ni potential. They are not, however, of the same type as the Särkisuo deposit.

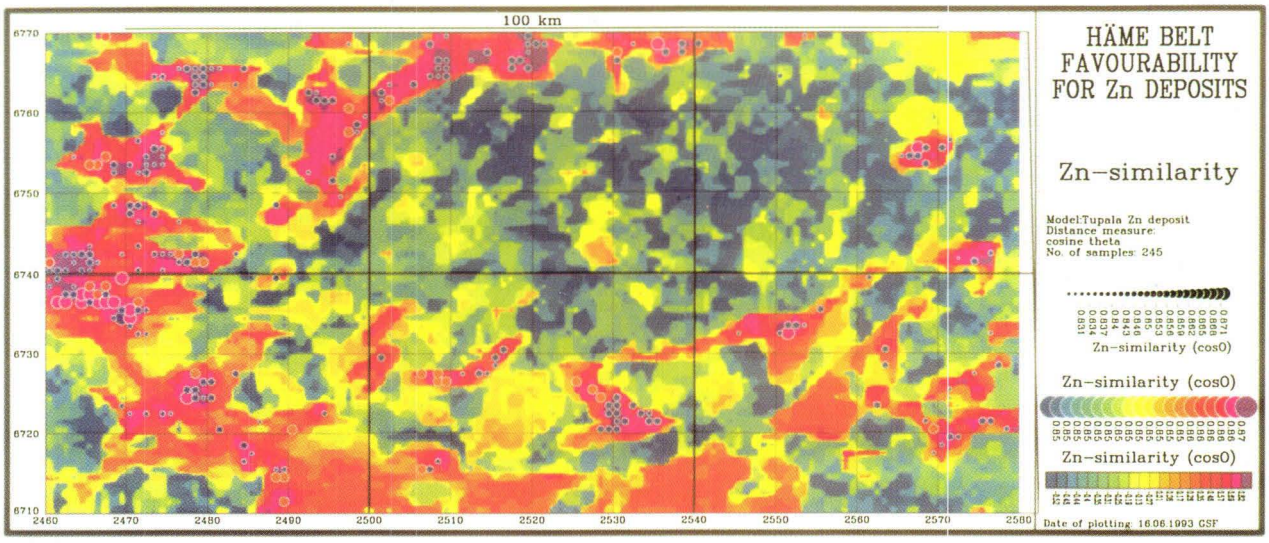

Fig.46. Similarity analysis with the Tupala Zn model. Cosine theta was applied as a distance measure. The most potential areas for Tupala type deposits are shown by the dark-red background, with dots indicating the similarity of the pixels in the most potential areas.

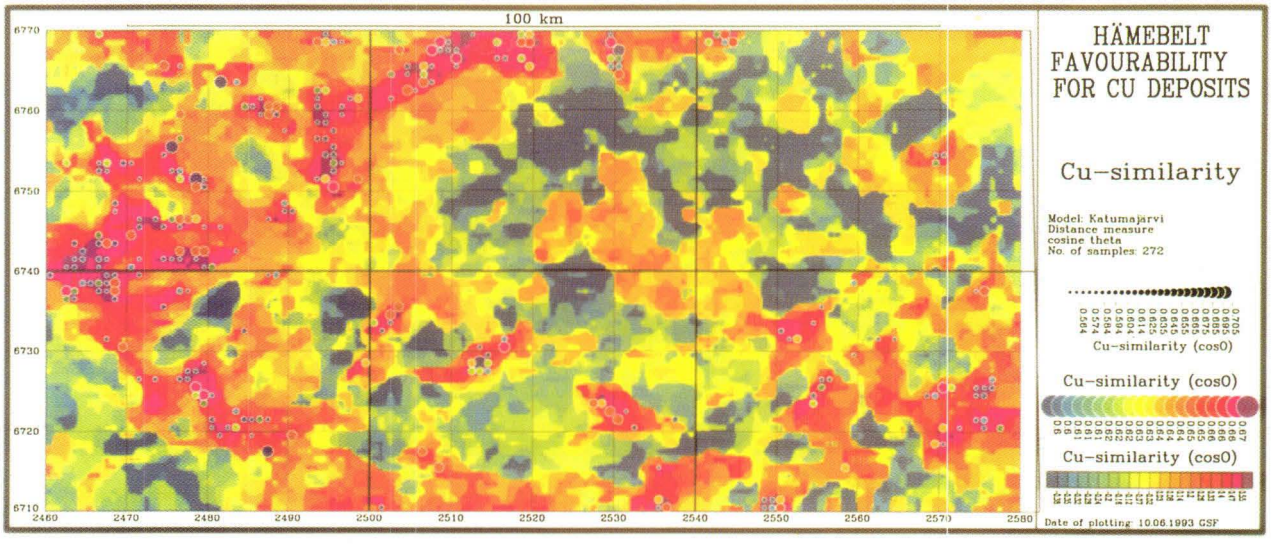

Fig. 47. Similarity analysis with the Katumajärvi Cu-Zn model.

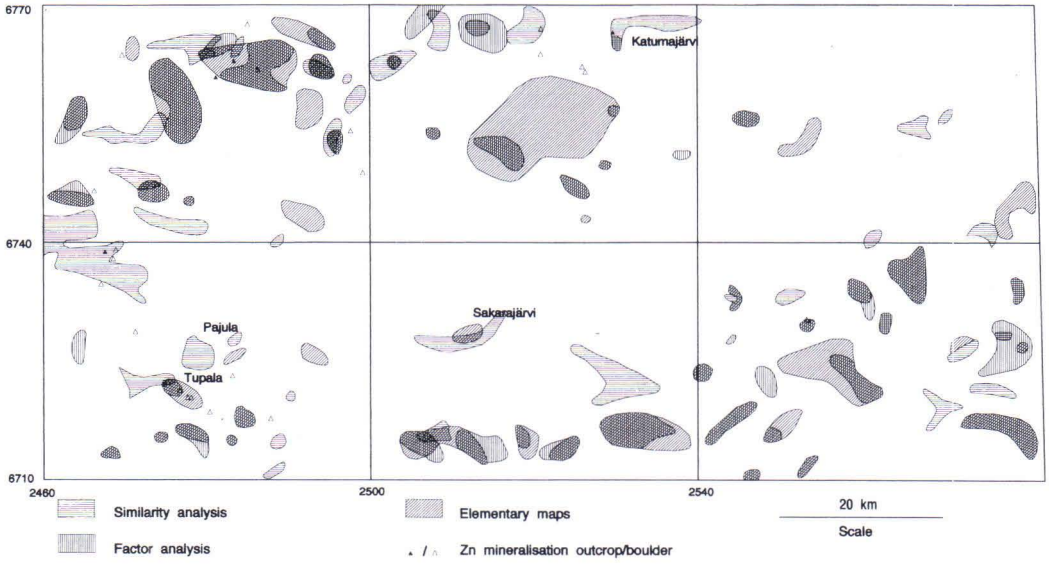

Fig. 48. Areas with high favourability for Zn deposits according to similarity analysis (Tupala model), factor analysis and element ratio maps.

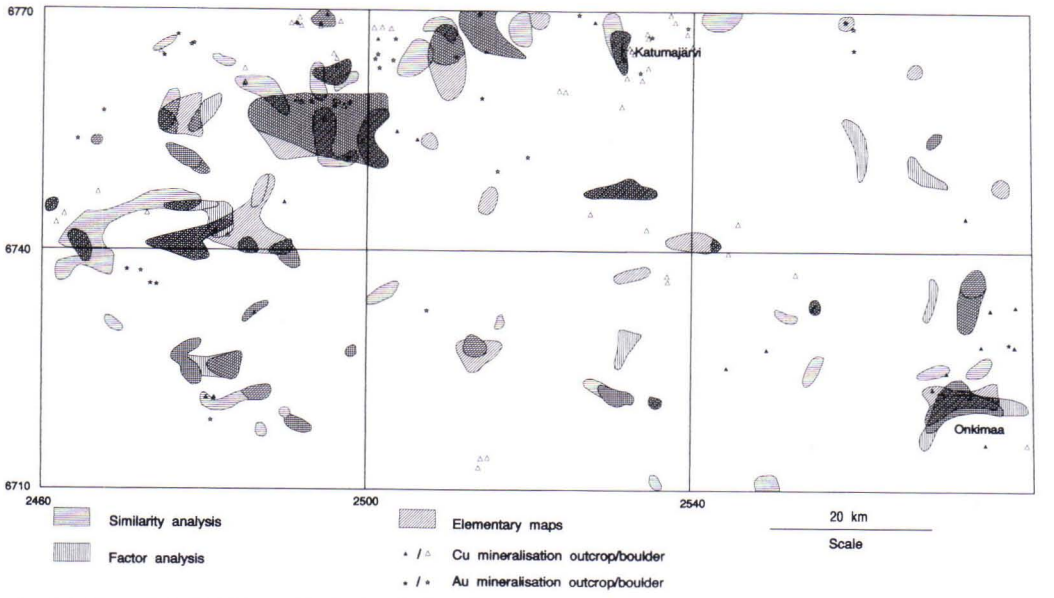

Fig. 49. Areas with high favourability for Cu deposits according to similarity analysis (Katumajärvi model), factor analysis and element ratio maps.

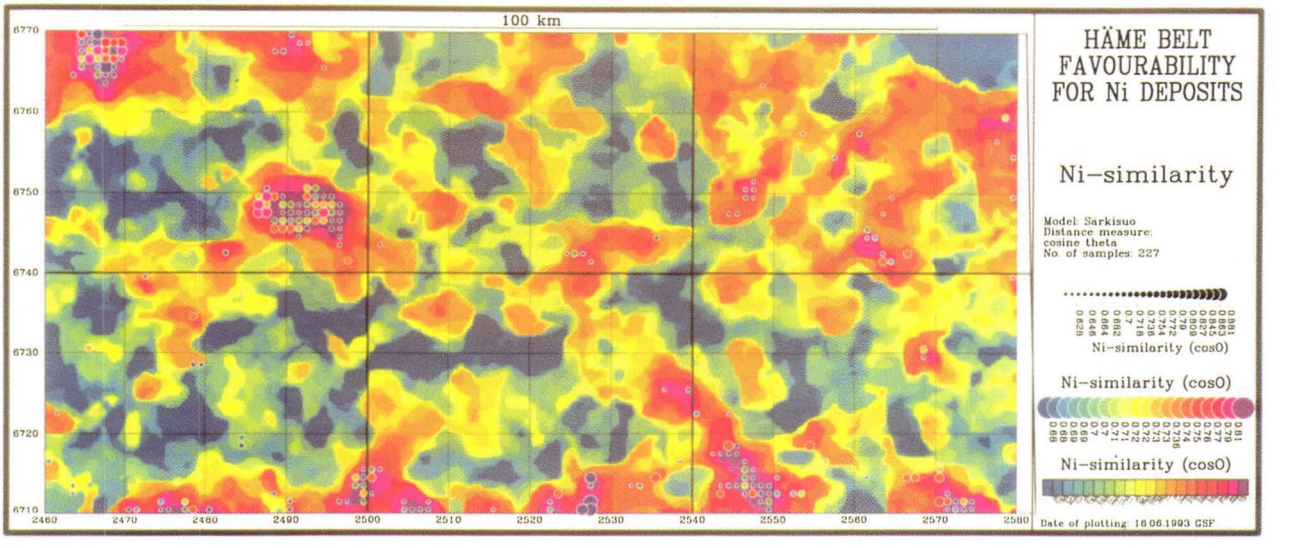

Fig. 50. Similarity analysis with the Särkisuo Ni-Cu model.

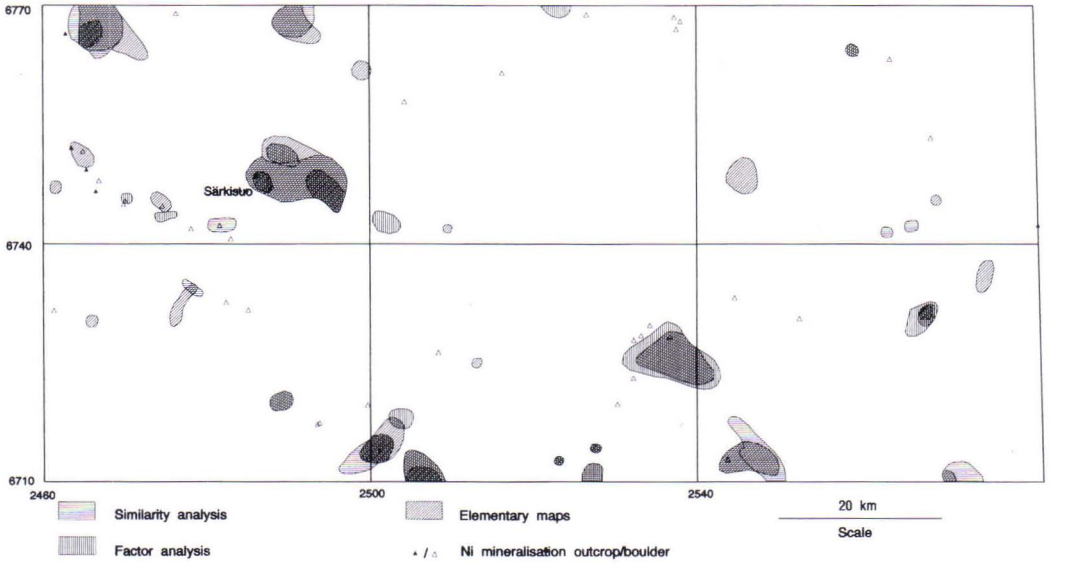

Fig. 51. Areas with high favourability for Ni-Cu deposits according to similarity analysis (Särkisuo model), factor analysis and element ratio maps.

CONCLUSION

The schists in the Häme belt consist mainly of calc-alkalic intermediate volcanites with some tholeiitic affinities. The volcanic belts are intruded by circular I-type granodioritic stocks and batholiths. The central part of the Häme belt consists of S-type migmatitic late-orogenic microcline granites. At the Tervakoski antiform the high metamorphic rocks are exposed beneath the microcline granites, probably being the lowest stratigraphical horizon in the Häme belt and slightly older than the Svecofennian volcanites in general. The southern part of the Häme belt consists of a mafic block that includes the Hyvinkää gabbro.

The Pääjärvi fault zone separates the Häme belt in the north from the Ni-bearing greywacke schist belt, and the Hirsjärvi fault zone in the south from the West Uusimaa complex. These fault zones are extremely important not only metallogenetically but also for understanding the geological development of southern Finland.

The main metallogenic types of the Häme belt are: Cu-Zn-Au deposits, Ni-Cu deposits, Au deposits, Fe-Ti-V(P) deposits and certain others, including W, Mo, U, Sn and some Cu deposit types. The Cu-Zn(-Au) deposits represent a hydrothermal volcanic hosted deposit type that has some features in common with Kuroko-type base metal deposits. Indications of Cu-bearing tourmaline breccias have been found in the surroundings of the Aulanko and Onkimaa batholiths. Gold-copper deposits typically occur in strongly sheared zones. Nickel-Copper deposits and Fe-Ti-V(-P) deposits are hosted by mafic or ultramafic intrusives, but of different types. Tungsten, Mo, Sn, U and some Cu deposits are related to granites, Sn and U especially to S-type late- orogenic granites.

The main targets for exploration were assessed by integrating the geological, geophysical and geochemical data with SIMANA and by analysing the till geochemical data, low-altitude geophysical and mineral indication data. The known deposits in the study area were not the best possible for deposit modelling and image processing of low-altitude geophysics. The Katumajärvi Cu-Zn deposit is small and the Tupala Zn deposit is under a thick clay cover, which makes it less suitable as a model with till geochemical and low-altitude geophysical data. Both the number and size of targets are therefore large. On the other hand, we tried to avoid the lost of potential targets at this stage of exploration.

The Cu-Zn potential is highest in the surroundings of the known deposits and prospects, e.g. Tupala, Katumajärvi, Forssa and Ypäjä—Jokioinen, and in the Lautaporras—Hämeenlinna area. In addition, there are some clusters of pixels and some single pixels that show distinct similarities to the Tupala and/or Katumajärvi deposits. One interesting target that has not been reported earlier and from which there are no indications in the mineral indication data bases of the GSF is the felsic volcanic belt of Pajula (map sheet 202405B-D).

The Ni potential is concentrated in the Särkisuo area, although there are a couple of other targets worth checking.In the assessment of the Ni potential the regional backgound level was filtered away from the till geochemistry data by regional factor 1. Interesting new areas were revealed using the same method for Cu and Zn.

Several targets for exploration of base metal deposits were detected. Some of them have already been partly surveyed, but some are new. The next stage is to prioritise the targets and to reduce the size of the target areas. This will require field checking in cooperation with expert geologists.

ACKNOWLEDGEMENTS

We wish to express our gratitude to the Economic Geology Department, especially its mineral assessment unit, the Geochemistry Department and the Geophysical Department of the GSF for providing us with the access to the data sets used. We are grateful to our colleagues Mikko Tontti and Viljo Kuosmanen for critically reading the manuscript and making valuable improvements; to Marja-Liisa Räisänen for enlightening discussions about till geochemistry; to Tuure Nyholm, Graeme Waller, Merja Mäkelä and Seija Suominen for digitizing the geological data and participating in the field work; to Pirkko Kurki for helping with the drafting; to Saija Tuiskula and Helena Korhonen for improving the photo copies; to Gillian Häkli for correcting the English; and to Stiina Seppänen for editorial work.

REFERENCES

Aarnisalo, J. 1984. Image processing and intergration of geophysical, Landsat and other data as a tool for mineral exploration in glaciated Precambrian terrain. In: Proceedings of the International Symposium on Remote Sensing of Environment.Third Thematic Conference: "Remote Sensing for Exploration Geology, vol 1. Colorado Springs, Colorado, 107-128.

Aarnisalo, J. 1990. Use of image processing and intergrated analysis in Exploration by Outokumpu Oy, Finland.In: Gaal, G. & Merriam, D. (ed.) Computer Applications in Resource Estimation Prediction and Assessmentfor Metals and Petroleum, 195-212.

Aarnisalo, J. , Franssila, E., Eeronheimo, J., Lakanen, E. & Pehkonen, E. 1982. On the integrated use of Landsat, geophysical and other data in exploration in the Baltic Shield, Finland. Photogramm. J. Finland 9 (1), 48-64.

Antón-Pacheo, C. & Gumiel, J.C. 1991. Multispectral analysis and digital classification of Landsat Thematic mapper data. In Development of new multi-disciplinary techniques for mineral exploration in several areas of the western Iberian Peninsula. Ed. by P. Gumiel, C. Anton-Pacheo and R. Campos.

Arkimaa, H. 1982. Some examples of multi-channel analysis of Landsat and geophysical data. Photogramm. J. Finland 9 (1), 38- 47.

Bleeker, W. 1990. Thompson area-general geology and ore deposits. In: Goodfellow, W.D. (ed.) Geology and mineral deposits of the Flin Flon and Thompson belts, Manitoba (Field trip 10). 8th IAGOD symposium, Field trip guidebook. Geol. Surv. Canada Open file 2165, 93-118.

CSIRO 1990. The Disimp Users Guide: An Introduction to Device - Independent Software for Image Processing, Apollo Disimp version 5.0, 487p. and The Disimp Utilities Refrence Manual: A Detailed Refrence to the Software Utilities in Disimp, version 5.0, 388p. CSIRO (Commonwealth Scientific and Industrial Research Organization), Division of Information Technology Centre for Spatial Information Systems, Canberra, Australia.

Drury, S.A. 1987. Image interpretation in Geology. Allen & Unwin, London, 243 p.

Front, K. & Nurmi, P. 1987. Characteristics and geological setting of synkinematic Svecokarelian granitoids in southern Finland. Precambrian Res. 35, 207-224.

Gaál, G. (ed.) 1988. Exploration target selection by intergration of geodata using statistical and image processing techniques: an example from Central Finland. Part I, (Text). Geol. Surv. Finland, Rep. Invest. 80, 156 p.

Gaál, G. & Gorbatschev, R. 1987. An outline of the Precambrian evolution of the Baltic Shield. Precambrian Res. 35, 15-52.

Gaál, G. & Koistinen, E. 1988. Deposit modelling.In: Gaál, G. (ed.) Exploration target selection by integration of geodata using statistical and image processing techniques: an example from Central Finland, Geol. Surv. Finland, Rep. Invest.

Gaál, G., & Rauhamäki., E. 1971. Petrological and structural analysis of the Haukivesi area between Varkaus and Savonlinna, Finland. Bull. Geol. Soc. Finland 43, 265-337.80, 102-112

Gaál, G., Autio, H., Lehtonen. M., Mäkinen, A., Oksama, M., Saltikoff, B., Tontti, M. & Vuorela, P. 1977. Pohjois-Suomen malmitiedostoprojekti. Summary: Ore Data File Project for Northern Finland. Geol. Surv. Finland, Rep. Invest. 26, 43 p.

Grant, F.S. 1985a. Aeromagnetics, geology and ore environments, I. Magnetite in igneous, sedimentary and metamorphic rocks: an overwiew. Geoexploration 23, 303-333.

Grant, F.S. 1985b. Aeromagnetics, geology and ore environments, II. Magnetite and ore environments. Geoexploration 23, 335-362.

Haataja, I. 1987. Hämeenlinnan Katumajärven alueen kallioperän kehityksestä ja malminmuodostuksesta. Unpubl. M. Sc. thesis. Univ. Oulu, Dep. Geology, 75 p.

Haavisto, M., Grönlund, T., Lahermo & Stèn, C. G. 1980. Geological map of Finland 1 : 100 000, sheet 2024 Somero. Explanation to the maps of Quaternary deposits (in Finnish, with English summary). Geol. Surv. Finland, 66 p.

Haga, I. 1984. Kaivoslain 19§ mukainen tutkimustyömaaselostus Somero, Satulinmäki, kaivosrekisterinro 3421/1. In the archives of The Ministry of Trade and Industry, 2 p.

Hakkarainen, G. 1989. Lahden-Someron vulkaniittimuodostuman stratigrafia, Sinkkiprojekti 1989. Publ. No. 20, Instutute of Geology and Mineralogy, University of Turku, Finland, 59 p.

Hakkarainen, G. 1990. Lithostratigraphic and geochemical relations in the Hämeenlinna-Somero Volcanic belt. In: Kähkönen, Y. (ed.) Proterozoic Geochemistry, Helsinki '90, abstracts, symposium by IGCP Project 217 Proterozoic

Härme, M. 1953. Pre-Quarternary rocks, Sheet 2042 Karkkila. Geological Map of Finland 1:100 000.

Härme, M. 1954. Geological map of Finland 1:100 000, sheet 2042 Karkkila. Explanation to the map of rocks (in Finnish, with English summary) Geological Survey of Finland, 42 p.

Härme, M. 1955. Kulonsuonmäen titaanirautamalmialueen geologiasta. On the geology of the titaniferous iron ore area of Kulonsuonmäki (in Finnish with English summary). Geoteknillisiä julkaisuja N:o 59. Geological Survey of Finland, 19 p.

Härme, M. 1965. On the potassium migmatites of southern Finland. Geol. Surv. Finland Bull. 219, 43 p.

Härme, M. 1978. Geological map of Finland 1:100 000, sheets 2043 Kerava and 2044 Riihimäki. Explanation to the pre-Quarternary rocks (in Finnish with English summary). Geological Survey of Finland, 51 p.geochemistry national working group of Finland, 12-15.

Hietanen, A. 1975. Generation of potassium-poor magmas in the northern Sierra Nevada and the Svecofennian in Finland. J. Res. U.S. Geol. Surv. 3, 631-645.

Himmi, R., Huhma, M. & Häkli, T.A. 1979. Mineralogy and metal distribution in the copper-tungsten deposit at Ylöjärvi, Southwest Finland. Econ. Geol. 74, 1183-1197.

Huhma, H. 1986. Sm-Nd, U-Pb and Pb-Pb isotopic evidence for the origin of the Early Proterozoic Svecokarelian crust in Finland. Geol. Surv. Finland Bull. 337, 48 p.

Huhtala, T. 1988. Exploration history and fingerprints. Pp. 70-76 in Exploration target selection by integration of geodata using statistical and image prossessing techniques: an example from Central Finland, Rep. Invest. 80, ed. by G. Gaál

Huopaniemi, P. 1978. Selostus tutkimustyöstä Malmikaivos Oy:n valtauksilla Särkijärvi, Kaiv.rek.no. 2454/1, kaiv.rek.no. 2454/2 ja Särkisuo 1-3, kaiv.rek.no. 2520/1-3, 1 p., in the archives of The Ministry of Trade and Industry.

Kaitaro, S. 1956. Pre-quaternary rocks, Sheet 2044 Riihimäki. Geological Map of Finland 1:100 000.

Ketola, M. 1989. The role of geophysics and geochemistry in sulphide and precious metal exploration in the light of some recent ore discoveries in Finland. In: Garland, G. D. (ed.) Proceedings of Exploration '87. Third Decennial International Conference on Geophycical and Geochemical Exploration for Minerals and Groundwater, Ontario Geological Survey, Special Volyme 3, 837-854

Kinnunen, A. 1987a. Kaivoslain 19§ mukainen tutkimustyöselostus Hämeenlinna, Katumajärvi, kaivosrekisterinro 3250/1. In the archives of The Ministry of Trade and Industry. 3 p.

Kinnunen, A. 1987b. Kaivoslain 19§ mukainen tutkimustyöselostus Kalvola, Kotka, kaivosrekisterinro 3252/1. In the archives of The Ministry of Trade and Industry. 3 p.

Kinnunen, K. 1979. Ore mineral inclusions in detrital quartz contained in basal till and the glacial transport from the Ylöjärvi copper-tungsten deposit, southwestern Finland. Geol. Surv. Finland Bull. 298, 55 p.

Koistinen, E. 1984. Matemaattiset menetelmät Vihannin sinkki-kupari -malmivyöhykkeen malmipotentiaalin arvioinnissa. Ph.Lic. thesis, TKK, Espoo, 93 p.

Koistinen, E., & Gaál, G. 1988. Factor analysis. In: Gaal, G. (ed.) Exploration target selection by integration of geodata using statistical and image processing techniques: an example from Central Finland, Geol. Surv. Finland, Rep. Invest. 80, 86-94.

Koljonen, T. (ed.) 1992. Suomen Geokemian Atlas, osa 2: Moreeni. The Geochemical Atlas of Finland, part 2: Till. Geol. Surv. Finland, 218 p.

Koljonen, T. & Malisa, E. 1991. Solubility in aqua regia of selected chemical elements occurring in the fine fraction of till. Geol. Surv. Finland, Spec. Pap. 9, 49-52.

Korhonen, J. 1980. Aeromagnetic Anomaly Map of Finland, 1 : 2 000 000, Geol. Surv. Finland.

Korhonen, J. 1985. A comparison of 1-,2-and 3-sensor aeromagnetic surveys. (Abstract). Geoexploration 23 (3), 438-439.

Kuosmanen, V. (ed.), 1988. Exploration target selection by intergration of geodata using statistical and image processing techniques: an example from Central Finland. Part II, (Atlas). Geol. Surv. Finland, Rep. Invest. 84, 47 p.

Lagerblad, B. 1988. Kemisk-stratigrafiska malmmodeller i Bergslagen. STU-Report 85-05150P, 15 p.

Lahtinen, R. 1991. Alueellisen moreenigeokemiallisen kartoituksen tulosten tulkinnasta. In: Salminen, R. & Roos, S.(eds.)Geokemian päivät Oulussa 28.-29.11.1990. Vuorimiesyhdistys B 50, 52-57.

Laine, E. 1952. Suomen vuoritoimi 1809-1884. III. Harkkohytit kaivokset konepajat. Historiallisia tutkimuksia XXXI, 3. Suomen Historiallinen Seura. The Hist. Soc. Finland, 267-271.

Latvalahti, U. 1979. Cu-Zn-Pb ores in the Aijala-Orijärvi area, Southwest Finland. Econ. Geol. 74, 1035-1059.

Lehijärvi, M. 1961. Pre-quarternary rocks, Sheet 2133 Kärkölä. Geological Map of Finland 1:100 000.

Lindmark, B. 1982a. Tutkimustyöselostus Mäntsälän kunnassa valtausalueella Kotkakorpi 1. kaiv. rek. n:o 3112/1 suoritetuista malmitutkimuksista. Intern. rep. M 06/2044/-82/1/10. Explor. Dep. Geol. Surv. Finland, 15 p.

Lindmark, B. 1982b. Malmitutkimukset Somerolla kesällä 1981. Intern. Rep. M 19/2024/-82/1/10. Explor. Dep. Geol. Surv. Finland, 4 p.

Lindmark, B. 1983. Hyvinkään gabron Cu-, Ni-tutkimukset vuosina 1979-1981. Intern. Rep. M 19/2042/-83/1/10. Explor. Dep. Geol. Surv. Finland, 12 p.

Lindroos, A. 1980. En zinkmineraliserings relation till metamorfa och hydrotermalt omvandlade vulkaniska bergarter i Ypäjä, Jockis, sydvästra Finland. Unpubl. M. Sc. thesis, Åbo Akademi, Dep. Geology, 89 p.

Lintinen, P. 1993. Moreenin hienoaineksen savipitoisuuden ja omainaispinta-alan alueellinen jakautuminen Suomessa - alustavia tuloksia. Regional differences in clay content and the specific surface area of till fines in Finland - preliminary results (in Finnish, with English summary). Geologi 2, 43.

Mäkelä, K. 1980. Geochemistry and origin of Haveri and Kiipu, Proterozoic strata-bound volcanogenic gold-copper and zinc mineralizations from southwestern Finland. Geol. Surv. Finland Bull. 310, 79 p.

Mäkelä, U. 1989. Geological and geochemical environments of precambrian sulphide deposits in southwestern Finland. Ann. Acad. Sci. Fennicae A III, 151, 102 p. 50.

Mäki, T. 1986. Lithogeochemistry of the Pyhäsalmi zinc-copper-pyrite deposit, Finland. In: Prospecting in areas of glaciated terrain. Seventh International Prospecting in Areas of Glaciated Terrain Symposium, Sept. 1-2, 1986 Kuopio, Finland. IMM, London, 69-82.

Mäkinen, J. 1987. Geochemical characteristics of Svecokarelidic mafic-ultramafic intrusions assosiated with Ni-Cu occurrences in Finland. Geol. Surv. Finland Bull. 342, 109 p.

Mäkinen, J. 1992. The relation between uunit weight and geochemical and mineralogical compositions in the fine fraction of till. Bull. Geol. Soc. Finland 64, Part 1, 59-74.

Makkonen, H. 1992. 1.9 Ga tholeiittinen magmatismi ja siihen liittyvä Ni-Cu-malminmuodostus Juvan alueella, Kaakkois-Suomessa. Unpubl. Ph. Lic. thesis, Univ. Oulu, Dep. Geology, 200 p.

Mason, B., 1966. Principles of Geochemistry. John Wiley & Sons, U.S.A., 329 p.

Multala, J. & Vironmäki, J. 1981. The new aerogeophysical equipment of Geological Survey of Finland. (Abstract). Geoexploration 19 (2). 150-151.

Naldrett, A.J. 1981. Nickel sulphide deposits: calssification, composition and genesis. Econ. Geol. 75th Anniversary Vol., 628-685.

Neuvonen, K. J. 1954. Pre-Quarternary rocks, sheet 2113 Forssa. Geological map of Finland.

Neuvonen, K. J. 1956. Geological map of Finland 1:100 000, sheet 2113 Forssa. Explanation to the map of rocks (in Finnish with English summary). Geological Survey of Finland, 37 p.

Nikander, J. 1988. Depositional types. In: Gaál, G. (ed.) Exploration target selection by integration of geodata using statistical and image processing techniques: an example from Central Finland, Geol. Surv. Finland, Rep. Invest. 80, 1, 65-70.

Norusis, M. J/SPSS Inc. 1988. SPSS/PC+ V2.0 Base Manual for the IBM PC/XT/AT and PC/2. Printed in USA.

Nurmi, P.A., & Isohanni, M. 1984. Rock, till and stream-sediment geochemistry in the search for porphyry-type Mo-Cu-Au deposits in the Proterozoic Rautio batholith, western Finland. J. Geochem. Explor., 21 (1-3), 209-228.

Nurmi, P.A. & Haapala, I. 1986. The Proterozoic granitoids of Finland: Granite types, metallogeny and relation to crustal evolution. Bull. Geol. Soc. Finland 58, 203-233.

Nurmi, P.A., Front, K., Lampio, E. & Nironen, M. 1984. Etelä-Suomen svekokarjalaiset, porfyyrityyppiset molybdeeni- ja kupariesiintymät; niiden granitoidi-isäntäkivet ja litogeokemiallinen etsintä. Summary: Svekokarelian porphyry-type molybdenum and copper occurrences in southern Finland; their granitoid host rocks and litogeochemical exploration. Geol. Surv. Finland, Rep. Invest. 67, 88 p.

Oksama, M. 1987. Basic characteristics of AEM system of Geological Survey of Finland. Intern. rep. Q16.2/24.8/87/1 Geophysics Dep. Geol. Surv. Finland, 20 p.

Pääkkönen, V., 1964a. Pusulan Tarkelan järven nikkelimalmiaihe. Intern. Rep. M 17/Ps-63/1. Explor. Dep. Geol. Surv. Finland, 2 p.

Pääkkönen, V., 1964b. Tutkimukset Arimajärven pohjoispuoleisella gabro- ja peridotiittialueella. Intern. Rep. M 17/Srn-63/1. Explor. Dep. Geol. Surv. Finland, 1 p.

Pakarinen, J. 1984. Esitutkimus Lounais-Suomen P-Ti-

aiheista. Intern. Rep. M 19/2042/-84/1/10 Explor. Dep. Geol. Surv. Finland, 27 p.

Papunen, H. (ed), 1990. Sinkkiprojektin raportti. Publ. No.22, Institute of Geology and Mineralogy, University of Turku, Finland, 143 p.

Patchett, J. & Kouvo, O., 1986. Origin of continental crust of 1.9-1.7 Ga age: Nd isotopes and U-Pb zircon ages in the Svecokarelian terrain of South Finland. Contrib. Mineral. Petrol. 92, 1-12.

Peltoniemi, M., 1982. Characteristics and results of an airborne electromagnetic method of geophysical surveying. Geol. Surv. Finland, Bull. 321, 299 p.

Peltoniemi, M., 1986. Systematic airborne electromagnetic surveys in Finland: an overview. Geol. Surv Canada, Paper 86-22, 159-167.

Poikonen, A., 1991. Geologian tutkimuskeskuksen geofysikaalinen lentomittausjärjestelmä. In: Häme, T. & Holm, M. (eds.) Kaukokartoitus lentokoneesta, VTT Symposium 127, 29-35.

Puranen, R., 1968. Hyvinkään gabron ja sen naapurikivilajien magneettisista ominaisuuksista. Unpubl. M. Sc. thesis, Univ. Helsinki, Dep. Geophysics, 83 p.

Puranen, R., 1971. Karkkilan - Riihimäen alueen kivilajien petrofysikaalisista tutkimuksista sekä tulosten geofysikaalisesta ja geologisesta soveltamisesta. Unpubl. Ph. Lic. thesis, Univ. Helsinki, Dep. Geophysics, 133 p.

Pyy, H., 1978. Om Borgnäs-skifferområdets struktur och stratigrafi. Unpubl. M. Sc. thesis, Åbo Akademi, Dep. Geology, 71 p.

Räisänen, M.L., Tenhola, M. & Mäkinen, J., 1992. Relationship between mineralogy and the physico-chemical properties of till in Central Finland. Bull. Geol. Soc. Finland 64, Part 1, 35-58.

Rasilainen, K., 1991. Geochemistry and wall rock alteration at the Kangasjärvi massive sulphide deposit, Central Finland. Geol. Surv. Finland, Spec. Pap. 12, 107-110.

Ruskeeniemi, T., 1990. Kiipun muodostuman muuttumisilmiöt ja niiden merkitys malminetsinnän kannalta. Unpbl. M.Sc. thesis, Univ. Turku, Dep. Geology, 119 p.

Saltikoff, B., 1984. Boulder tracing and the Mineral Indication Data Bank in Finland. Prospecting in areas of glaciated terrain 1984, IMM, London, 179-191.

Saltikoff, B., 1992. Lounais-Suomen malmiviitteiden jaottelu malmityyppeihin. Intern. rep. M 10.1/1992/2. Econ. Geol. Dep. Geol. Surv. Finland 9 p.

Saltikoff, B. & Tarvainen, T., 1990. Explorational databases at the Geological Survey of Finland. In: Gaál, G. D.F.Merriam, D. F. (eds.) Computer Applications in Resource Estimation, Prediction and Assessment for Metals and Petroleum,. Pergamon Press, Oxford, 453 p.

Sawkins, F.J., 1990. Metal deposits in relation to plate tectonics. Springer-Verlag, Berlin, 461 p.

Schwarzer, T.F. & Adams, J.A.S., 1973. Rock and soil discrimination by low altitude airborne gamma-ray spectrometry in Payne County, Oklahoma. Econ. Geol. 68, 1297-1312.

Siegal, B.S. & Gillespie, A.R. (eds.), 1980. Remote sensing in geology. Wiley & Sons, New York, 702 p.

Sillitoe, R.H., 1982. Extensional habitats of rhyolite-hosted massive sulfide deposits. Geology 10, 403-407.

Simonen, A., 1948. On the petrology of the Aulanko area in southwestern Finland. Bull. Comm. Geol. Finlande 143, 66 p.

Simonen, A., 1949a. Pre-Quarternary rocks, Sheet 2131 Hämeenlinna. Geological Map of Finland 1:100 000.

Simonen, A., 1949b. Geological map of Finland 1:100 000, sheet 2131, Hämeenlinna. Explanation to the map of rocks (in Finnish with English summary), Geological Survey of Finland, 45 p.

Simonen, A. 1955. Pre-Quarternary rocks, Sheet 2024 Somero. Geological Map of Finland 1:100 000.

Simonen, A. 1980. The Precambrian in Finland. Geol. Surv. Finland, Bull. 304, 58 p.

Sipilä, P. 1981. Lounais-Suomen rautamalmeista. Unpubl. M. Sc. thesis, Univ. Turku, Dep. Geology, 106 p.

SPSS Inc. 1988. SPSS-X User's quide. 3rd ed. Printed in USA, 1072 p.

Talvitie, J. & Paarma, H. 1980. Precambrian basic magmatism and the Ti-Fe ore formation in central and northern Finland. In: Siivola, J. (ed.) Metallogeny of the Baltic Shield: Proceedings of the symposium held in, Finland, June 12-21, 1978, Geol. Surv. Finland, Bull. 307, 98-107.

Tiainen, M. 1989. The South-West Finland Mineral-assessment project. Geol. Surv. Finland, Spec. Pap. 10, 129-130.

Tiainen, M. 1991. Oblique rotation - a new aspect to geochemical factor analysis. Geol. Surv. Finland, Spec. Pap. 12, 219-224.

Tiainen, M. Lahtinen, R. & Salminen, R., 1991. Similarity analysis applied to till geochemical data from southwest Finland - Geochemical signatures of Vammala and Kylmäkoski nickel deposits. IMM, vol. 100, B 209-215.

Tontti, M., Koistinen, E., & Seppänen, H. 1981. Vihannin Zn-Cu-malmivyöhykkeen geomatemaattinen arviointi. Summary: Geomathematical evaluation of the Vihanti Zn-Cu ore zone (In Finnish with English summary). Geol. Surv. Finland, Rep. Invest. 54, 58p.

Wester, K. 1992. Spectral signature measurements and image processing for geological remote sensing. Meddelanden från naturgeokrafiska institutionen vid Stockholm universitet Nr A273, 130 p.

Virkkala, K. Hyyppä, J. & Valovirta, V., 1969. Geological map of Finland 1:100 000, sheet 2131 Hämeenlinna. Explanation to the map of Quarternary deposits (in Finnish, with English summary). Geol. Surv. Finland, 67 p.

Tätä julkaisua myy

GEOLOGIAN
TUTKIMUSKESKUS (GTK)
Julkaisumyynti
02150 Espoo
☎ (90) 46 931
Teleksi: 123185 geolo sf
Telekopio: (90) 462 205

GTK, Väli-Suomen
aluetoimisto
Kirjasto
PL 1237
70211 Kuopio
☎ (971) 205 111
Telekopio: (971) 205 215

GTK, Pohjois-Suomen
aluetoimisto
Kirjasto
PL 77
96101 Rovaniemi
☎ (960) 3297 130
Teleksi: 37295 geolo sf
Telekopio: (960) 3297 289

Denna publikation säljes av

GEOLOGISKA
FORSKNINGSCENTRALEN (GFC)
Publikationsförsäljning
02150 Esbo
☎ (90) 46 931
Telex: 123185 geolo sf
Telefax: (90) 462 205

GFC, Distriktsbyrån för
Mellersta Finland
Biblioteket
PB 1237
70211 Kuopio
☎ (971) 205 111
Telefax: (971) 205 215

GFC, Distriktsbyrån för
Norra Finland
Biblioteket
PB 77
96101 Rovaniemi
☎ (960) 3297 130
Telex: 37295 geolo sf
Telefax: (960) 3297 289

This publication can be obtained
from
GEOLOGICAL SURVEY
OF FINLAND (GSF)
Publication sales
FIN-02150 Espoo, Finland
☎ +358 0 46 931
Telex: 123185 geolo sf
Telefax: +358 0 462 205

GSF, Regional office of
Mid-Finland
Library
P.O. Box 1237
FIN-70211 Kuopio, Finland
☎ +358 71 205 111
Telefax: +358 71 205 215

GSF, Regional office of
Northern Finland
Library
P.O. Box 77
FIN-96101 Rovaniemi
☎ +358 60 3297 130
Telex: 37295 geolo sf
Telefax: +358 60 3297 289

ISBN 951-690-553-6
ISSN 0781-4240

Vammalan Kirjapaino Oy 1994